# FABRICATION AND ANALYSIS OF KEVLAR FIBER REINFROCED POLYMER COMPOSITES USING FUSED DEPOSITION MODELLING

Thesis Submitted for the Award of the Degree of

**DOCTOR OF PHILOSOPHY**

**in**

**Mechanical Engineering**

**By**

**KAMAL KUMAR OJHA**

**Registration No: 41900107**

**Supervised By**

**Dr. Vishal Francis (24813)**

**School of Mechanical Engineering (Assistant Professor)**

**Lovely Professional University**


**LOVELY PROFESSIONAL UNVERSITY**
**2025**

## DECLARATION

I, hereby declared that the presented work in the thesis entitled "Fabrication and analysis of Kevlar fiber reinforced Polymer Composites using Fused deposition modeling" in fulfilment of degree of **Doctor of Philosophy (Ph. D.)** is outcome of research work carried out by me under the supervision Dr,Vishal Francis, working as Associate Professor, in the Department of Mechanical Engineering Lovely Professional University, Punjab, India. In keeping with general practice of reporting scientific observations, due acknowledgements have been made whenever work described here has been based on findings of other investigator. This work has not been submitted in part or full to any other University or Institute for the award of any degree.

**(Signature of Scholar)**

Name of the scholar: Kamal Kumar Ojha
Registration No.:41900107
Department/school: Department of Mechanical Engineering
Lovely Professional University,
Punjab, India

## CERTIFICATE

This is to certify that the work reported in the Ph. D. thesis entitled "Fabrication and analysis of Kevlar fiber reinforced Polymer Composites using Fused deposition modeling" submitted in fulfillment of the requirement for the reward of degree of **Doctor of Philosophy (Ph.D.)** in the Department of Mechanical Engineering is a research work carried out by Kamal Kumar Ojha,41900107, is bonafide record of his/her original work carried out under my supervision and that no part of thesis has been submitted for any other degree, diploma or equivalent course.

**(Signature of Supervisor)**

Name of supervisor: Dr.Vishal Francis

Designation: Associate Professor

Department/school: Mechanical Engineering

University: Lovely Professional University

**ABSTRACT**

The fabrication of intricate geometries holds significant importance in industry. Fused deposition modeling (FDM) an additive manufacturing (AM) technique has proved to be a good candidate to fabricate complex shapes in small lead time. FDM offers a platform to produce polymeric objects for prototyping, tooling and even end-use parts. The materials properties of the FDM parts lacks integrity compared to its counterpart manufacturing processes due to layer structure and inherent porosity issues. Utilizing composite materials, particularly FRCP in FDM process for improved mechanical properties holds significant capability. Moreover, the continuous fiber reinforcement can further enhance the mechanical properties of FDM parts. The volume fraction of fiber and orientation are among few of the important parameters that needs to be investigated. There is a scarcity of literature in FDM of continuous FRCPs. Therefore, the aim of the study is to investigate the effect of impregnating continuous Kevlar fiber into thermoplastic material for fabrication of FDM parts. Tensile and impact specimen was fabricated and tested in accordance with ASTM standards. Experimental investigations were conducted by varying factors such as fiber orientation, patterns and volume fraction. Tensile performance exhibited significant disparities between specimens with concentric pattern and those with isotropic pattern. Results indicates a positive correlation between increased reinforcement and enhanced tensile properties. A peak tensile strength of 405 MPa with 58% volume fraction was achieved. Unreinforced specimens exhibited tensile strength of 21 MPa. 3D printed Onyx composite showed a ductile failure pattern. With increased reinforcement, strain decreased, and the tensile modulus increased. Alignment of continuous fibers along the load-bearing axis yielded the maximum strength. Failure modes varied from fiber pull-out to delamination, on increasing the reinforced volume fraction, exhibiting, brittle fracture. Strength and ductility were inversely correlated with an increase in reinforcement.

Rule of mixture and Halpin Tsai models were used to predict the mechanical properties and compared with the experimental values. Macroscopic analysis unveiled that when volume fraction of the reinforcement is increased beyond 30%, it resulted in delamination. Increment in Young's modulus was achieved on increasing the volume

fraction up to 60%, a threshold point. Beyond this point complete detachment of the reinforcement from the matrix was observed.

Impact properties of FDM parts were evaluated by varying fiber orientation, volume fraction and fiber pattern. A comparative analysis was conducted between unreinforced impact specimens and their reinforced counterparts. The experimental results revealed a significant impact of impregnating continuous fiber on impact properties of FDM printed specimen. The study observed superior strength when laying the fiber along the print bed orientation compared to the transverse direction of loading.

On comparing the mechanical behaviour of FDM fabricated continuous FRCP to conventionally manufactured specimen it was found the tensile strength of printed specimen were found to be 56.1 MPa. On the other hand, the strength of conventional specimens was 31.38 MPa. The strain of printed specimens was 0.035 and that of conventional specimens was 0.025. Fiber pull outs were observed on the conventionally fabricated specimens. Possibility of fiber entanglement and uneven distribution due to compression may have caused the weakening of the specimens as compared to FDM printed parts.

The key objective of the thesis to enhance the performance of FDM parts by continuous fiber reinforcement has been successfully achieved. Investigations carried out in this research work suggest the threshold value of volume fraction of fiber reinforcement to achieve maximum strength. Moreover, the influence of fiber direction and pattern was also investigation. The research work serves to fill the gap in the knowledge of FDM of continuous fiber composite.

Keywords: FDM, continuous fiber composite, Kevlar, additive manufacturing.

## LIST OF ACRONYMS

| | |
|---|---|
| 3D | Three dimensional |
| ABS | Acrylonitrile Butadiene Styrene |
| AM | Additive manufacturing |
| ASTM | American society for testing and materials |
| CAD | Computer aided Design |
| CFRCP | Continuous fiber reinforced composite |
| FDM | Fused deposition modeling |
| FFF | Fused filament fabrication |
| FRCP | Fiber reinforced composite |
| KFRCP | Kevlar fiber reinforced composite |
| LOM | Laminated object Manufacturing |
| PA | Polyamide |
| PC | Polycarbonate |
| PE | Polythene |
| PEEK | Polyethere ketone |
| PLA | Poly lactic acid |
| PP | Polypropylene |
| PE | Polythene |
| PPS | Polyphenylene sulphide |
| SLS | Selective laser sintering |
| STL | Standard triangle language |
| TS | Tensile Strength |
| U | Expanded Uncertainty |
| UTS | Ultimate tensile strength |

## LIST OF SYMBOLS

| | |
|---|---|
| $V_f$ | Volume fraction |
| $C_t$ | Sensitivity coefficients of thickness. |
| $C_w$ | Sensitivity coefficients of width |
| $C_t$ | Sensitivity coefficients of thickness |
| $E_t$ | Total Energy |
| $E_i$ | Impact Energy |
| $h_i$ | Initial Height |
| $u_c$ | Combined standard uncertainty |
| $h_f$ | Final Height |
| $u_c$ | Combined standard uncertainty |
| $u_{con}$ | Uncertainty contribution |
| c | Standard uncertainty of parameter or equipment |
| k | Student's t-distribution |
| m | mass |
| n | Number of specimens tested |
| g | Gravity |
| w | Width |
| u | Standard uncertainty |
| s | standard deviation of tensile strength values |
| t | thickness |

## LIST OF FIGURE

## LIST OF TABLE

TABLE OF CONTENTS

# Contents

# CHAPTER 1
# INTRODUCTION

## 1.1. Additive Manufacturing

Additive Manufacturing (AM) represents a revolutionary method of production, where items are built layer by layer (Hasan, 2020). This innovative process enables the fabrication of intricate geometries with remarkable ease, breaking traditional manufacturing constraints. Initially confined to prototyping, AM has transcended into the realm of manufacturing end-use products, marking a significant evolution in manufacturing technology (Tofail et al., 2018). Figure 1.1 shows the evolution of the AM process from prototyping to manufacturing.

The versatility of AM extends across diverse sectors, including Defense, Aerospace, Biomedical, and Automobile industries (Ngo et al., 2018).. Its adaptability and precision make it crucial in creating components and structures that were once challenging or impossible to produce using conventional methods (Bozkurt & Karayel, 2021). AM's impact across these sectors highlights its potential to reshape manufacturing paradigms and drive innovation in various fields (Yan et al., 2021).

ASTM 52900 categorizes additive manufacturing technologies into seven primary groups. These include Vat photo-polymerization, where liquid photopolymers are solidified through photo-polymerization; Sheet lamination, which bonds sheets of material together to form parts; Powder bed fusion, where thermal energy melts and fuses powdered materials; Material jetting, a process where droplets of materials are deposited layer by layer; Binder jetting, which uses a liquid bonding agent to join powdered materials during deposition; Direct energy deposition, employing thermal energy to fuse materials directly; Material extrusion, wherein pressurized and heated material is dispensed through a nozzle hole. Additionally, Energy Deposition utilizes thermal energy to fuse materials, allowing for the creation of intricate and durable structures. These classifications provide a detailed understanding of additive manufacturing processes and their applications across various industries (Radhika et al., 2024) (Blakey-Milner et al., 2021)..

Fused deposition modeling (FDM) is recognized as one of the most widely used AM processes, primarily due to its numerous advantages over other AM techniques. The

process, characterized by extrusion-based technology, is preferred for its versatility, cost-effectiveness, and accessibility. FDM's ability to produce robust parts with intricate geometries, coupled with its relatively simple setup and operation, has made it a preferred choice across various industries. Its widespread adoption underscores its efficiency and effectiveness in realizing complex designs and prototypes with precision and reliability.

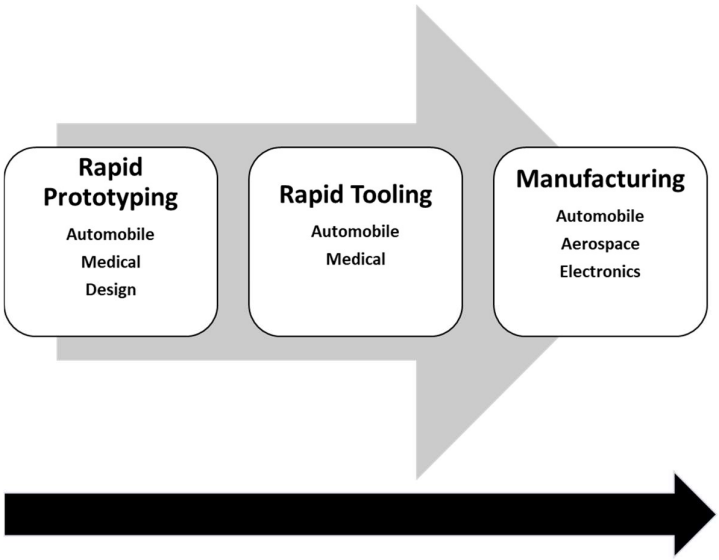


Figure 1.1. Evolution of 3D printing process from prototyping to manufacturing

## 1.2. Applications

AM has found extensive applications across various industries, showcasing its versatility and transformative potential (figure 1.2). In the realm of biomedical applications, AM technologies have revolutionized the production of medical implants, prosthetics, and anatomical models, offering customized solutions that enhance patient care and outcomes. In the automotive sector, AM techniques are employed for rapid prototyping, tooling, and manufacturing of lightweight components, contributing to improved performance and fuel efficiency. Likewise, in defense and aerospace industries, AM facilitates the production of complex parts, components, and even entire structures with reduced lead times and enhanced design flexibility. The space sector leverages AM for manufacturing lightweight and durable components for spacecraft and satellites, enabling space exploration endeavors. Moreover, AM has made

significant inroads in electronics manufacturing, allowing for the creation of intricate circuitry and miniaturized components. Additionally, AM plays a pivotal role in rapid tooling and prototyping across various sectors, enabling agile product development cycles and reducing time-to-market. The breadth of applications underscores the profound impact of AM across diverse industries, driving innovation and reshaping traditional manufacturing paradigms.

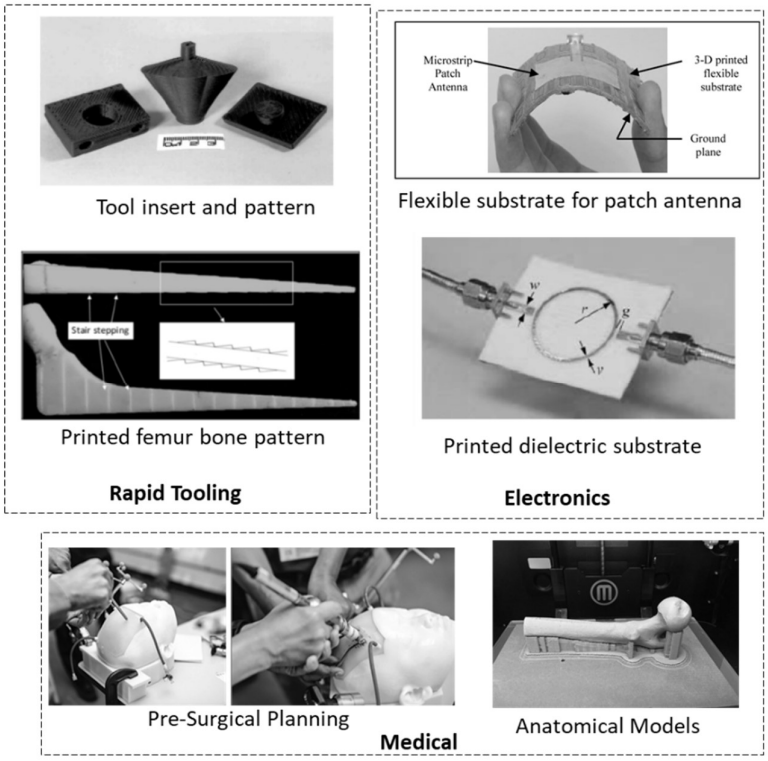


Figure 1.2. Some applications of FDM technique (Penumakala et al., 2020)

### 1.3. Fused deposition modeling

Among the diverse array of additive manufacturing (AM) techniques, Fused Deposition Modeling (FDM) is recognized as one of the most prominent and extensively utilized methods. Patented by Scott Crump, co-founder of Stratasys, in 1989, FDM was subsequently introduced to the commercial market in the early 1990s (Jaisingh Sheoran & Kumar, 2020). FDM process employs a continuous supply of thermoplastic filament, provided through a spool, to fabricate components layer by layer. The core operating principle of FDM involves the extrusion of a semi-liquid thermoplastic that does not

solidify instantaneously upon deposition. Instead, the materials for each layer fuse together before undergoing curing and solidification, resulting in a component constructed in a layer-wise manner, influenced by the surrounding ambient temperature.

The advantages of FDM include its process simplicity, rapid printing capabilities, and cost-effectiveness. However, the technique also presents several disadvantages: the mechanical properties are dependent on process parameters (resulting in anisotropic characteristics), there is a tendency for poor surface finish, and the range of printing materials is limited to thermoplastic polymers due to the necessity of thermos plasticity for 3D printing via FDM .Continuous fibers, such as carbon fiber or glass fiber, are introduced into the process to improve strength, stiffness, and impact resistance (Karimi et al., 2024).Thermoplastics like PLA, ABS, PETG, and Nylon, combined with continuous fibers, are common (Penumakala et al., 2020).The fibers are typically aligned in the direction of the load to maximize strength. Continuous fibers provide greater tensile strength compared to standard FDM without reinforcement (Melenka et al., n.d.) .Offers high strength-to-weight ratios, making parts lighter and more efficient. Improved thermal and chemical resistance. Aerospace components, Automotive parts Sporting goods Prototyping for structural applications Adjustments in temperature, print speed, and layer height may be necessary to accommodate the additional material Specialized printers designed to handle continuous fibers are often required, as they must manage the feed of both thermoplastic and fiber materials (Jayakrishna et al., 2018) .

### 1.4. Limitations of FDM

The application domain of FDM parts faces certain limitations primarily due to the relatively restricted availability of compatible materials. Unlike traditional manufacturing processes that may offer a broader selection of materials, FDM relies on materials specifically formulated for extrusion-based printing. This constraint can sometimes limit the types of parts that can be effectively produced using FDM technology.

Furthermore, the strength and durability of FDM parts may not always match those manufactured through conventional methods. This discrepancy in strength often arises from the inherent characteristics of FDM, where layers of material are deposited and

partially bonded together. While FDM parts can be structurally sound, they may exhibit weaknesses at the interfaces between layers, affecting overall strength and reliability (figure 1.3.).

However, the integration of composite materials represents a promising avenue for overcoming these limitations. By incorporating composite materials into the FDM process, manufacturers can enhance the mechanical properties of printed parts. Composite materials, which typically consist of a combination of fibers and resins, offer improved strength, stiffness, and durability compared to traditional FDM materials alone. The use of composite materials in FDM opens up new possibilities for designing and producing parts with enhanced performance characteristics. Components fabricated with composite materials can withstand higher stresses, exhibit better resistance to wear and fatigue, and possess superior mechanical properties overall. As a result, the application domain of FDM parts can be significantly expanded, enabling their use in a broader range of industries and applications where strength and durability are paramount.

Integration of composite materials into the FDM process represents a strategic approach to address the inherent limitations of traditional FDM materials. By leveraging the unique properties of composites, manufacturers can unlock new opportunities for innovation and advancement in additive manufacturing, ultimately enhancing the capabilities and utility of FDM technology in diverse fields and sectors.

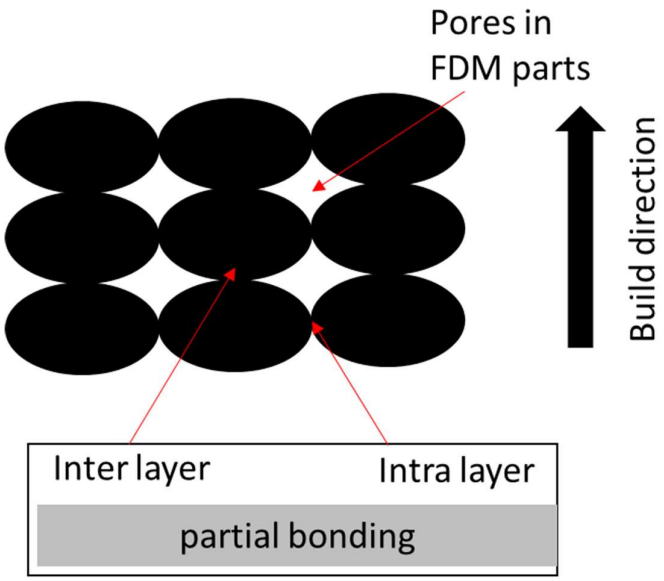


Figure 1.3Pores and partial bonding issue associated with FDM technique

### 1.5. Fiber-reinforced composites

Fiber-based composites hold significant interest in various industries for several compelling reasons. Firstly, their lightweight nature combined with high strength makes them particularly appealing. By utilizing fiber-based polymer composites, manufacturers can achieve a favorable strength-to-weight ratio, ensuring that components remain sturdy without adding unnecessary bulk. FRCPs find applications in several sectors such as aerospace, infrastructure, renewable energy and transportation (figure 1.4.).

Moreover, the incorporation of fibers, whether carbon or glass, serves to bolster the polymer matrix, thereby enhancing mechanical properties significantly. These reinforced composites exhibit improved tensile strength, stiffness, and impact resistance, all of which are crucial for maintaining the structural integrity of FDM-printed parts. Such enhancements not only contribute to the overall durability of the parts but also expand the range of potential applications where strength and reliability are paramount. One of the key advantages of fiber-based composites lies in their ability to tailor mechanical performance according to specific application requirements. By selecting appropriate fibers and adjusting their orientation within the composite matrix,

manufacturers can customize mechanical properties to suit diverse needs. This flexibility allows for the creation of components optimized for various environments and usage conditions.

Additionally, fiber reinforcement plays a pivotal role in mitigating common issues associated with FDM printing, such as warping and shrinkage. By integrating fibers into the polymer matrix, the composite material exhibits reduced susceptibility to dimensional distortions during the printing process. This results in improved dimensional accuracy and minimization of defects in the final printed components, ultimately enhancing overall product quality and reliability.

The utilization of fiber-based composites offers a host of benefits, including lightweight construction, enhanced mechanical properties, tailored performance characteristics, and reduced printing-related issues. These advantages position fiber-based composites as a valuable resource for advancing additive manufacturing technologies, particularly in applications where strength, durability, and precision are paramount concerns.

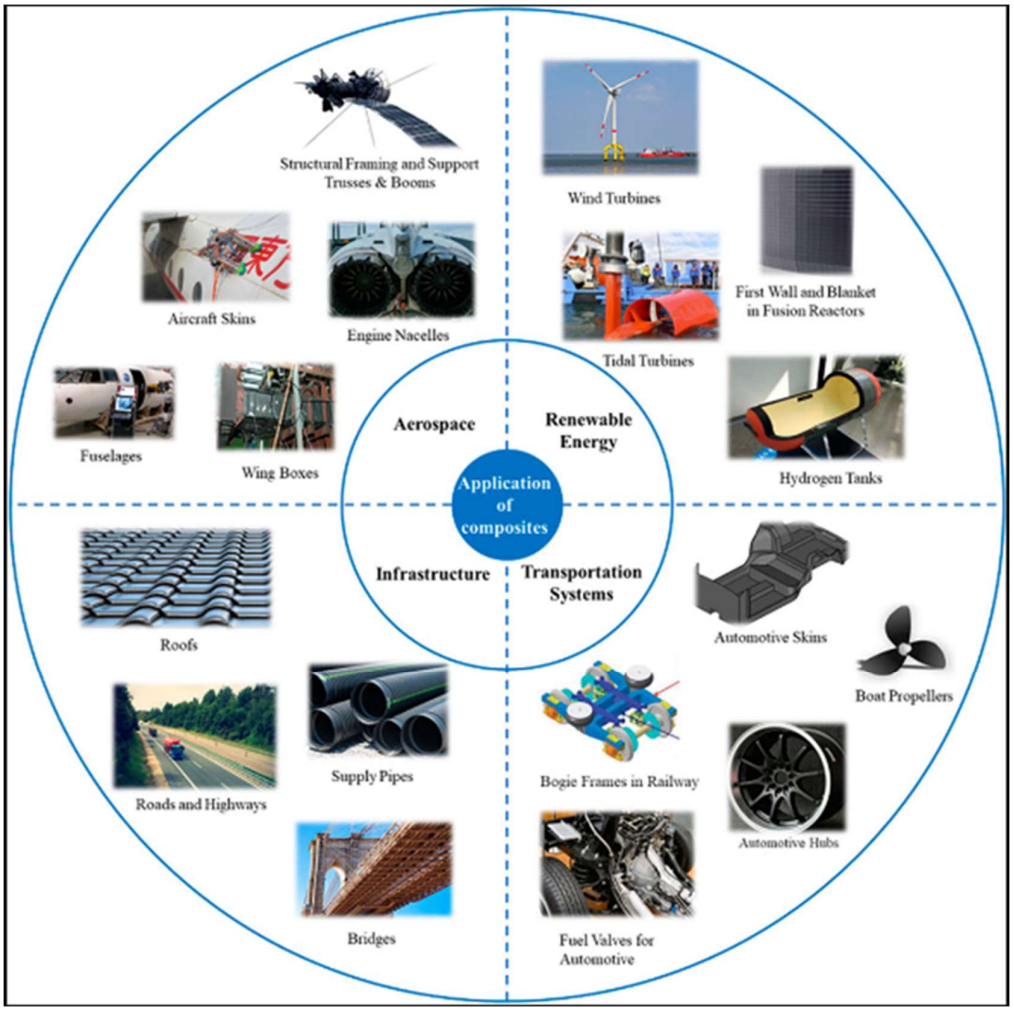


Figure 1.4 Application domain of FRCPs [(Chen et al., 2022)]

### 1.6. Types of FDM printers for FRCP

The working principle of FDM involves a systematic process in which preheated filaments are pressurized and extruded through a nozzle onto the printing bed. The extruded filament is carefully guided by the nozzle to create each layer of the object. Once the first layer is complete, the print bed moves upwards in the z-direction to begin the next layer. This layer-by-layer technique continues until the final CAD model is fully constructed. Within the realm of FDM, there are three primary techniques identified by (Naranjo-Lozada et al., 2019).

Type A utilizes a single nozzle through which both the thermoplastic material and the fiber are extruded. In Type B, two different types of filament are employed: one for the thermoplastic material and the other for the fiber material. Finally, Type C incorporates

two separate nozzles, one for the filament and the other for the reinforcement material. The Mark Two 3D printer exemplifies a Type C printer renowned for its capability to print continuous Carbon fiber, Kevlar, and Glass fiber composites. Mark Two printer features a dual extrusion nozzle system. One nozzle dispenses the matrix material, while the other disperses the reinforcing fiber. The extrusion nozzles operate sequentially: the first nozzle deposits the matrix material and pauses, allowing the second nozzle to extrude the reinforcing fiber material before pausing in turn. This process is continuous, ensuring the seamless integration of both materials to achieve the desired 3D printed object with enhanced structural properties and performance characteristics. Due to the benefits of type C printers, they are utilized to fabricate the specimens in the current research work

Fibers like glass, carbon, and Kevlar are brittle and sensitive to deformation when subjected to external loads. Binding agent like epoxy when glue fiber and matrix create composite material which is robust and capable in distributing load. The process contributes to improve excellent strength to weight ratio. State-of-the-art 3D printing technology has made it possible to print for these reinforced fibers, paving new possibilities for creating strong lightweight material and application in various industries. Both continuous as well as discontinuous fibers can be fabricated however each has a unique way of printing procedure and the choice of it depends upon end user application. The choice between continuous and discontinuous fiber depends upon end user requirement. Chopped fiber (discontinuous) like carbon fiber when impregnated with weak thermoplastic material (Nylon, ABS or PLA) results in an increase in strength, dimensional stability, good surface finish. Using continuous fiber is a cost-effective method to replace traditional metals resulting in an excellent Strength to weight ratio. Plethora of materials are suitable for FFF printing, Acrylonitrile Butadiene Styrene (ABS), Onyx, Polyamide (Nylon), Polylactic Acid (PLA), Polyethylene Terephthalate Glycol Modified (PETG), Polyether Ether Ketone (PEEK), Polycarbonate and ULTEM etc. In this present research work thermoplastic material onyx® is impregnated with Kevlar to 3D print composite.

Onyx is composite base material for composite. It’s a thermoplastic material which can be melted multiple time and marketed by Mark forged which is an amalgamation of

chopped nylon (polyamide 6) and carbon fiber filled with approximately 10% to 20% volume fraction of short carbon fiber (Hetrick et al., 2021).Thermoplastic material is type of polymer can be heated and reshaped because of weak intermolecular forces. Thermoplastic materials like nylon, PLA and ABS are sensitive to moisture. Moisture negatively affects the mechanical performance of 3D printed parts like voids formation, poor surface finish. Onyx is a thermoplastic material which is affected less when exposed to moisture. It imparts high toughness and strength when printed unreinforced. When reinforced with fiber like Kevlar, glass and carbon then strength is comparable to aluminum (Nikiema et al., 2022.6) Kevlar are aromatic polyamide fiber which possesses good impact strength properties. It provides excellent strength to weight ratio, low density, low thermal conductivity developed in 1965 by Stephanie Kwolek. Kevlar have anti-impact properties therefore, it finds applications in bullet proof jacket, biomedical etc (Mohammadizadeh & Fidan, 2021)

### 1.7. Overview of the Thesis

As discussed in the above section, continuous FRCPs hold immense applications in various fields. Capability to produce complex shaped geometrical features via FDM technique provides an opportunity to fabricate end-use products. However, the exhaustive investigations on the effect of fiber direction, pattern and volume fraction is critical in achieving the desired enhanced mechanical properties. Utilizing the FDM technique to fabricate continuous FRCPs parts can open great avenues for various structural applications.

The current study focuses on the fabrication of Kevlar reinforced polymer composite using FDM technique. By considering various fiber orientations and different infill patterns the mechanical behavior of the fabricated samples was investigated and analyzed. Moreover, the crucial effect of fiber volume fraction is also taken into account for the investigation. A threshold value of volume fraction is determined for fabrication of composite specimens via FDM process. The 3D printed samples were compared with the conventionally manufactured composite samples and a contrast is discussed. Finally, the experimental values were compared with the Rule of mixture and Halpin Tsai models for the fabricated composites.

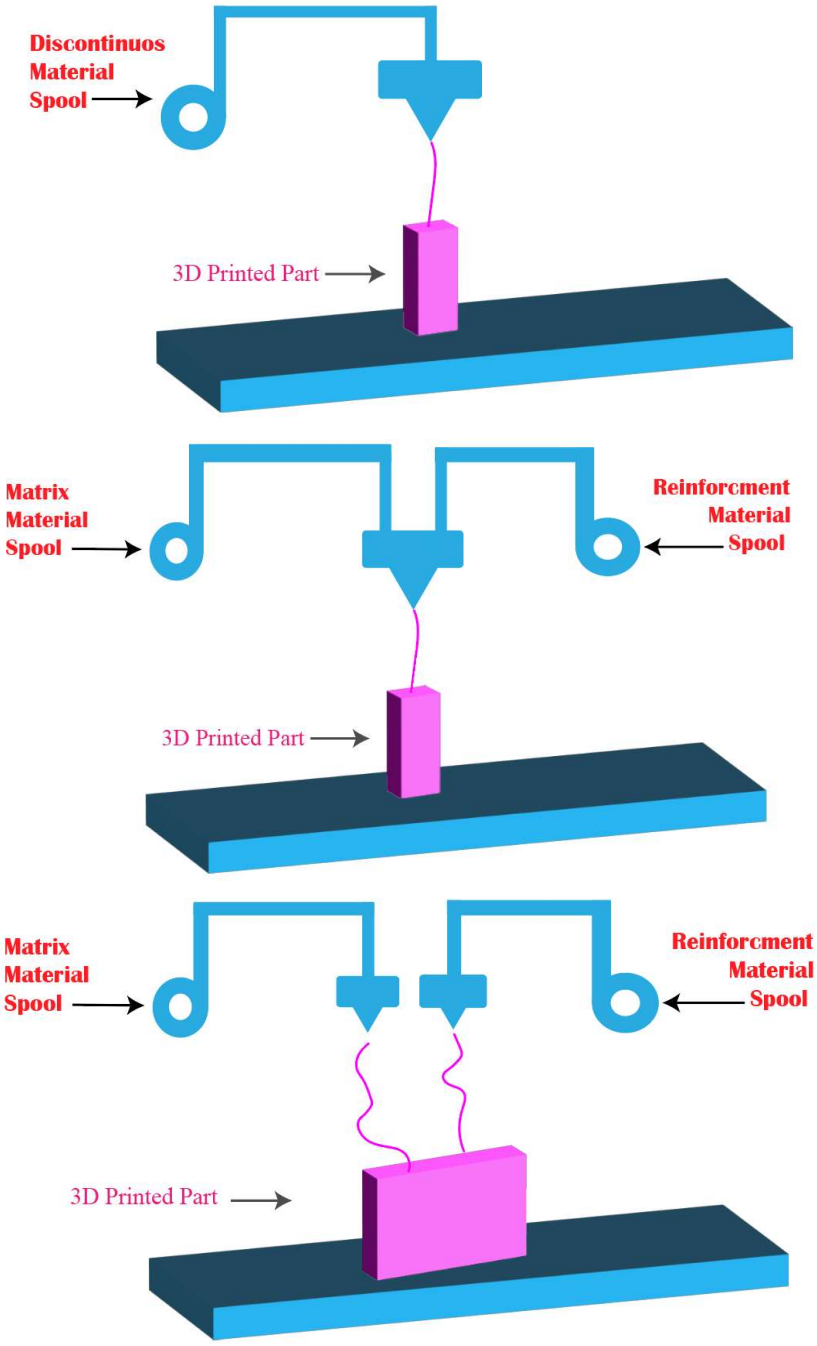


Figure 1.5 Various configuration of extrusion-based 3D printers (Pereira et al., 2019)

## CHAPTER 2

## LITERATURE REVIEW

In this chapter, a comprehensive literature review is presented to identify existing gaps and establish the research objectives for the current study. The literature review categorizes studies based on several key aspects related to fiber conditions, types of printers, mechanical properties investigated, and the effects of various parameters. Firstly, it examines the condition of fibers used in additive manufacturing processes, considering factors such as their composition, length, orientation, and distribution within the matrix material. Understanding these aspects helps researchers evaluate how different fiber characteristics influence the final properties of composite materials. Secondly, the review delves into the types of printers utilized in the studies focusing on extrusion-based printers. Thirdly, the literature review investigates the mechanical properties under examination, including tensile strength and impact resistance. Understanding how these properties vary based on fiber orientation, volume fraction, and build orientation is crucial for optimizing composite material performance for specific applications. By organizing the literature review according to these key categories, valuable insights are drawn into the current state of knowledge and potential avenues for further investigations are identified for improvement in the field of additive manufacturing of composite materials.

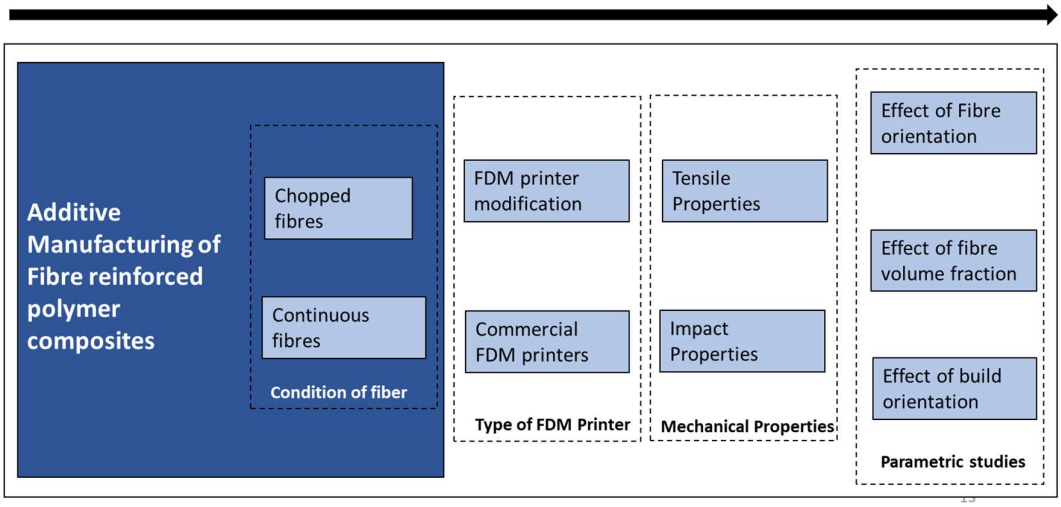


Figure 2.1 Literature review classification

Section 2.1 Discusses the literature review related to tensile properties of 3D printed FRCPs. Section 2.2 deliberates about impact properties of fiber reinforced polymer composites.

### 2.1. Tensile properties

Tensile testing of fiber-reinforced composites is essential for evaluating their mechanical properties and structural integrity. By subjecting these materials to tensile forces, important properties such as tensile strength, elastic modulus and elongation at break can be evaluated. Understanding these properties is crucial for the design and optimization of composite structures for various applications, including the aerospace, automotive, construction and sports industries. The tensile test provides valuable information about the behavior of fiber-reinforced composites under load, helping in material selection, quality control and performance prediction. A plethora of authors reported FDM of thermoplastic materials and investigated the mechanical behavior of the fabricated parts. Focusing on the tensile strength, Sood *et al.* utilized the ABS polymeric filament for 3D printing and reported the experimental value of 16.7 MPa (Sood et al., 2010).Rodríguez-Panes *et al.* reported tensile strength and modulus of elasticity for ABS to be 51 MPa and 3.5 GPa respectively (Rodríguez-Panes et al., 2018).Nabeel *et al.* reported tensile strength and modulus of elasticity of 43.83 MPa and 3.09 GA respectively for PLA material(Maqsood & Rimašauskas, 2021) .Todd Letcher *et al.* reported Ultimate Stress of 59.65 MPa and modulus of elasticity (GPa) of 3.256 for PLA (Letcher & Waytashek, 2014).Jatti *et al.* reported that various printing parameters of FDM like infill percentage extrusion temperature, printing speed etc., significantly affects the mechanical properties (Jatti et al., 2019).Cristina *et al.* reported that increase in raster orientation and layer thickness decreased the mechanical strength of the 3D printed parts (Vălean et al., 2020) .Moreover, attempts have been made to incorporate macro and nano sized particles in the polymer matrix for FDM of composites (Vălean et al., 2020). Singh *et al.* explored the effect of impregnating single, double, and triple particle sizes of $Al_2O_3$ into a Nylon-6 matrix, which significantly improved the tensile strength of the material (Singh & Singh, 2015).Farina *et al.* recycled Nylon-6 granules with ABS and titanium dioxide ($TiO_2$), resulting in a varying

range of strengths between 55.79 to 86.91 MPa and a Young's modulus of 1.64 GPa(Farina et al., 2019).

### 2.1.1. Effect of chopped fiber

In order to improve the mechanical properties of FDM parts fiber reinforced polymer composites have been developed and investigations have been carried out on the printed specimens. A general approach to develop such filaments is to mix the chopped fibers with the polymer matrix for filament fabrication. Nings *et al.* research findings unveiled a clear correlation between the percentage of chopped carbon fiber impregnation and mechanical performance of the FDM fabricated composite ,As the content of chopped carbon fiber increased from 0 wt.% to 15 wt.%, a discernible enhancement in tensile strength was observed, with values progressively increasing from 32 MPa to 42 MPa. Furthermore, the Young's modulus displayed a corresponding increment, evolving from 1.9 GPa to 2.5 GPa within the same range of carbon fiber content. Experimental result revealed tensile strength and Young's modulus increased and toughness and ductility decreased. This study highlights the direct impact of chopped carbon fiber reinforcement on the material's tensile properties (Ning et al., 2017).

Tekinalp *et al.* reported impregnation of ABS with chopped carbon fiber which resulted in a substantial increase in tensile strength to 71 MPa and a Young's modulus of 12.5 GPa when utilizing a 40 wt% proportion of chopped carbon fiber (Tekinalp et al., 2014).Liao *et al.* (2018) reported that the inclusion of chopped carbon fiber at a 10% weight fraction led to a significant enhancement in the tensile strength of polyamide material, increasing it from 46.4 MPa to 93.8 MPa (Liao et al., 2018).

Incorporation of short carbon fibers, impregnated with a 15% weight fraction of carbon fiber, resulted in a notable 1.2-fold improvement in the tensile strength of pure PLA (Ferreira et al., 2017)..The literature reports increment of mechanical properties of polymer materials on incorporation of chopped fibers for filament fabrication(Ferreira et al., 2017).

### 2.1.2. Effect of continuous fiber

Incorporation of continuous fiber in polymer matrix for composite fabrication yields much better results compared to chopped/short fibers. The incorporation of continuous fiber in 3D printed samples has been challenging. Hao *et al.* research findings

demonstrated that continuous carbon fiber composites exhibited significantly improved tensile strength, measuring 792.8 MPa and 1641.4 MPa, when compared to short carbon fiber impregnated with PLA having experimental tensile strength of 91MPa. The elastic modulus and flexural strength were found to be 2020 MPa and 143.9GPa(Hao et al., 2018).Nabeel Maqsood *et al.* reported that impregnating continuous carbon fiber in thermoplastic material using modified printed increased its tensile strength from 43.83 to 245.40 MPa. In a similar fashion Young's modulus was increased from 3.09 GPa to 25.94 GPa, while ductility decreased (Maqsood & Rimašauskas, 2021).

James Sauer & James reported that thermoplastic material nylon has low tensile strength of 28 MPa resulting in larger strain compared to reinforced specimen. With successive increment in reinforcement strain was reduced resulting it decreased strain and increase in Young's modulus up to 586 MPa with 70 % volume fraction (James Sauer & James, 2018). Figure 2.2. shows the effect of fiber reinforcement fraction on mechanical properties of printed specimens (James Sauer & James, 2018).

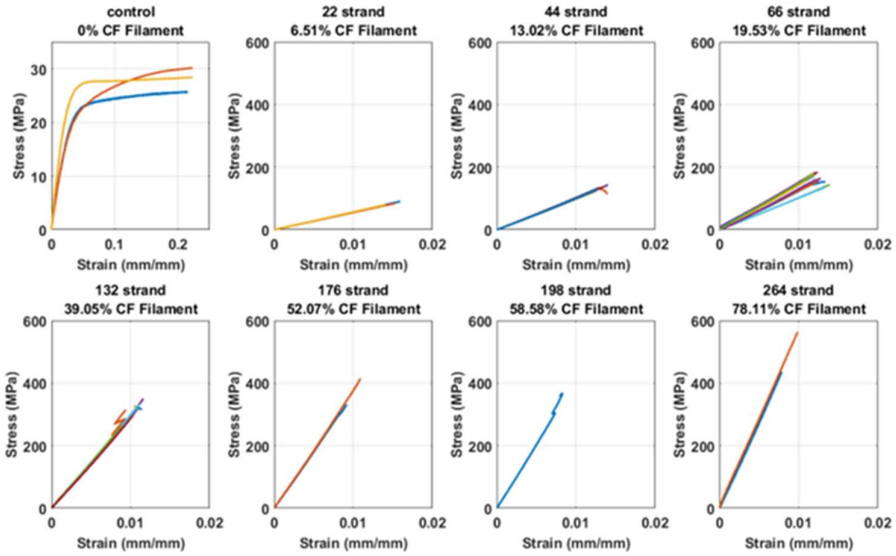


Figure 2.2 Stress –Strain Plot of 3D printed nylon composites with varying reinforcement (James Sauer & James, 2018).

Mohammadizadeh reported that impregnating continuous carbon fiber into the nylon matrix at different volume fractions of 8%, 18%, 33%, and 60%, resulting in a notable enhancement in tensile strength, with values ranging from 19.17 MPa to an impressive 446.87 MPa(Mohammadizadeh & Fidan, 2021).Compared to chopped fibers, continuous fibers yield better mechanical properties, however, limited work is reported due to the restrictions imposed by the availability of dedicated setup for achieving 3D printing of continuous fiber.

### 2.1.3. Effect of Modified Printer

Due to the unavailability of 3D printers capable of printing continuous FRCPs, investigations have been carried out to modify the existing 3D printers to accommodate continuous fiber impregnation. Chaudhry *et al.* reported that the modification of the printer nozzle into a dual nozzle setup allowed for the production of continuous reinforced composites. When PLA was impregnated with continuous carbon fiber using this setup, the tensile strength notably increased to 112 MPa, and the flexural strength reached an impressive 164 MPa. These findings highlight the advantages of modifying 3D printers to incorporate continuous carbon fiber. These reinforcements can enhance the mechanical properties of the printed materials, making them suitable for a wide range of applications (Chaudhry et al., 2022). Moreover, 3D-printed parts impregnated with continuous filaments such as carbon, glass, and Kevlar exhibited qualities on par with traditional composite materials manufactured through manual layup techniques. In the context of 3D printed thermoplastic materials, the initial unreinforced onyx material exhibited a modest tensile strength of 32.630 MPa. However, when this material was reinforced with different fibers, namely glass fiber, carbon fiber, and Kevlar fiber, substantial improvements in tensile strength were observed. Specifically, the tensile strengths of the reinforced materials were recorded as 276.134 MPa, 290.570 MPa, and 261.957 MPa, respectively (Florin Cofaru et al., 1964).Additionally, Kabir *et al.* reported in 2021 that 3D printed composites were limited in their volume fraction, not exceeding 45% (Kabir et al., 2021). In their study, they observed a noteworthy tensile strength of 395.1 MPa for 3D printed nylon when reinforced with glass fiber.

These findings highlight the remarkable correlation of fiber reinforcement on enhancing the mechanical properties of 3D printed thermoplastic materials, making them suitable for a variety of engineering applications (Kabir et al., 2021).Yu *et al.* reported a modified open-source 3D printer for impregnating PLA with continuous carbon fiber. This resulted in a substantial increase in tensile strength of pure plastic from 52 MP to 80 MPa and flexural strength to 59 MPa (Yu *et al.*, 2019).

The modification of 3D printers to accommodate continuous fiber composite fabrication has shown promising results, outperforming chopped fibers in terms of mechanical properties and structural integrity. However, one significant challenge lies in the lack of standardized setups for these modified printers, which are not readily available commercially. As a result, investigations into commercially available 3D printers capable of printing continuous fiber composites are imperative.

### 2.1.4. Effect of Fiber Orientation

It is evident that continuous fiber reinforced polymer composites offer better mechanical performance. However, it is crucial to study the effect of fiber orientation on mechanical properties of the composites. During 3D printing the continuous fibers can be deposited in various orientations as shown in Figure 2.3. The fiber orientation direction can be varied from 0° to 90°. Few common orientations investigated in literature are 0°, 15°, 45°, 60° and 90°. Apart from these orientations, continuous fibers can be deposited in concentric manner (usually referred as concentric pattern) in commercially available composite 3D printers. Dickson *et al.* reported that the depositing fibers in 0° orientation exhibits a higher tensile strength when compared to concentric pattern with same volume fraction of glass fiber impregnated in a 3D printed nylon composite (8-10%), elastic modulus and tensile strength for the concentric pattern were measured to be 156 MPa and 3.29 GPa, respectively. The tensile strength for isotropic 0° pattern, was found to be 212 MPa, and the elastic modulus was determined to be 4.29 GPa (Dickson et al., 2017).

3D printed nylon composite with continuous carbon fiber and an isotropic pattern achieved a higher tensile strength of 450 MPa, whereas the concentric pattern yielded 250 MPa, both with a 50% volume fraction of carbon fiber (Hao et al., 2018).Mohammadizadeh *et al.* findings reported lower mechanical strength in

concentric pattern compared to isotropic pattern. Despite similar volume fraction, the lower fiber content in the concentric pattern may have contributed to this observed difference. This shows that there is a correlation between fiber orientation and the achieved mechanical properties (Mohammadizadeh & Fidan, 2021).

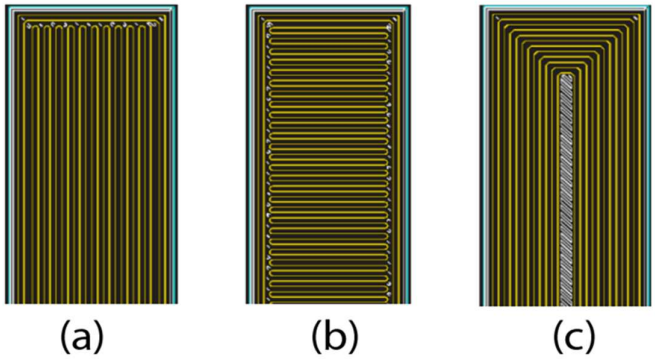


Figure 2.3. Fiber orientation (a) 0° orientation, (b) 90° orientation and (c) Concentric pattern

Kaiwen Shi *et al.* reported a decrease in yield stress with decrease in orientation angle. The difference is due to rotation of fiber at different angels. Smaller fiber angles result in smaller force component causing fiber rotation (Shi et al., 2021)..Pyl *et al.* reported the spectrum of tensile strength in the order 0, 0/90, ±45. The strain rate was four-fold in case of sample having ± 45 fiber direction (Pyl et al., 2018).

Goh *et al.*, observed two distinct types of failure in 3D printed composites with glass and carbon fiber. The type of fiber orientation played a crucial role in determining the mode of failure. When the fibers were laid in the direction of the loading, the dominant failure modes were shear rupture and shear damage along the fiber direction. This indicated strong bonding between the fiber and the matrix, leading to effective load-carrying capabilities by the reinforcement. Conversely, when the fibers were laid in the transverse direction, a different failure mode was observed indicating tensile rupture. This failure mode was attributed to the brittle nature of the composite, where the load was being transferred to the matrix rather than the reinforcement. This undermines the crucial role of fiber orientation in load bearing capacity of 3D printed composite (Goh et al., 2018) .

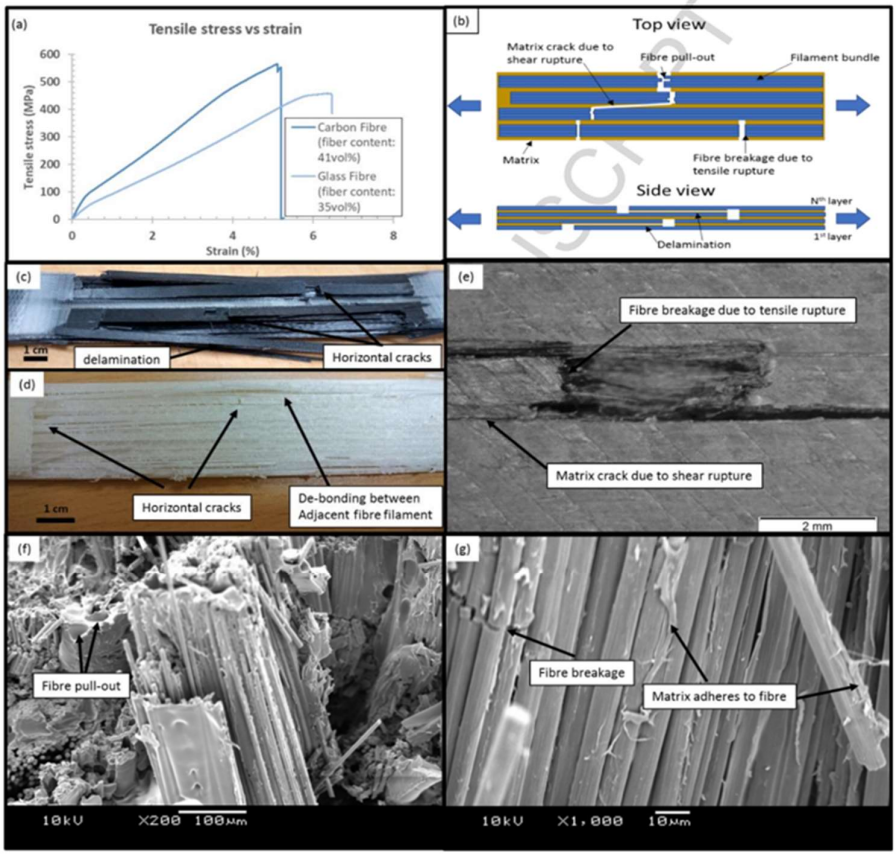


Figure 2.4 Schematic diagram showing types of failure in case of when the fiber is loaded in (Goh et al., 2018).

### 2.1.5. Effect of Volume Fraction

The volume fraction of the deposited fiber is also one of the major parameters that governs the performance of the composites. The volume fraction may significantly affect the mechanical properties. Cersoli *et al.* investigated the effect of varying the ber volume fraction. They incorporated the fibers into PLA matrix with different volume fractions (3.46%, 4.74%, and 20.53%). The selection of volume fraction significantly affected the mechanical properties of the composites. Ultimate tensile strength values were measured as 35.8, 47.4, 71.5, and 84.1MPa for the various volume fractions of Kevlar fiber. These results indicate a significant increase in tensile strength with higher volume fractions, suggesting that more fiber reinforcement leads to stronger composites. Young's modulus values were recorded as 3.26, 3.22.6, 4.5, and 3.68 GPa. The variations in Young's modulus highlight the changes in stiffness with different fiber

volume fractions and orientations. These findings emphasize the importance of considering the volume fraction of fibers in composite materials to achieve the desired mechanical properties for specific applications, especially when dealing with materials like Kevlar and PLA (Cersoli et al., 2021).

Naranjo-Lozada *et al.* investigated the affect of varying volume fraction of carbon fiber in composite printing. The tensile strength of thermoplastic material 9.8MPa for onyx, 9.6 MPa for nylon was observed and significant improvement in tensile strength was observed as 304.3 MPa with 54% volume fraction of carbon fiber and elastic modulus of 24 GPa. Onyx failure mechanism was different from that of nylon 3D printed specimens. A linear type of stress-strain graph shows brittle type of fracture. The increase in reinforcement restricts the elongation and decreased strain suggesting a brittle type fracture (Naranjo-Lozada et al., 2019)Hao *et al.* reported a compromised ductility with increase in reinforcement and strength and suggests that higher reinforcement levels tend to make the material less ductile but potentially stronger (Hao et al., 2018) .Mohammadizadeh *et al.* reported in 2019 demonstrated that the primary cause of failure was fiber pullout in case of nylon-carbon fiber composites. However, in the case of nylon- glass fiber composites, the failure mechanism involved both fiber pullout and fiber breakage. These insights further highlight the complex interplay between fiber orientation, composite configuration, and the resulting mechanical properties in 3D printed composites (Mohammadizadeh & Fidan, 2021)

Gonzalez-Estrada *et al.* reported decrease in tensile strength in 3D printed nylon composite reinforced with 25% volume fraction of glass fibers. The reported Young's modulus and tensile strength were 1610, 558, 391 MPa and 83, 37 and 22 MPa for 0, 45 and 90°respectively (González-estrada & Pertuz, 2018)

### 2.1.6 Effect of Build Orientation

AM offers flexibility to print parts in various orientation. The orientation significantly affects the properties and surface finish of the parts. Previous research work indicates a change in mechanical properties due to part orientations since it introduces anisotropy in the parts. (Caminero et al., 2018;. reported that the tensile strength of parts fabricated in flat orientation were about 8.4% higher than that of the parts fabricated on edge as shown Figure 2.5. Higher fiber volume content was achieved in flat oriented samples

due to internal structure. Reduction in fiber volume content was observed for the case of edge orientation which resulted in reduction of mechanical strength. On edge samples need more time as compared to flat samples. They reported that build orientation is an important parameter in affecting mechanical properties dictates the failure behavior and ductility. Mechanical performance was more in case of flat and edge sample. Upright orientation resulted weaker mechanical performance. Failure modes in above said modes is inter–layer fusion bond failure and trans layer failure. For the upright orientation, the samples were pulled parallel to the layer which leads to inter layer bond failure. In this case the adjacent layers of the fibers take the maximum load and not the fiber. In case of on edge and flat orientation the fibers are pulled perpendicular to the printing direction resulting in trans layer failure (Chacón et al., 2017)

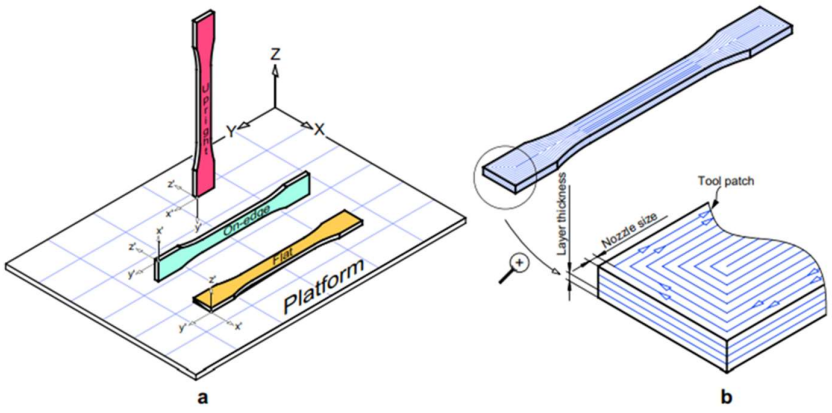


Figure 2.5 Schematic diagram showing different types of build orientation (Chacón et al., 2017)

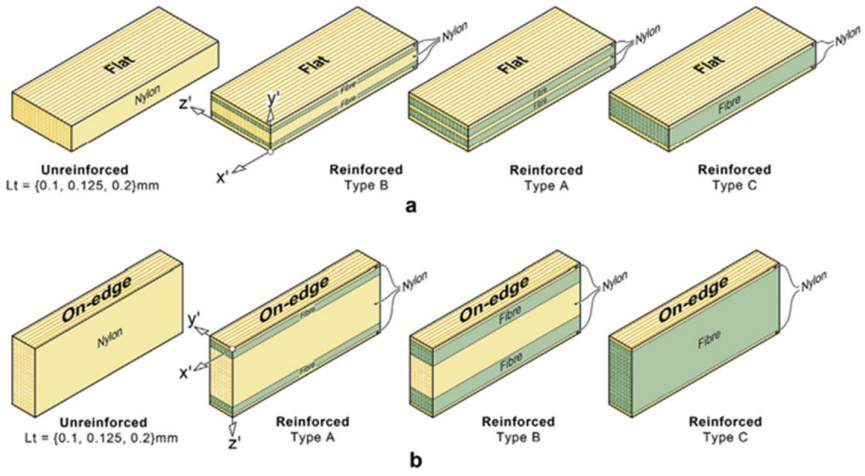


Figure 2.6 Schematic diagram showing various build orientation and fiber reinforcing strategy (Chacón et al., 2017a)

Table 2.1 Tensile Properties Reported in Literature

| Matrix | Fiber Reinforcement | Volume Fraction (%) | Fiber Pattern | Tensile strength (MPa) | Young's Modulus (GPa) | References |
|---|---|---|---|---|---|---|
| Nylon | Carbon | 25 | Iso 0° | 83 | 1.610 | (Shi et al., 2021a) |
| Nylon | Carbon | 25 | Iso 45° | 37 | .558 | (Shi et al., 2021a) |
| Nylon | Carbon | 25 | Iso 90° | 22 | .391 | (Shinde et al., 2020) |
| Nylon | Carbon | 25 | Iso 0° | 83 | 1.610 | (González-estrada & Pertuz, 2018) |
| Nylon | Carbon | 25 | Iso 45° | 37 | .558 | (González-estrada & Pertuz, 2018) |
| Nylon | Carbon | 25 | Iso 90° | 22 | .391 | ((González-estrada & Pertuz, 2018) |
| PLA | - | - | Iso 0° | 43.83 | 3.09 | (Maqsood & |

| | | | | | | |
|---|---|---|---|---|---|---|
| | | | | | | Rimašaus kas, 2021) |
| PLA | Carbon | - | Iso 0° | 245.40 | 25.94 | (Maqsood & Rimašaus kas, 2021) |
| Nylon | - | - | | 61 | .53 | (Dickson et al., 2017) |
| Nylon | Carbon | 50% | Concentr ic | 250 | | (Moham madizade h & Fidan, 2021) |
| Nylon | Carbon | 50% | Concentr ic | 350 | - | (Moham madizade h & Fidan, 2021) |
| Nylon | Carbon | - | Iso 0° | 701 | 60.9 | (Todoroki et al., 2020) |
| Nylon | Carbon | - | Iso 45° | 90 | 3.97 | (Todoroki et al., 2020) |
| Nylon | Carbon | - | Iso 90° | 60 | 2.27 | (Todoroki et al., 2020) |
| Nylon | Glass | 33 | | 156 | 3.29 | (Dickson et al., 2017) |
| Nylon | Glass | 33 | | 212 | 4.91 | (Moham madizade h & Fidan, 2021) |
| Nylon | Carbon | 58% | Iso 0° | 404.3 | 51.40 | (Moham madizade h & Fidan, 2021) |

| | | | | | | |
|---|---|---|---|---|---|---|
| Nylon | Glass | 28% | Iso 0° | 372.1 | 21.70 | (Mohammadizadeh & Fidan, 2021) |
| Nylon | Carbon | | Iso 0° | 436 | 51.40 | (Chacón et al., 2017) |
| Nylon | Glass | | Iso 0° | 305 | 21.70 | (Chacón et al., 2017) |
| Nylon | Carbon | 41 | | 600 | - | (Goh et al., 2018) |
| Nylon | Glass | 35 | | 450 | - | (Goh et al., 2018) |
| Onyx | Carbon | 9.8 | | 304 | 24 | (Naranjo-Lozada et al., 2019) |
| Onyx | Carbon | - | | 560 | 25 | (Ghebretinsae et al., 2019) |
| PLA | Glass | 50 | | 479 | 38 | (Akhoundi et al., 2019) |
| Onyx | Carbon | - | | 136 | - | (Shinde et al., 2020) |
| Onyx | Carbon fiber | 8.6 | | | 5.19 | (Yu et al., 2019) |

### 2.2. Impact Properties

The evaluation of impact energy absorption in FRCP materials is a critical parameter in preventing catastrophic failures. This assessment encompasses various phenomena such as delamination, matrix cracking, fiber breakage, and debonding between fibers

and the matrix. Therefore, the evaluation of impact absorption in composite materials is pivotal for numerous applications. The primary objective of an impact test is to quantify the material's toughness. Toughness, a fundamental mechanical property, measures the material's ability to absorb energy and undergo plastic deformation before fracture.

In this experimental procedure, the material undergoes a rapid impact from a swinging pendulum. Standardized specimen incorporates a stress concentrator which is in the form of a V-shaped notch which assess material's resistance against impact forces, accesses mechanical performance of the material against crack propagation (Es-Said et al., 2000) .Roberson *et al.* concluded that there was an insignificant difference in the part printed to that of milled in case of V -Shaped notch (Roberson et al., 2015).

Patterson *et al.* evaluated the impact strengths of various thermoplastic materials commonly used in different applications. The specimens were 3D printed, with ABS, PLA, and HIPS demonstrating impact strengths of 14.6 KJ/$m^2$, 15.8 KJ/ $m^2$, and 14.8 KJ/ $m^2$ respectively. Nylon exhibited significantly higher impact strength at 31.9 KJ/$m^2$, while PETG showed a notable impact strength of 22.6.2 KJ/ $m^2$. These findings provide valuable insights into material selection and design considerations for diverse engineering and manufacturing applications (Patterson et al., 2021).

### 2.2.1. Effect on Discontinuous and Continuous Fiber

The effect of fiber type (chopped and continuous) may affect the impact strength of the 3D printed composites. Delamination, fiber pullout and efficient load transfer on impact loading can be influenced by the type of fiber used in composite.

Lia *et al.* reported increase in impact strength of 24.8 KJ/$m^2$ in additively manufactured composite by impregnating 10% of chopped carbon fiber reinforced in polyamide matrix (Liao et al., 2018) .3D printed nylon composite impregnated with 37% of continuous glass fiber reported 224% more impact strength(Kabir et al., 2021).An increase in impact strength for 3D printed composite with an increase in reinforcement was observed. 3D printed composite reinforced with glass fiber showed maximum impact strength (280.9 MPa) because of matrix and fiber bonding as shown in SEM image (Fig 2.5). SEM images showed poor wettability between nylon and Kevlar as

well as nylon and carbon fiber (184.7 KJ/$m^2$) and least for carbon fiber (82.26 KJ/$m^2$)(Caminero, Chacón, García-Moreno, & Rodríguez, 2018).

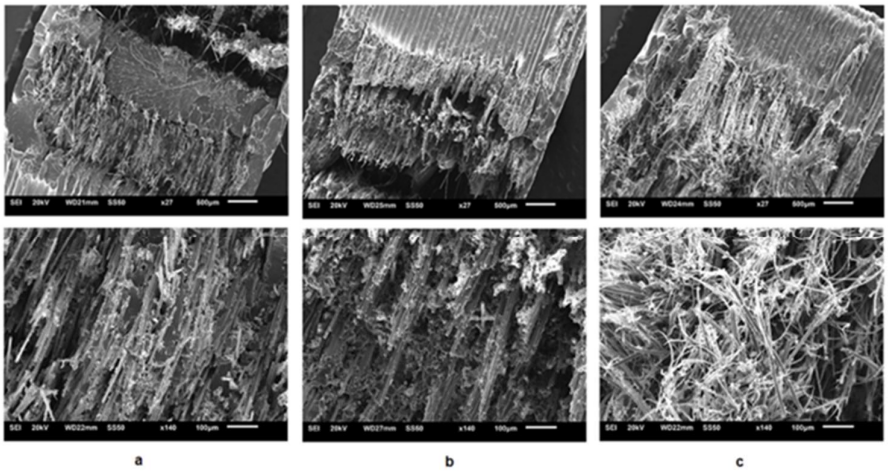


Figure 2.7: Schematic diagram showing comparing wettability between nylon and Kevlar (Caminero et al., 2016)

### 2.2.2. Effect of Fiber Orientation

The impact strength of 3D printed composite specimens is significantly influenced by fiber orientation. The orientation of fibers within the composite material affects how the applied force is distributed and absorbed during impact events. Therefore, careful consideration of fiber orientation during the 3D printing process is crucial for optimizing the impact strength and overall mechanical performance of composite specimens.

Ziemian *et al.* reported that mechanical properties of FFF printed part are dependent on raster direction and concluded that specimen exhibit superior impact resistance property with 0° raster orientation (printing direction in the direction of bed Anisotropy arises with the alignment of fiber with the direction of flow commonly known as direction of printing of extrusion process). Weak interlayer bonding of the material is another major reason for anisotropy(Ziemian et al., 2012).

Hetrick *et al.* reported that Kevlar fiber are anisotropic and energy absorbed by Kevlar reinforced composite to be around 31 J by varying angle with volume fraction of 30% and fiber when loaded in the transverse direction yielded least strength of 21 J (Hetrick et al., 2021)Prajapati *et al.* reported that impact strength decreases with increase in

raster angle. Since the fiber overall length decreased, short fiber length are the reason for decreased impact strength

They reported brittle fracture in fiber reinforced impact specimen. Increase in concentric pattern provided more impact strength properties as compared to isotropic pattern (Prajapati et al., 2020).

### 2.2.3. Effect of Build Orientation and Fiber volume Fraction

Fiber build orientation and content plays a significant role in impact performance of additively manufactured composite. Increase in layer thickness decrease the manufacturing cost and increase the mechanical strength. The reason is reduction in void. In case of flat sample as shown in fig 2.7 impact loading is parallel and in case of on edge sample the nature of loading is perpendicular. In the former case layer to layer bonding performance enhanced the impact strength of the surface material. However, in case of on edge sample it's the individual fiber which took the maximum load and fiber breakage was predominant. Flat sample was observed to have ductile fracture and on edge sample was observed to have brittle type fracture. Figure 2.8 shows the possible build orientation for fabrication of impact testing specimens.

.

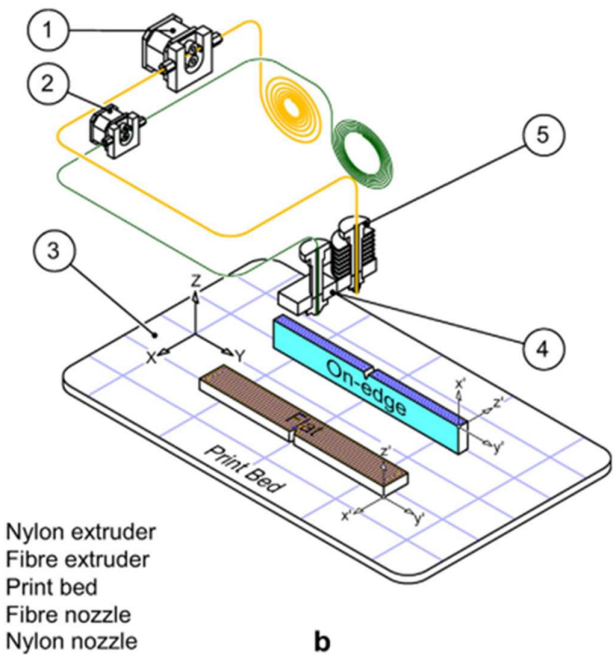


Figure 2.8 Schematic diagram showing details of printing parameters (Caminero et al., 2016)

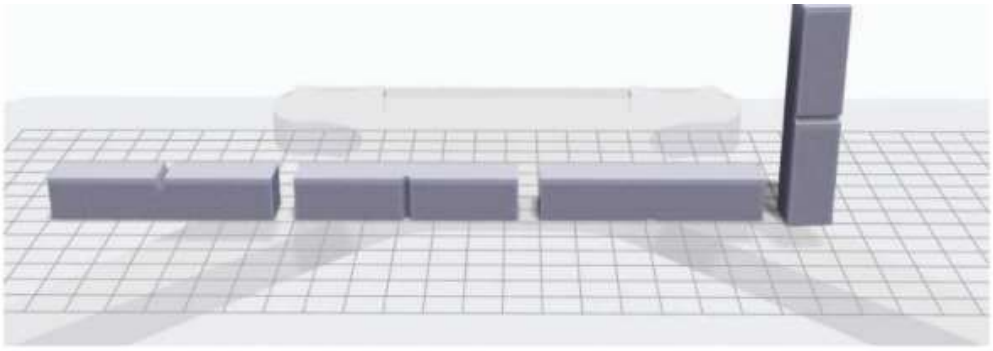

Figure 2.9 Possible build orientation for impact test (Prajapati et al., 2020)

Prajapati et al. reported consolidated stacking sequence has much more impact strength carrying capacity as compared to alternate stacking sequence. More binding agent's onyx holds the reinforcement material which produces strong adhesion and synergy between the matrix and the reinforcement material Prajapati et al. reported that impact strength in case of flat sample shows more impact of 2457.25J/m with 50% volume fraction for HSHT. However experimental impact strength was found to be 905J/m in case of on edge (Prajapati et al., 2020)

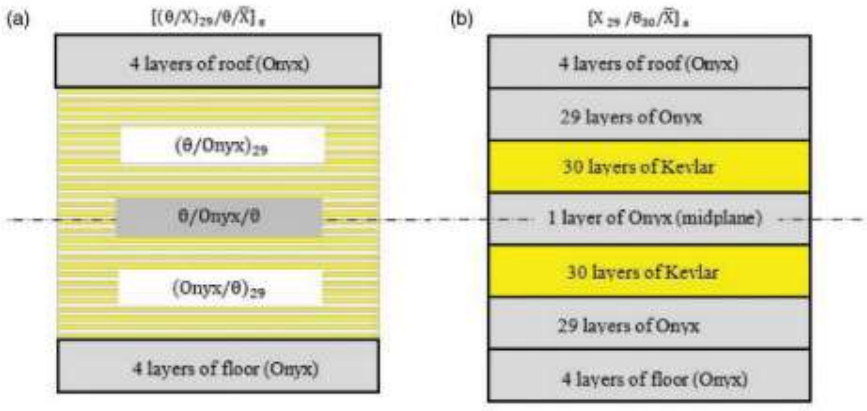


Figure 2.10 Schematic diagram showing stacking sequence in 3D printed KFRCP (Prajapati et al., 2020)

Table 2.2 Impact properties reported in the literature

| Matrix | Fibre | Volume Fraction (%) | Fibre Pattern | Impact Strength | References |
|---|---|---|---|---|---|
| Nylon | | - | | 1.8 | (Kabir et al., 2021) |
| Nylon | Glass Fiber | 35 | Isotropic 0° | 11.8 | (Kabir et al., 2021) |
| PLA | Carbon | 10 | Chopped | 24 KJ/$m^2$ | (Liao et al., 2018) |
| Nylon | HSHT | - | Isotropic 0°, One edge | 3555.18 KJ/$m^2$ | (Chacón et al., 2017) |
| Nylon | Carbon | 25 % | Isotropic 0°, flat surface | 12.6 KJ/$m^2$ | (Chacón et al., 2017) |
| Nylon | Carbon | 53% | Isotropic 0°, flat surface | 1045.1 KJ/$m^2$ | (Caminero et al., 2016) |
| Nylon | HSHT | 50% | Isotropic 0° $+45^{\circ}, -45^{\circ}$,Flat | 2455 KJ/$m^2$ | (Prajapati et al., 2020) |

**2.3 Advancements in Additive Manufacturing Technologies.**

Additive manufacturing (AM) technologies have advanced significantly, enhancing the capacity to fabricate complex, high-performance components for sectors such as aerospace, healthcare, and automotive. Recent developments include multi-material printing, which has become increasingly precise, enabling the integration of diverse

materials within a single print. This allows for the production of components with tailored mechanical, electrical, or thermal properties. Techniques such as multi-jet fusion (MJF) and direct ink writing have been optimized to facilitate smooth material transitions, enhancing functionality by targeting specific properties like electrical conductivity or impact resistance. (Karimi et al., 2024) as with FDM advances, continuous fiber-reinforced 3D printing now enables stronger, lightweight components by embedding materials like carbon or glass fibers directly into printed parts. This is especially relevant for structural applications that demand high strength-to-weight ratios (Jamal et al., 2024).Methods such as selective laser melting (SLM) and electron beam melting (EBM) have evolved, now capable of producing intricate metal parts with enhanced mechanical properties and reducing post-processing needs. These processes also focus on reducing residual stresses and minimizing material waste, critical for aerospace and biomedical applications (Karimi et al., 2024).Advances in bio-printing are making it possible to print tissues and, eventually, organs. Techniques like extrusion-based bio printing and laser-assisted bio-printing now achieve greater cell viability and structural integrity, critical for complex biological structures .AI and Machine Learning in AM is being used to optimize printing parameters in real-time, enhancing the accuracy, speed, and reliability of the printing process. Machine learning algorithms analyze data from the manufacturing process to predict and adjust for potential defects before they occur (Kumar et al., 2022.6; Qin et al., 2022; Wang et al., 2020).4D Printing adds the dimension of time, where materials are printed to change shape or properties in response to environmental factors like temperature or humidity. This is particularly useful in applications requiring adaptable structures or self-healing materials (Qin et al., 2013)

These advancements demonstrate AM's growing role in customizable, sustainable production, where reduced waste, energy efficiency, and material versatility are leading its adoption in advanced industries.

### 2.3. Scope of Study and Research Gap Identification

This section presents the scope of the research work undertaken and includes the identification and analysis of research gaps in the field of additive manufacturing of

continuous fiber-reinforced composites. With an aim to close the critical gaps through formulated objectives, the research focuses to bring valuable insights and advances to the sector, improving understanding and supporting innovation.

### 2.3.1. Scope of Study

The literature reveals that there is a scarcity of published work and available knowledge on the utilization of Kevlar fiber for reinforcing polymers. Moreover, fabrication of these composites via extrusion-based 3D printing further requires exhaustive investigations. The process parameters have a significant effect on the mechanical performance of these composites. Therefore, comprehensive research work needs to be carried in this direction.

The scope of the study includes a multi-faceted study of various aspects related to the fabrication and performance evaluation of Kevlar Fiber Reinforced Polymer Composites the application of fused deposition modeling. The aim of the research is initially to investigate the performance properties of Kevlar fiber-reinforced composites and to investigate how different fiber orientations influence the mechanical properties of the composites. In addition, the study will investigate the effect of changing the volume fraction of the reinforcement (Kevlar fiber) on the mechanical behavior of the composites. A comparative analysis of composites produced by additive manufacturing (FDM) and traditional manufacturing methods is conducted to evaluate differences in mechanical properties. In addition, study investigates the anisotropic properties of Kevlar fiber composites, a critical issue in FDM parts. The aim of this comprehensive study is to provide valuable insights into the fabrication and mechanical behavior of FDM printed Kevlar fiber-reinforced polymer composites, thereby bringing significant advances in the field of additive manufacturing and composites.

### 2.3.2. Research Gap

Based on the above-mentioned literature review, the following gaps have been identified:

i. Limited exploration of FDM-printed continuous fiber composites in existing research.

ii. Scarcity of studies on the effect of incorporating Kevlar fiber in FDM printed composites.
iii. Lack of investigation into the effects of fiber direction and volume percentage on the mechanical behavior of FDM-printed continuous fiber structures.
iv. Anisotropic behavior of FDM-printed parts requires further in-depth studies.
v. Vital need for expanded research to enhance understanding of additive manufacturing of continuous fiber composite.

## 2.4. Research Objectives

The research was planned with the following objectives based on the identified gaps in the literature:

- To study the performance of Kevlar FRCP using Fused deposition modeling with different fiber orientation.
- To investigate the effect of changing volume percentage of both the reinforcement as well as matrix on the composite.
- To compare the mechanical properties of Kevlar fiber when manufactured by additive manufacturing to that of conventional method of manufacturing.
- To investigate the anisotropic properties of Kevlar fiber.

## CHAPTER 3

## MATERIALS AND METHODOLOGY

The chapter covers the information related to 3D printer machine, materials and methodology used in the research work.

### 3.1. Materials and Manufacturing Process

The 3D printer used in this study is the Mark Two from Markforged. The printer has two extrusion functions, one extruder is dedicated to thermoplastic polymer/composite deposition and the other is dedicated to fiber deposition (Figure 3.1). The thermoplastic polymer examined in this study is Onyx, a Markforged-patented material made from nylon and shredded carbon fiber. The fiber reinforcement used in the composite manufacturing process is Kevlar fiber, also a proprietary material from Markforged. The manufacturing process involves the deposition of Onyx polymer and Kevlar fiber's using the Mark Two printer's dual extrusion capabilities.

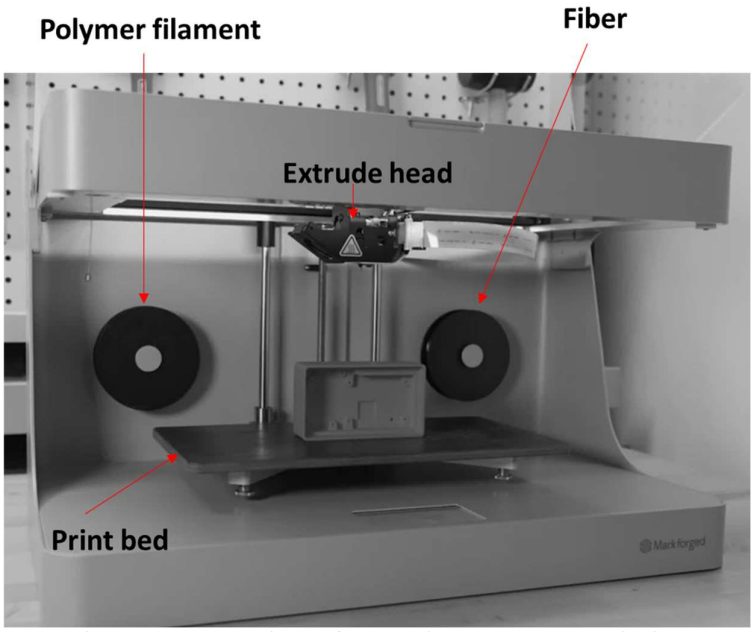


Figure 3.1 3D printer for continuous FRCP printing

The material properties of the onyx and Kevlar fiber as per the datasheet provided by the manufacturer is illustrated in table 3.1 and 3.2. Respectively.

Table 3.1. Material properties of onyx

| S.No. | Properties | Values |
|---|---|---|
| 1 | Tensile Modulus (GPa) | 2.4 |
| 2 | Tensile Stress at Yield (MPa) | 40 |
| 3 | Tensile Stress at Break (MPa) | 37 |
| 4 | Tensile Strain at Break (%) | 25 |
| 5 | Flexural Strength (MPa) | 71 |
| 6 | Flexural Modulus (GPa) | 3.0 |
| 7 | Heat Deflection Temp (°C) | 145 |
| 8 | Izod Impact - notched (J/m) | 330 |
| 9 | Density ($g/cm^3$) | 1.2 |

Table 3.2. Material properties of Kevlar

| S.No. | Properties | Values |
|---|---|---|
| 1 | Tensile Strength (MPa) | 610 |
| 2 | Tensile Modulus (GPa) | 27 |
| 3 | Tensile Strain at Break (%) | 2.7 |
| 4 | Flexural Strength (MPa) | 240 |
| 5 | Flexural Modulus (GPa) | 26 |
| 6 | Flexural Strain at Break (%) | 2.1 |
| 7 | Compressive Strength (MPa) | 130 |
| 8 | Compressive Modulus (GPa) | 25 |
| 9 | Compressive Strain at Break (%) | 1.5 |
| 10 | Heat Deflection Temp (°C) | 105 |
| 11 | Izod Impact - notched (J/m) | 2000 |
| 12 | Density ($g/cm^3$) | 1.2 |

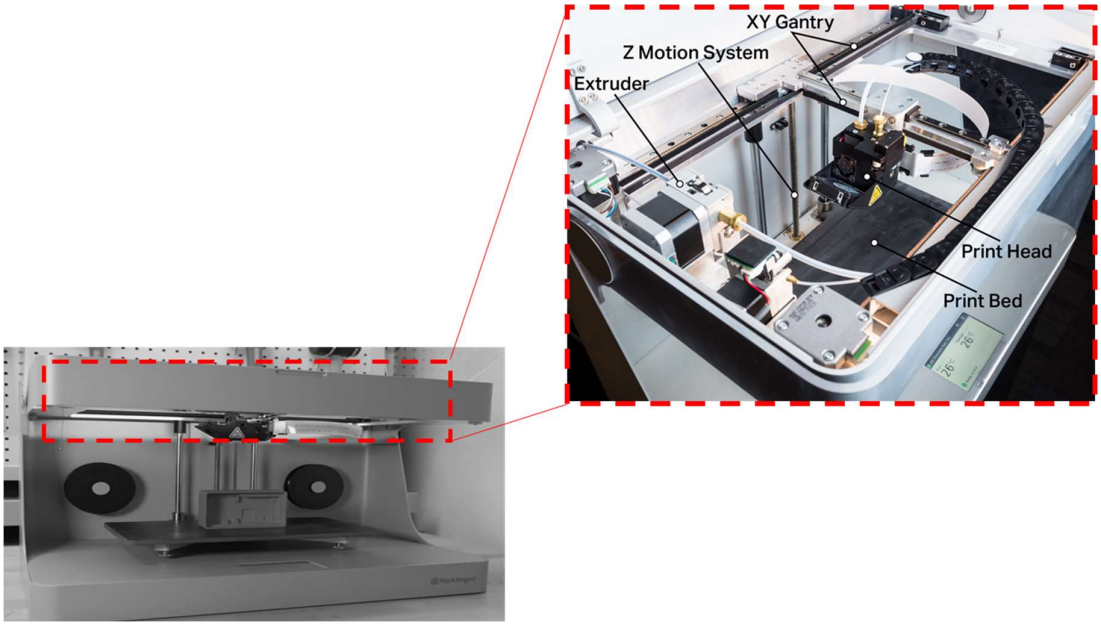


Figure 3.2 Details of Continuous fiber 3D printer (Make: Markforged, Mark Two)

The 3D printer used in the study consist of three main electromechanical systems that greatly affect the quality of prints. First the print head and the extrusion system. This part heats the thermoplastic material and pushes it through a nozzle to create the desired object. Then there is the print bed and the Z-motion system. The print head places the material on the print bed while the Z-motion system moves the bed at precise intervals, creating layers of the printed object. Finally, the XY gantry movement system controls the lateral movement of the print head along the X and Y axes, essentially making the shape of each layer. The layers are deposited by each nozzle consisting of polymer and fiber. The layers can be deposited as per the desired structure of the composite part. The position and numbers of the polymer as well as fiber layers can be decided and tool path is created in Eiger cloud-based software. Figure 3.3 illustrates the deposition strategy for continuous FRCP fabrication by 3D printing. The polymer matrix layers (as per the required volume fraction of fiber) are deposited and then fiber layers are deposited which are sandwiched between polymer layers.

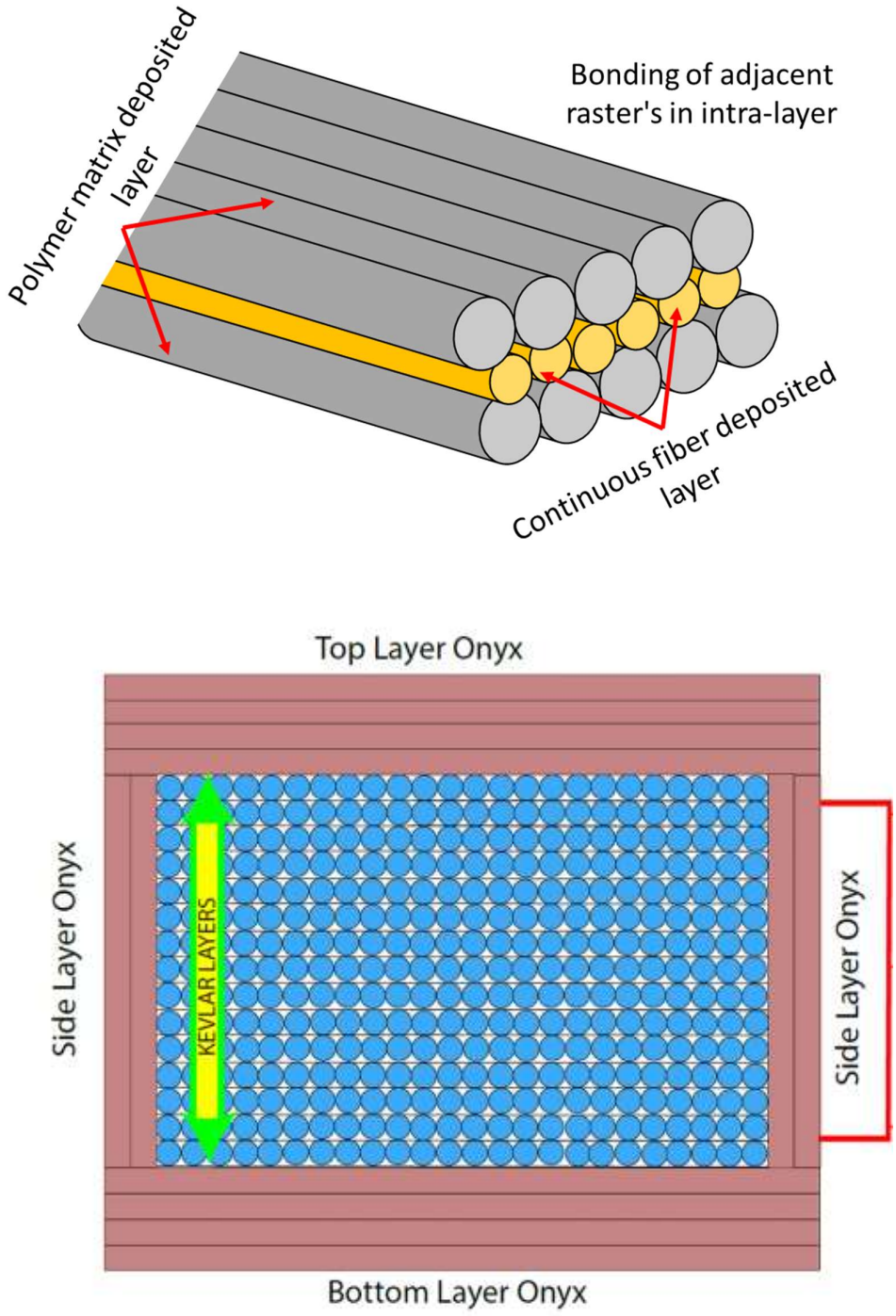


Figure 3.3 Fiber deposition strategy (number of layers varies as per volume fraction) for composite fabrication by 3D printing: top (fibers sandwiched between polymer matrix), below (cross-sectional view)

### 3.2. Specimen Fabrication

The specimens were fabricated using Onyx filament, a proprietary blend from Markforged, with a nominal diameter of 1.75 mm. A continuous Kevlar fiber with a nominal diameter of 0.35 mm was used for reinforcement. Both filament types were stored in a modified dry box, specifically a Pelican 1430, to maintain a moisture-tight environment and prevent filament deterioration. A Mark Two 3D printer (Make: Markforged) was used to produce 3D printed objects. Table 3.3 shows the fixed printing parameters. The extruder temperature was set at 270 °C and the infill percentage was set be 100% to ensure solid part. The layer thick ness was set be 0.1 mm in order to achieve better resolution and finish of specimen. The printing process for fabrication of specimens utilizing dual nozzle is illustrated in figure 3.4.

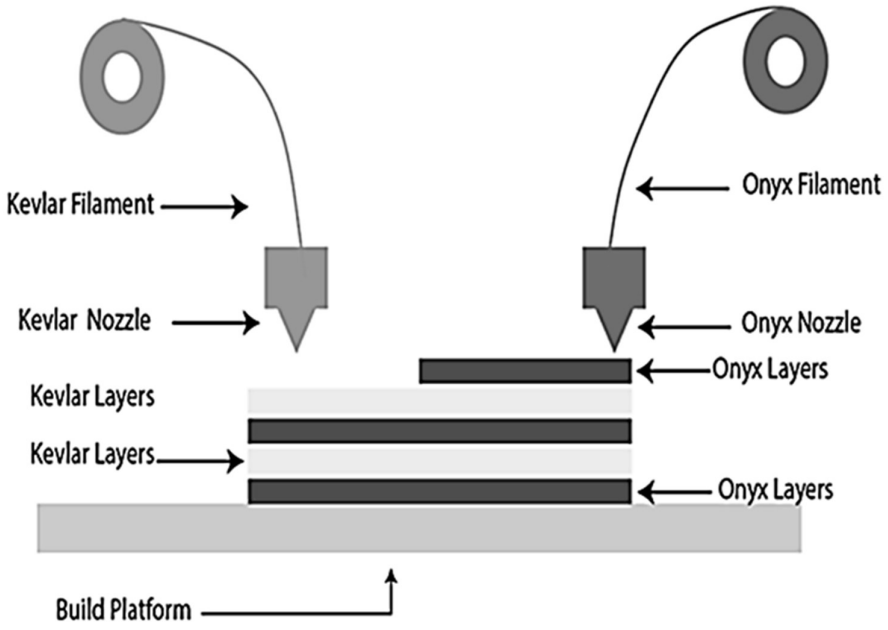


Figure 3.4 Schematic diagram of dual nozzle continuous fiber reinforced polymer composite 3D printing

Table 3.3 Fixed parameters for printing of specimens

| Parameters | Parametric value |
|---|---|
| **Bed Size** | 320 mm × 132 mm × 154 mm |
| **Nozzle temperature (℃)** | 270 |
| **Fill type** | Solid |
| **Fill density** | 100% |
| **Layer thickness** | 0.1 mm |

The capability of dual extrusion is utilized to deposit polymer layers and the Kevlar fiber. The pattern of deposition of onyx and Kevlar can be selected as per the reinforcing strategies adopted. In the present work the Kevlar fibers are sandwiched between onyx layers. The number of fiber layers deposited is varied as per the volume fraction selected for investigation. Figure 3.5 shows the fiber layering pattern used for specimen fabrications. The steps involved in fabrication of specimens involves creation of CAD model of the specimens to be fabricated which then converted into .stl file format. This file is taken to the slicing software for data preparation for the 3D printer. The orientation, infill density, infill pattern and layer height are decided and selected at this stage. The model is sliced and tool path is generated for both the nozzles for deposition of onyx and Kevlar fiber. Figure 3.6 illustrates the procedure.

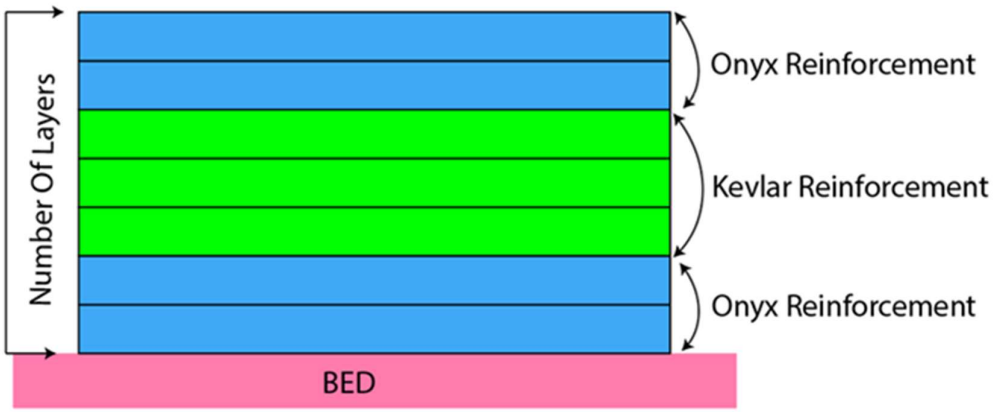


Figure 3.5 Schematic diagram showing fibre layering pattern

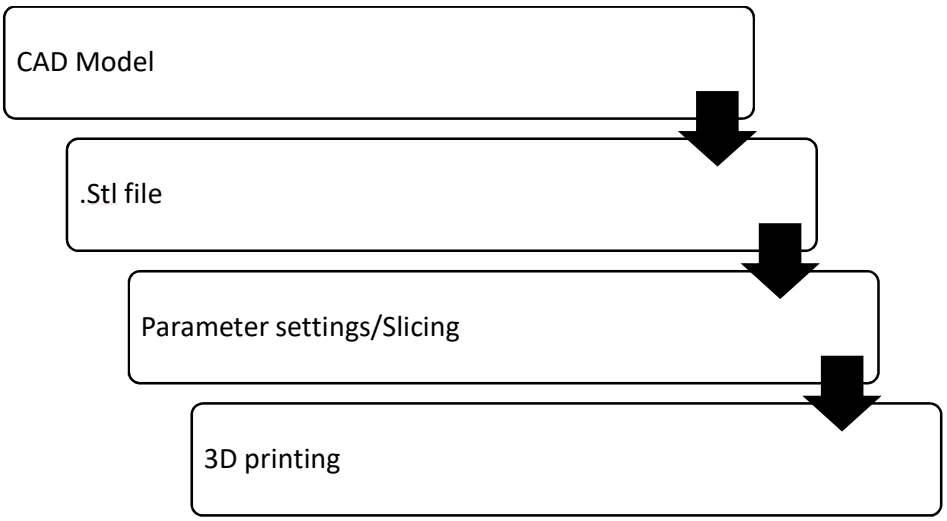


Figure 3.6 3D printing process flow for fabrication of specimens

### 3.2.1. Build Direction

The build direction of the specimens fabricated by 3D printing process plays an important role in determining the part quality and mechanical properties. Moreover, when fabricating parts with deposition of continuous fibers, the importance of build directions is further increased. The literature suggests that deposition of raster's along the loading direction can yield better performance of the parts. Therefore, the build orientation for fabrication of tensile and impact specimens was selected flat in nature as depicted by figure 3.7.

### 3.2.2. Fiber Orientation

For fabrication of parts using continuous fiber by 3D printing requires proper selection of fiber orientation. This will ensure the load bearing capacity of the parts fabricated. In order to investigate the effect of the Kevlar fiber orientation on tensile and impact properties of the 3D printed parts various orientations were considered. The investigations were carried out on linear fiber pattern/orientation, in which 0° and 90° orientations were selected. Moreover, a concentric pattern of fibers was also investigated. The orientation selected was based on the literature and available options on Eiger software. Figure 3.8 illustrates the fiber orientation considered for the investigations.

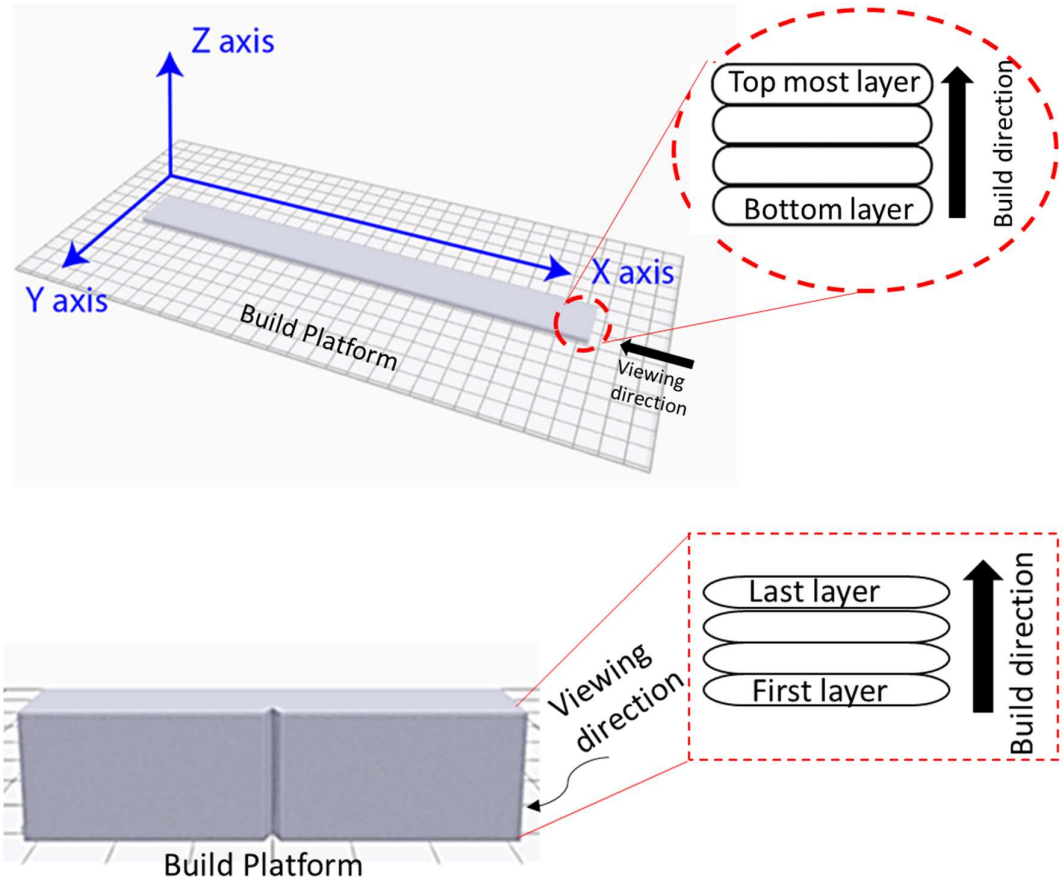


Figure 3.7 Build direction for fabrication of tensile and impact specimens

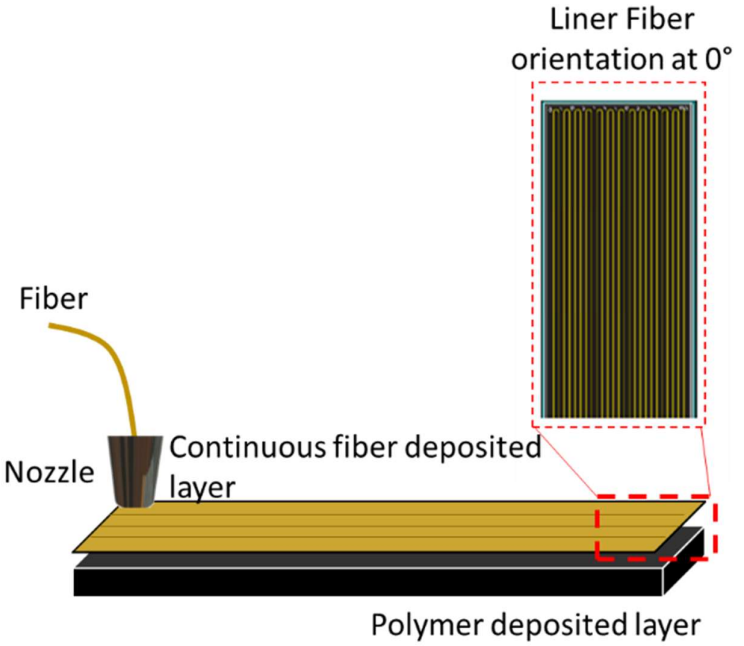
Liner Fiber
orientation at 0°
Fiber
Nozzle
Continuous fiber deposited
layer
Polymer deposited layer

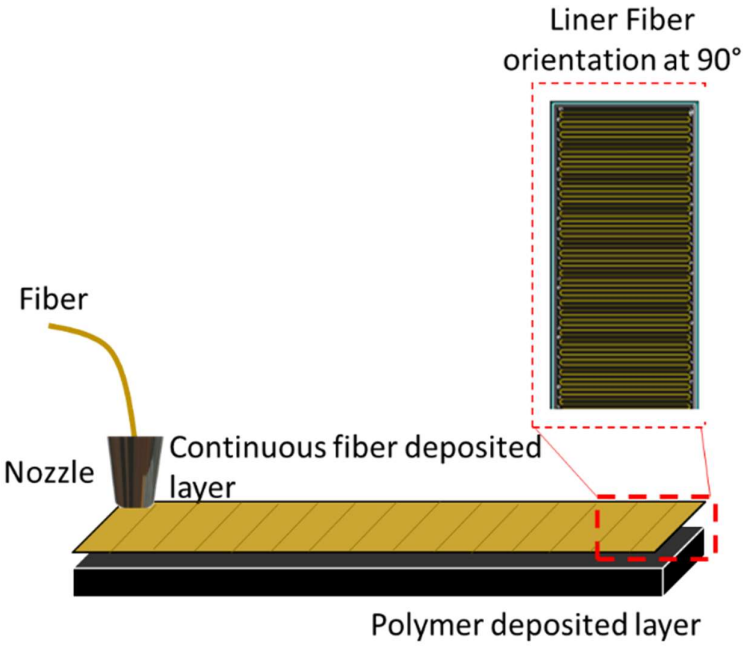
Liner Fiber
orientation at 90°
Fiber
Nozzle
Continuous fiber deposited
layer
Polymer deposited layer

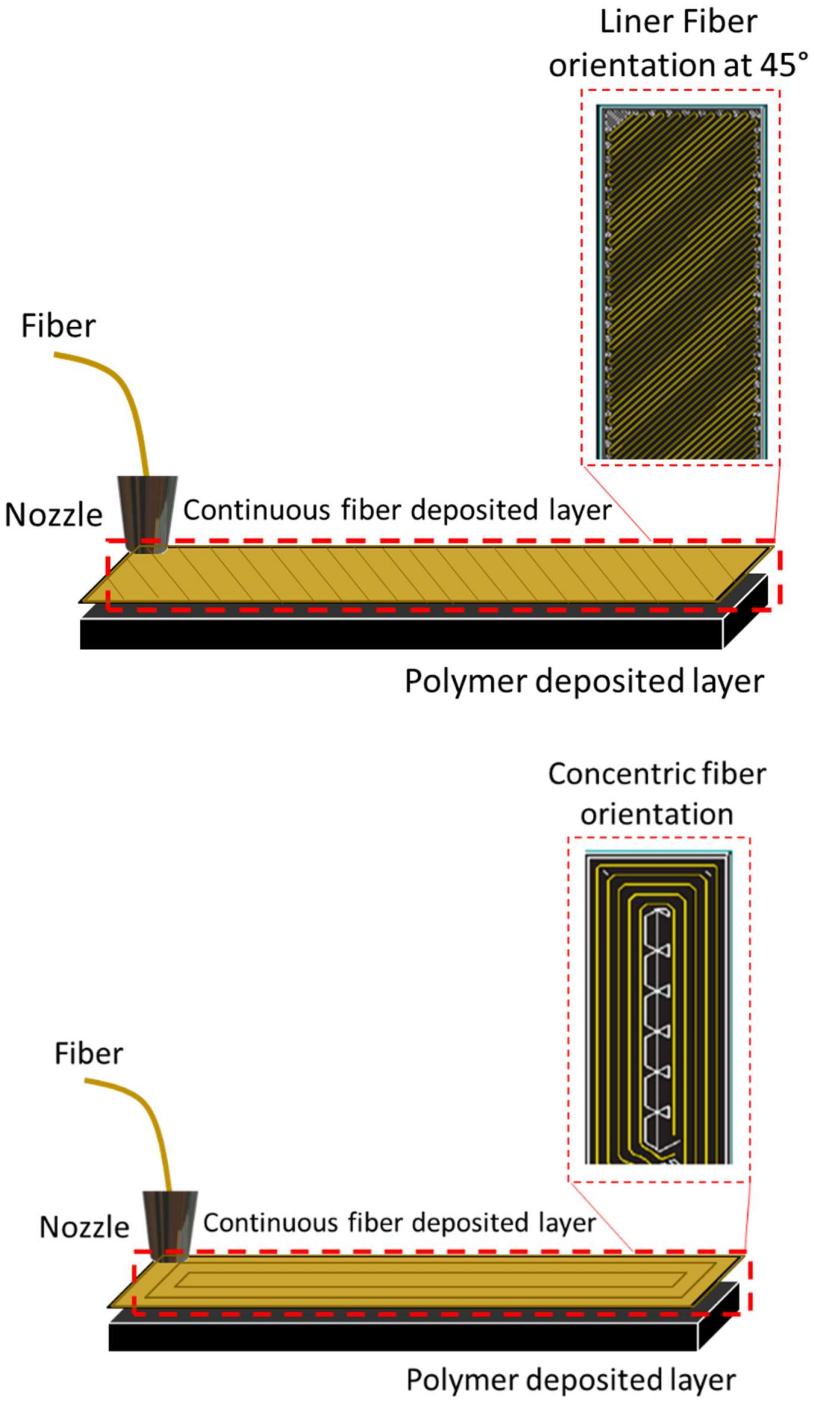


Figure 3.8 Continuous fiber orientations Process

### 3.2.3. Stacking Sequence of 3D Printed Specimen

The stacking sequence of a 3D printed specimen refers to the specific order and orientation of layers that make up the final printed object. This sequence is crucial in determining the mechanical properties, strength, and aesthetic appearance of the printed part. Key Factors in Stacking Sequence involved

- Layer Orientation: The direction in which each layer is printed can significantly affect the properties of the part. Common orientations include horizontal, vertical, or at an angle (e.g., 0°, 45°, or 90°).
- Layer Thickness: The thickness of each layer can vary based on the printing settings. Thicker layers may result in faster prints but can affect surface finish and resolution. The thickness on 0.1mm was used since the nozzle diameter for reinforcement as 0.1 mm .s
- Fill Pattern: The internal structure (infill) of the layers can be modified. Common fill patterns include honeycomb, grid, and line, affecting strength and weight. In this present work solid infill pattern was used.

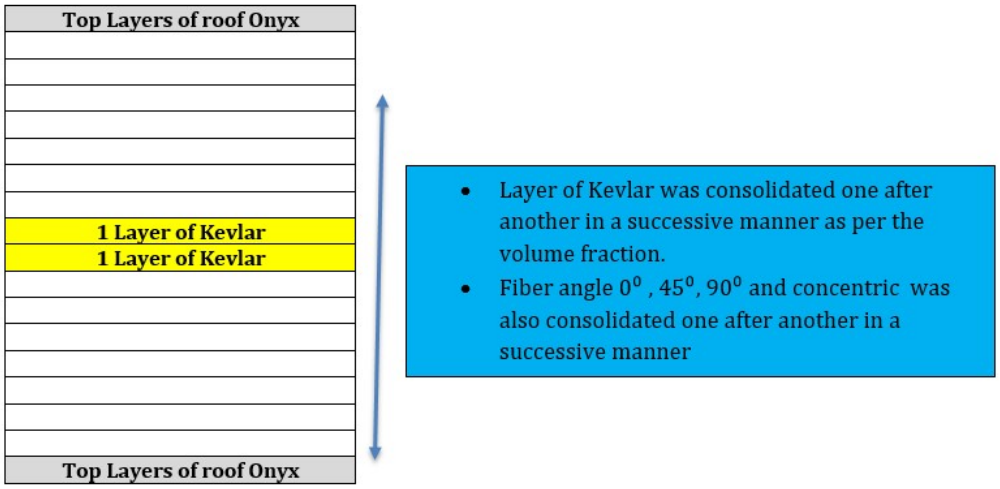


Figure 3.9 Schematic showing consolidated stacking sequence in case of 3D printed specimen

### 3.2.4. Volume Fraction of 3D printed specimen

The fiber volume fraction in this study is defined by the slicing software, Eiger, as the ratio of the reinforcement fiber volume to the total volume of the printed specimen. For example for 2 layers of kevlar the volume fraction was obtained by the ratio of palstic

volume by the total volume of plastic and reinforcement .This calculated fiber volume fraction does not include contributions from the chopped carbon fibers within the Onyx matrix, the binder material within the fiber bundles, or any porosity present both within and between layers of fiber and Onyx. For consistency, the fiber volume fraction was held constant across all configurations in this study.

A set of control specimens was fabricated using pure Onyx, without the addition of continuous fiber reinforcement, to establish a baseline for comparison with the reinforced specimens. These control specimens were printed with identical parameters, notch placement, and dimensions as the reinforced specimens to ensure reliable comparative analysis (Hetrick, Sanei, Ashour, et al., 2021).

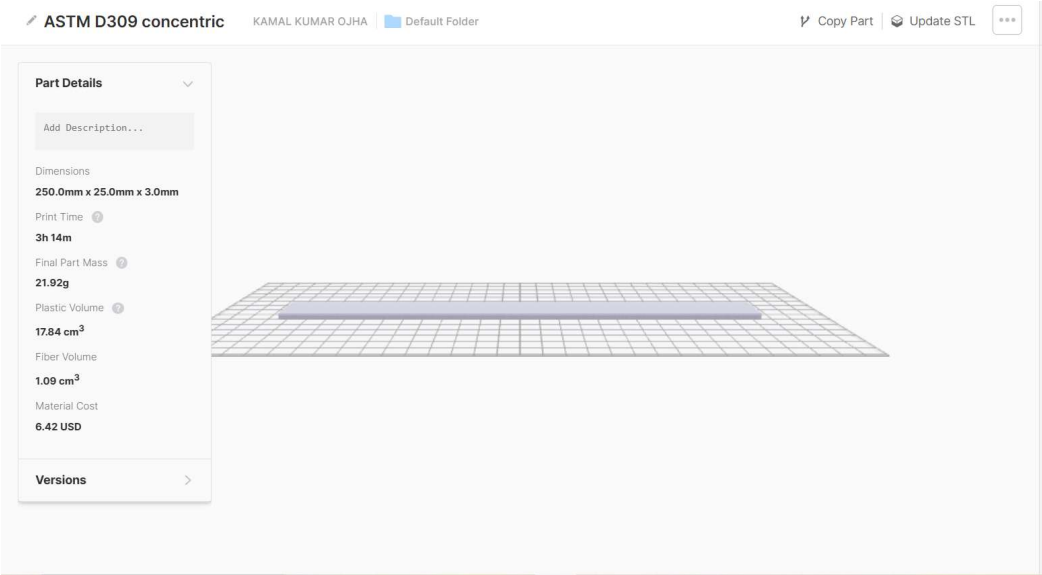


Figure 3.10 Schematic showing procedure to calculate volume fraction of the 3D printed specimen.

### 3.3. Testing

The specimens were fabricated to perform tensile and impact testing of the composites. The tensile test has its ability to yield fundamental mechanical properties, including tensile strength, yield strength, and Young's modulus. Unlike specialized tests, which measure material behavior under specific stresses, tensile testing generates a complete stress-strain curve, providing a comprehensive view of a material's elastic and plastic behavior, such as ductility and brittleness. Additionally, tensile testing follows

standardized procedures (e.g., ASTM, ISO), ensuring consistent, reproducible results. Its simplicity in setup and interpretation also makes it efficient compared to shear and torsion tests, which often require complex setups, or drop tests, where results are highly dependent on variables like impact angle and surface properties. Tensile properties are central to engineering calculations, giving tensile tests broad applicability in structural and material design.

Impact testing is critical for Kevlar because it provides insights into how this high-strength material behaves under sudden, intense loads, simulating real-world conditions where Kevlar is often used, such as in ballistic protection, body armor, and high-impact sports gear. Kevlar's unique molecular structure allows it to absorb and dissipate large amounts of energy, making it excellent at resisting impacts, but its performance can vary under different impact speeds and angles.

The ASTM standards were followed to design the specimens and to perform the testing's on calibrated machines. ASTM D30339 standard was followed for the tensile test. The geometry and the dimensions of the specimen is illustrated in (figure 3.7.) The impact tests were conducted as per ASTM D256-10. Figure 3.9 shows the dimensions and geometry of the impact specimens fabricated. The parallelepiped tensile specimen was manufactured having dimension 250 mm × 25mm × 3mm, as shown in (figure 3.9.) Three samples made up for each sample set for a particular set of process parameters were made. Average tensile strength was considered. Thirty layers, each 0.1 mm thick, were superimposed to give the specimen its thickness of 3 mm. The effect of increasing reinforcement on tensile properties was evaluated by changing fiber volume fraction. An MTSE45.105 machine with a 50 KN rated force capacity was used for unidirectional tensile testing. The lower end was secured with a grip that extended 56 mm. As seen in figure 3.9, the lengths for the fixed end and load grasping were both adjusted to 56 mm. The sample was tested to the point of failure. The entire testing process took place at ambient temperature.

To investigate the impact characteristics of the composites sample, an Izod impact test was performed. The specimen is set up as depicted in the (figure 3.9.) The specimen is held vertically like a cantilever beam and fixed at one end. A fixed-mass pendulum is hoisted to a known height and allowed to descend from that height in a circular motion. The impact sample's notch direction is the inverse of the hammer direction (figure 3.10).

The impact strength characteristics of composites were measured using BOT 633 D with an energy of 10 J. The energy needed to break the specimens is measured using pendulum impact testing. By breaking the test specimen with standardized type pendulums and hammers, the impact test is performed to evaluate the resilience of composite materials. It is the total amount of energy needed to cause a specimen to fracture, spread a fracture, bend, produce vibration, and imprint. Because the notch is a zone of concentrated stress, it increases the risk of fracture from brittle rather than ductile materials. Complete break, hinge break, partial break, and non-break are the several types of specimen failure. The breakage of a notch occurs when it is reversed or faces the opposite direction as the weight. The energy per unit area absorbed to break the sample is measured by all test techniques. Only entire breaks are used in this work. The difference in height provides the necessary energy to fracture the specimen. Total fracturing energy is supplied by $E_t$ which is the total energy ($kJ/m^2$) consumed where m is the mass of the anvil, $h_i$ is the initial height and $h_f$ is the final height.

$$E_t = mg(h_i - h_f) \quad 3.1$$

The absorbed impact energy $E_i$ is defined as follows where w is width and t is thickness of the specimen:

$$E_i = \frac{E_t}{wt} \quad 3.2$$

Figure 3.10 illustrates the Schematic diagram holding pattern and direction of loading for impact specimen. Table 3.4 shows the details of the impact testing.

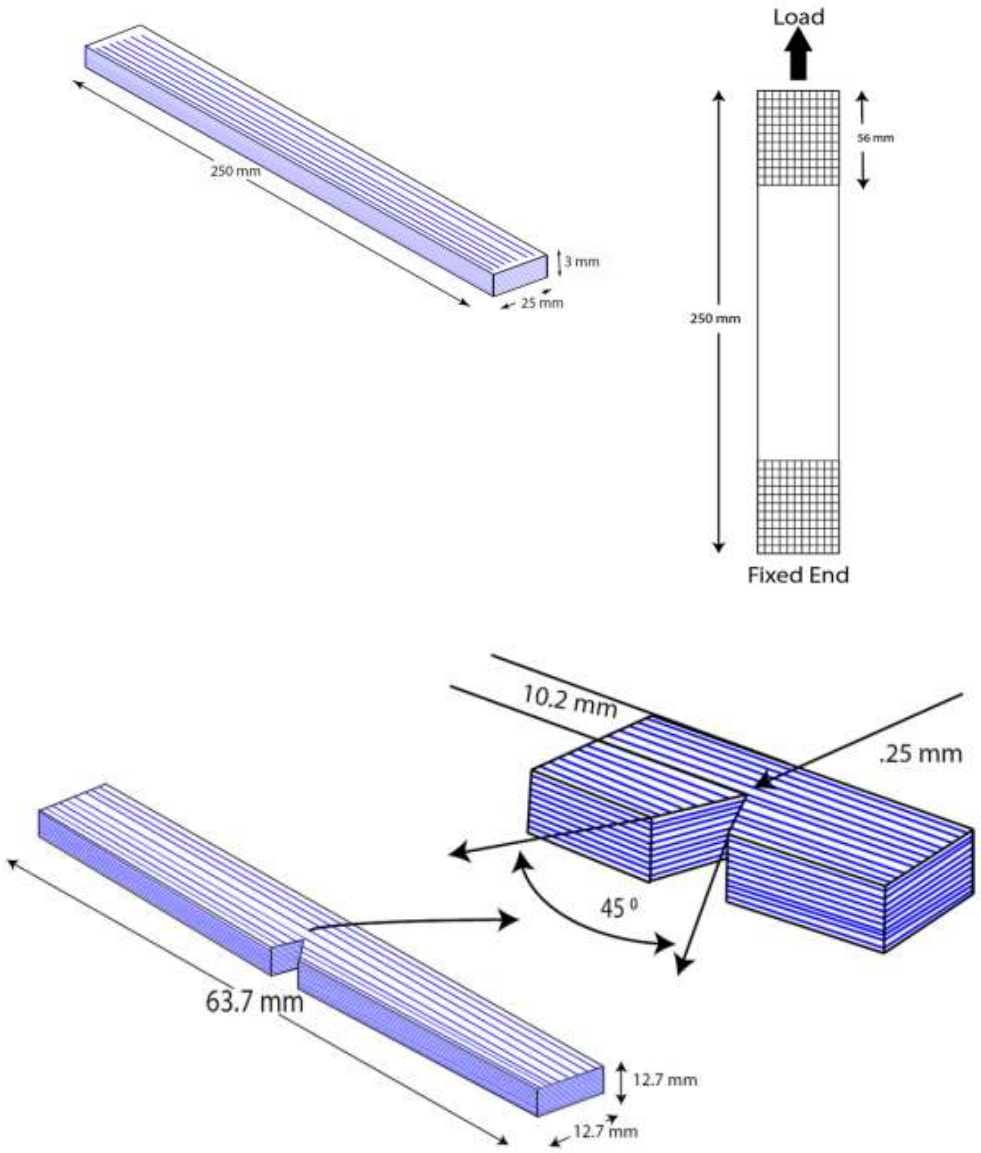


Figure 3.11 Tensile and Impact testing specimen dimensions and geometry as per ASTM standards

Table 3.4 Impact test machine specification for Izod impact test

| Description | Values |
|---|---|
| Hammer Weight load | 4260 gm |
| Hammer length | 340 mm |
| Falling height | 605 mm |
| Hammer weight | 1811 gm |
| Hammer weight with load | 3309 gm |

In any measurement process, it is essential to evaluate and report the associated uncertainty. This practice ensures that the reported results are accompanied by quantified limits within which they can be assumed to lie. Such a statement of uncertainty may be required by customers to assess the reliability of the results or by the test laboratory itself to identify aspects of the test procedure that significantly influence the outcomes, allowing for more precise control.Its purpose is to standardize and simplify the evaluation of uncertainties. The aim is to provide a series of documents in a consistent format, ensuring they are comprehensible and readily accessible to customers, testing laboratories, and accreditation authorities.

Table 3.5 Uncertainty in Dimension of 3D printed Tensile Specimen

| **Fiber Layer** | **Vf** | **X-dimension** | | | **Mean** | **Dev.** | **Y-dimension** | | | **Mean** | **Dev.** | **Z-dimension** | | | **Mean** | **Dev** |
|---|---|---|---|---|---|---|---|---|---|---|---|---|---|---|---|---|
| | | **X1** | **X2** | **X3** | | | **Y1** | **Y2** | **Y3** | | | **Z1** | **Z2** | **Z3** | | |
| 0 | 0 | 252.6 | 251.5 | 249.7 | 251.27 | 1.46 | 25.3 | 25.09 | 24.98 | 25.12 | 0.16 | 3.09 | 2.87 | 3.1 | 3.02 | 0.13 |
| 2 | 5.8 | 250.1 | 250.2 | 248.7 | 249.67 | 0.84 | 25.82 | 25.11 | 25.21 | 25.38 | 0.38 | 2.99 | 3.47 | 3.68 | 3.38 | 0.35 |
| 4 | 10 | 250.8 | 251.7 | 253.1 | 251.87 | 1.16 | 25.13 | 25.12 | 25.34 | 25.20 | 0.12 | 3.41 | 3.05 | 3.37 | 3.28 | 0.20 |
| 6 | 14.2 | 252.4 | 252.6 | 249.8 | 251.60 | 1.56 | 22.6.52 | 25.66 | 25.76 | 25.71 | 0.07 | 3.21 | 3.22 | 3.47 | 3.30 | 0.15 |
| 8 | 18.4 | 249.1 | 252.1 | 250.1 | 250.43 | 1.53 | 25.43 | 25.83 | 22.6.92 | 25.63 | 0.28 | 2.61 | 3.16 | 3.08 | 2.95 | 0.30 |
| 10 | 22.6 | 251.4 | 253.6 | 252.4 | 252.47 | 1.10 | 24.93 | 25.01 | 25.03 | 24.99 | 0.05 | 3.14 | 2.77 | 3.31 | 3.07 | 0.28 |
| 12 | 26.8 | 252.9 | 249.9 | 250.7 | 251.17 | 1.55 | 22.6.11 | 25.12 | 25.2 | 25.16 | 0.06 | 2.8 | 3.42 | 2.5 | 2.91 | 0.47 |
| 14 | 31 | 253.6 | 252.3 | 252.3 | 252.73 | 0.75 | 25.48 | 25.43 | 24.99 | 25.30 | 0.27 | 3.02 | 3.5 | 2.86 | 3.13 | 0.33 |
| 16 | 35.2 | 252.1 | 252.3 | 248.5 | 250.97 | 2.14 | 24.7 | 24.87 | 25.16 | 24.91 | 0.23 | 3.41 | 3.27 | 3.36 | 3.35 | 0.07 |
| 18 | 39.4 | 248.5 | 249.9 | 249.8 | 249.40 | 0.78 | 25.1 | 25.22.6 | 24.78 | 24.94 | 0.23 | 3.18 | 3.18 | 2.73 | 3.03 | 0.26 |
| 20 | 43.6 | 250.2 | 253.3 | 250.3 | 251.27 | 1.76 | 25.48 | 25.43 | 25.78 | 25.56 | 0.19 | 2.95 | 2.88 | 3.47 | 3.10 | 0.32 |
| **Fiber Orientation** | **Vf** | **X-dimension** | | | **Mean** | **Dev.** | **Y-dimension** | | | **Mean** | **Dev.** | **Z-dimension** | | | **Mean** | **Dev** |
| | | **X1** | **X2** | **X3** | | | **Y1** | **Y2** | **Y3** | | | **Z1** | **Z2** | **Z3** | | |
| 45 | 22.6 | 249.601 | 249.86 | 250.13 | 249.86 | 0.26 | 26.33 | 24.83 | 24.82 | 25.327 | 0.87 | 2.83 | 3.4 | 3.22.6 | 3.12 | 0.40 |
| 90 | 22.6 | 248.9 | 252.6 | 250.3 | 250.60 | 1.87 | 25.43 | 24.53 | 24.72 | 24.893 | 0.47 | 3.22.6 | 3.83 | 3.13 | 3.48 | 0.49 |
| Conc | 22.6 | 253.3 | 250 | 251.7 | 251.67 | 1.65 | 25.13 | 24.78 | 25.353 | 25.088 | 0.29 | 2.99 | 2.987 | 3.029 | 3.00 | 0.02 |

Table 3.6 Uncertainty in Dimension of 3D printed Impact Specimen

| | | X-dimension | | | | | Y-dimension | | | | | Z-dimension | | | | |
|---|---|---|---|---|---|---|---|---|---|---|---|---|---|---|---|---|
| **Fiber Layer** | **Vf** | **X1** | **X2** | **X3** | **Mean** | **Dev.** | **Y1** | **Y2** | **Y3** | **Mean** | **Dev.** | **Z1** | **Z2** | **Z3** | **Mean** | **Dev** |
| 0 | 0 | 63.75 | 63.65 | 64.03 | 63.81 | 0.197 | 12.63 | 12.85 | 12.78 | 12.75 | 0.11 | 12.62 | 12.65 | 12.51 | 12.59 | 0.074 |
| 10 | 5.81 | 63.92 | 64.1 | 64.18 | 64.07 | 0.133 | 12.75 | 12.72 | 12.57 | 12.68 | 0.10 | 12.78 | 12.82 | 12.76 | 12.79 | 0.031 |
| 20 | 8.09 | 63.52 | 63.71 | 64.29 | 63.84 | 0.401 | 12.89 | 12.88 | 12.69 | 12.82 | 0.11 | 12.74 | 12.71 | 12.69 | 12.71 | 0.025 |
| 30 | 16.41 | 62.78 | 63.2 | 64.39 | 63.46 | 0.835 | 12.62 | 12.73 | 12.72 | 12.69 | 0.06 | 12.89 | 12.77 | 12.54 | 12.73 | 0.178 |
| 40 | 25 | 63.96 | 62.8 | 63.56 | 63.44 | 0.589 | 12.68 | 12.89 | 12.62 | 12.73 | 0.14 | 12.72 | 12.73 | 12.82 | 12.76 | 0.055 |
| 50 | 33.81 | 64.15 | 63.91 | 62.88 | 63.65 | 0.675 | 12.79 | 12.5 | 12.84 | 12.71 | 0.18 | 12.69 | 12.57 | 12.53 | 12.60 | 0.083 |
| 60 | 42.79 | 63.82 | 63.83 | 64.09 | 63.91 | 0.153 | 12.68 | 12.82 | 12.85 | 12.78 | 0.09 | 12.78 | 12.88 | 12.65 | 12.77 | 0.115 |
| **Fiber Orientation** | **Vf** | **X1** | **X2** | **X3** | **Mean** | **Dev.** | **Y1** | **Y2** | **Y3** | **Mean** | **Dev.** | **Z1** | **Z2** | **Z3** | **Mean** | **Dev** |
| 45 | 25 | 63.87 | 64.52 | 64.39 | 64.26 | 0.344 | 12.83 | 12.68 | 12.83 | 12.78 | 0.087 | 12.59 | 12.93 | 12.46 | 12.66 | 0.24 |
| 90 | 25 | 64.45 | 64.44 | 63.94 | 64.28 | 0.292 | 12.91 | 12.57 | 12.6 | 12.69 | 0.188 | 12.51 | 12.57 | 12.65 | 12.58 | 0.07 |
| Conc | 25 | 64.45 | 64.44 | 62.94 | 63.94 | 0.869 | 12.78 | 12.76 | 12.74 | 12.76 | 0.020 | 12.92 | 12.54 | 12.67 | 12.71 | 0.19 |

# CHAPTER 4

# INVESTIGATIONS ON THE INFLUENCE OF THE KEVLAR FIBER OREINTATION ON MECHANICAL PROPERTIES OF COMPOSITES

The present chapter focuses on the investigations of Kevlar fiber orientation on mechanical properties of composites. As the literature suggests that the orientation of the deposited fibers plays an important role in determining the mechanical performance of the composites. Therefore, the central objective of the chapter is to establish a correlation between tensile and impact strength and fiber orientation or fiber pattern. The thermoplastic matrix, Onyx, is impregnated with continuous Kevlar fiber to create these composite materials. The study primarily investigates the tensile and impact behavior of these composite components, considering factors such as fiber patterns (concentric and unidirectional). Moreover, the unidirectional/linear orientation was varied as 0°, 45°, and 90°. A comparative analysis is conducted, contrasting the mechanical properties of KFRCP with unreinforced Onyx.

## 4.1. Tensile Properties with Varying Fiber Orientation

To investigate the effect of fiber orientation on tensile properties of the 3D printed composites samples. Three distinct fiber orientations/patterns were selected for the investigation. For this study the other parameters related to fibers were fixed such as volume fraction and infill density. The fiber pattern in the 3D printer are characterized as unidirectional and concentric. These fiber patterns are generally referred as Isotropic pattern as shown in Fig 4.1. In case of unidirectional fiber orientation, the fibers are positioned parallel to each other at various angles. Fig 4.1 illustrates 0°, 45°, 90° and concentric pattern where fiber is laid along, at 45° and in transverse direction and in in circular ring like pattern to the print bed.

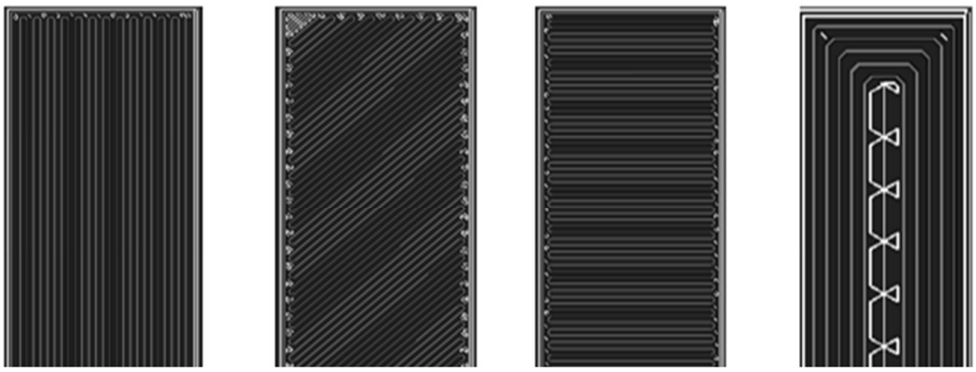

Figure 4.1 Fiber orientations in unidirectional and concentric, 0°, 45°, 90° and concentric (left to right)

### 4.1.1 Effect of Fiber Orientation on Tensile Properties

Unidirectional fiber orientation in 3D printed samples can significantly influence the tensile properties of the composites. In order to investigate the effect of unidirectional fiber orientation tensile tests were performed on the fabricated specimens with 0°, 45°, 90° fiber orientations. In case of longitudinal 0° fiber orientation the maximum mean ultimate strength was found to be 171 MPa. In contrast, the transverse 90° fiber orientation displayed the lowest mean ultimate strength 16.2 MPa. In similar fashion when the fiber laid in 45° raster orientation exhibited 16.3 MPa of mean tensile strength. It was observed that the 3D printed composite gives maximum strength when fibers are laid in the direction of loading and are weak when laid in different direction. The same observations have been reported in the literature (Shi et al., 2021b) .Experimental result provides strong evidence that fiber orientation plays a pivotal role in influencing the tensile strength of the 3D printed specimens. Detailed physical inspection at macroscopically level revealed that the failure pattern was a function of fiber orientation. In case of 0° direction fiber pull out in longitudinal direction and delamination was witnessed. In this fiber orientation the molecules are aligned in the direction of applied load which created strong bonding subjected to tensile loading. Figure 4.2 shows the stress-strain plot for 0° oriented fiber composite. On observing the plot, it is evident that a brittle type of fracture resulted for this orientation.

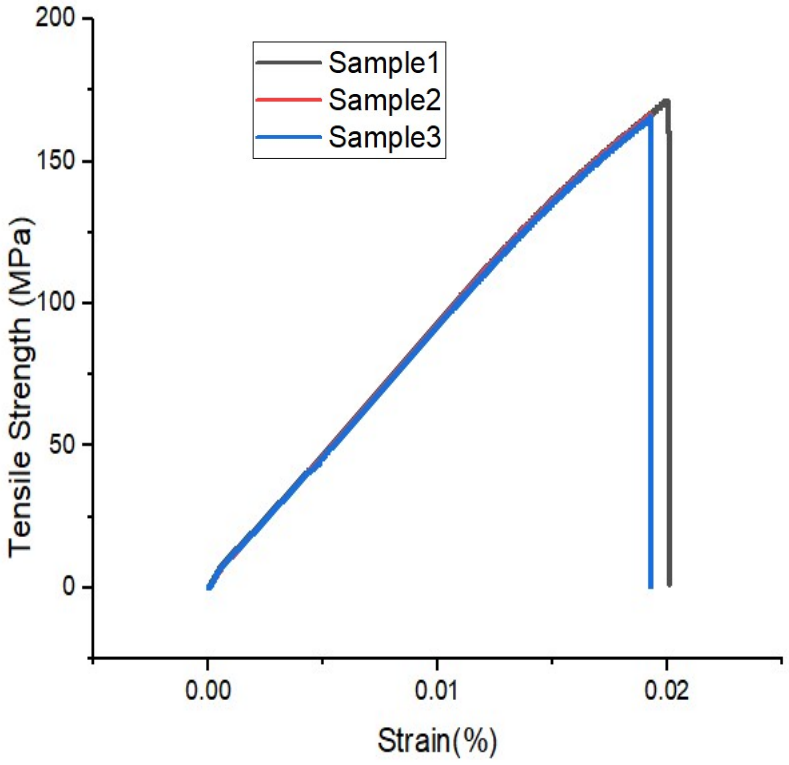


Figure 4.2 Stress Strain diagram for 0° orientated fiber composite

When fiber was laid perpendicular to loading direction it resulted in ductile fracture as observed in stress strain graph (Figure 4.3). There was no role of reinforcement, and the complete load was taken by the matrix material. The mechanical was worse than thermoplastic material onyx. The strain in case of 90° was more compared to 0°oriented fibers. Stress strain graph was observed to be nonlinear and ductile type of fracture was observed (Chacón et al., 2017) .Strain in case 45° was more Nonlinear graph obtained represent ductile fracture. Similar results were obtained for 45° oriented fiber pattern. Figure 4.4 illustrates the stress-strain plot for 45° fiber orientation samples.

.

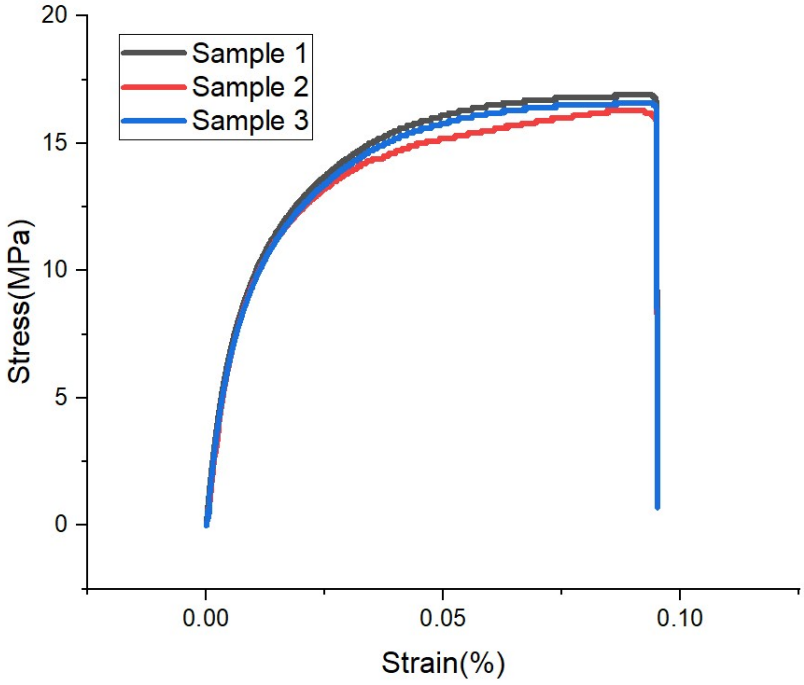


Figure 4.3 Stress Strain diagram for 90° oriented fiber composite

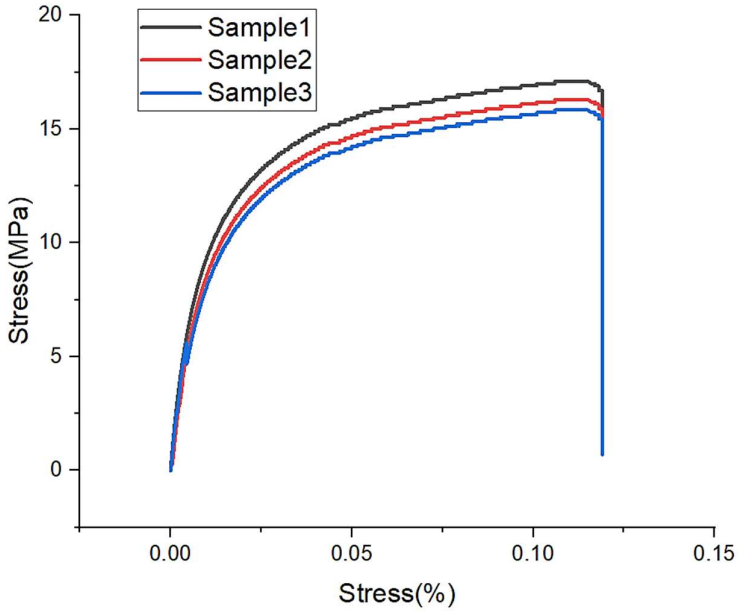


Figure 4.4 Stress Strain diagram for 45° oriented fiber composite

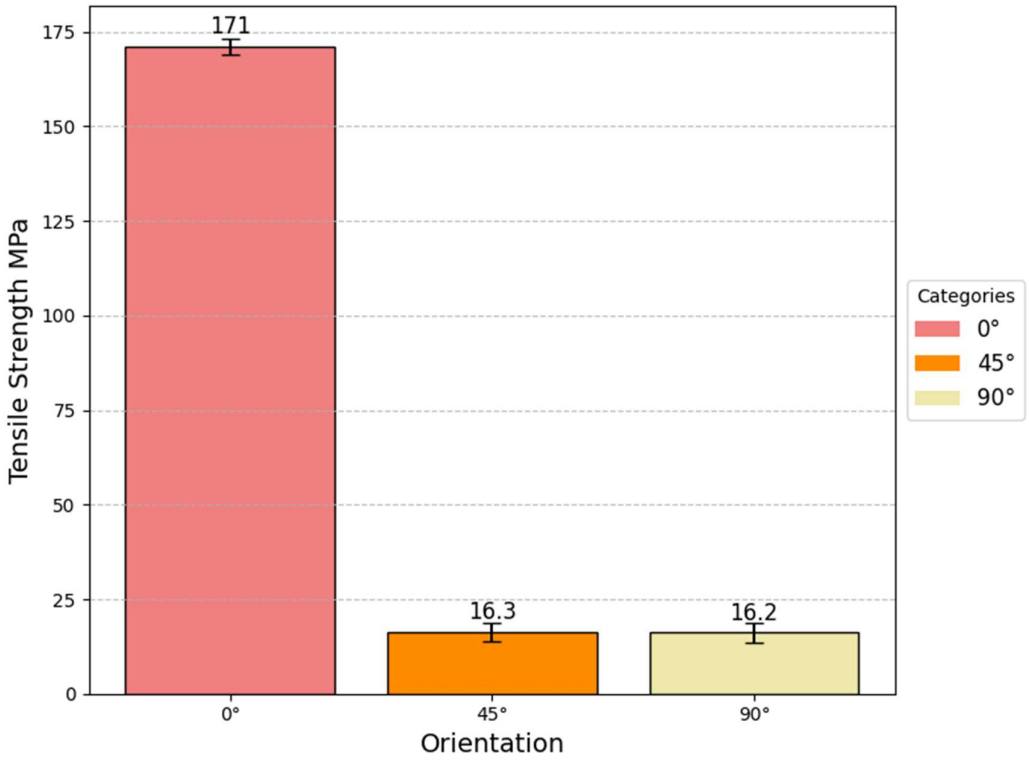


Figure 4.5 Comparison of Tensile strength of various fiber orientations

The observation that the 0° oriented fiber pattern provides the maximum strength compared to all other configurations (figure 4.5), while fiber loaded in the transverse direction at 90° and 45° yields the least strength, correlates the influence of fiber orientation on the tensile strength of the material

For the case of fiber deposition along the loading direction, the applied load needs to overcome the resistance offered by the entire polymer raster's and also the fiber. Since these are laid along the length of the specimens as illustrated in figure 4.6 a. However, for the case of increment in fiber deposition angle such as 45°, the applied load has to primarily overcome the resistance offered by the partial bonding between the deposited raster's. This is considerably less compared to the previous case (figure 4.6 b).

Moreover, in case of 0° pattern the fiber has more surface area as compare to other two direction which was the reason of increase in tensile strength. In case of 3D printed composite, the load shared by the fiber can be expressed as proportional to the cosine angle.

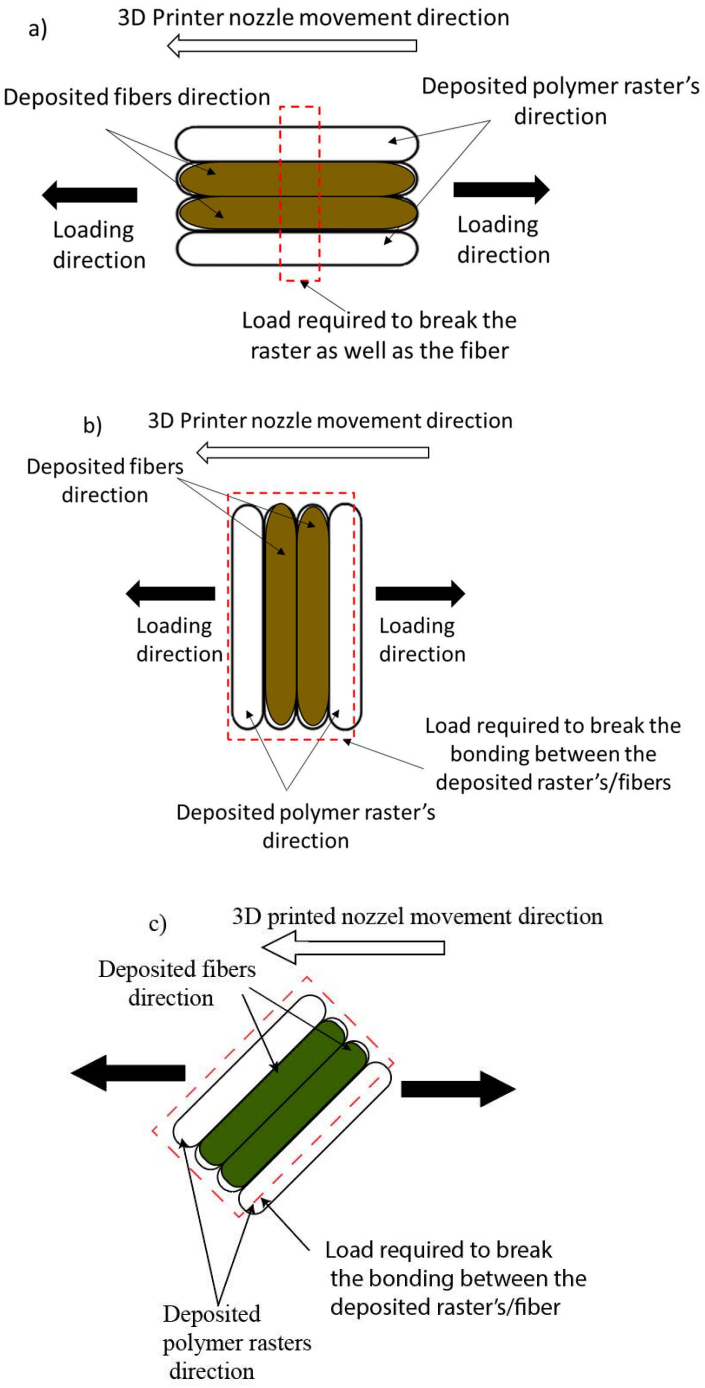


Figure 4.6 Load requirement for fracture of specimens for a) 0° and b) 45°, 90° fiber orientation

Fibers in composites are the primary load-bearing component, while the matrix binds the fibers and transfers loads between them. The orientation of fibers relative to the applied load determines how effectively the composite can carry the load. In 0° the fibers are aligned with the load direction, allowing the load to be directly borne by the strong, stiff fibers. Tensile stresses are efficiently transferred to the fibers through the matrix. The composite takes advantage of the high tensile strength of the fibers, resulting in a maximum strength of 171 MPa. The matrix plays a secondary role in this case, mainly providing support to hold the fibers in place. In 90° Orientation (Transverse), the fibers are perpendicular to the load direction, meaning the matrix must carry most of the load. The matrix is much weaker and less stiff compared to the fibers, leading to the lowest strength of 16.2 MPa. Stress transfer from the matrix to the fibers is inefficient because the fibers cannot directly resist the tensile forces. In 45° Orientation the fibres are angled relative to the load, and the applied force is resolved into both longitudinal and transverse components along the fibres. This creates significant shear stresses within the matrix, which is weaker in shear. Tensile strength is therefore low (16.3 MPa), only slightly better than the 90° case. When a load is applied in the longitudinal direction, the fibers bear most of the stress, with minimal reliance on the weaker matrix.In the transverse direction, the matrix must bear the stress, as the fibers cannot resist forces perpendicular to their orientation. This exposes the inherent weakness of the matrix. At 45°**,** stress is shared between fibers and matrix. However, the fibers' orientation leads to significant shear stresses, which the matrix cannot handle effectively. In case of 0° orientation Failure occurs when the tensile stress exceeds the fibers' tensile strength, typically by fiber breakage. In case of 90° orientation failure is dominated by matrix cracking, as the fibers do not contribute significantly to strength in this direction of 45° orientation. Shear failure occurs within the matrix, alongside potential delamination between fibers and the matrix. The 0° orientation leverages the superior tensile properties of fibers, while the 90° and 45° orientations reveal the weaknesses of the matrix under tensile and shear loads**,** respectively.

The anticipated tensile strength is maximum for cosine ($0^{\circ}$) and decreases with increase in angle  A smaller fiber orientation angle results in a lower force component driving fiber rotation, thereby enhancing resistance to deformation. This phenomenon is further corroborated by the stiffness characteristics presented in. However, a smaller fiber angle also reduces the time required for fiber rotation, leading to an earlier transition to the plateau region in the stress-strain curve. A smaller fiber orientation angle results in a lower force component driving fiber rotation, thereby enhancing resistance to deformation. This phenomenon is further corroborated by the stiffness characteristics presented in. However, a smaller fiber angle also reduces the time required for fiber rotation, leading to an earlier transition to the plateau region in the stress-strain curve.(Shi et al., 2021a)Void was apparent in case of case of 90° and 45° at macroscopic level which was apparent as seen in Fig 4.7. Mechanical performance decreased with increase in angle. The proper adhesion between matrix and the reinforcement lags when there is void (Ning et al., 2017).

The change in raster angle towards higher value leads to poor interfacial adhesion between the matrix and reinforcement which leads to compromised mechanical strength.An increase in raster angle alters the fiber orientation within the composite, leading to a reduction in interfacial adhesion between the matrix and the reinforcement. This weakened interfacial bonding negatively impacts stress transfer efficiency, resulting in diminished mechanical properties such as tensile strength, flexural strength, and impact resistance. Consequently, higher raster angles contribute to structural inconsistencies, increasing susceptibility to delamination and failure under mechanical loading conditions.Void is comparably less in case of 0° which lead to the enhanced tensile strength. An incremental angle in print orientation led to diminution on mechanical performance of 3D printed composites. This emphasizes the importance of

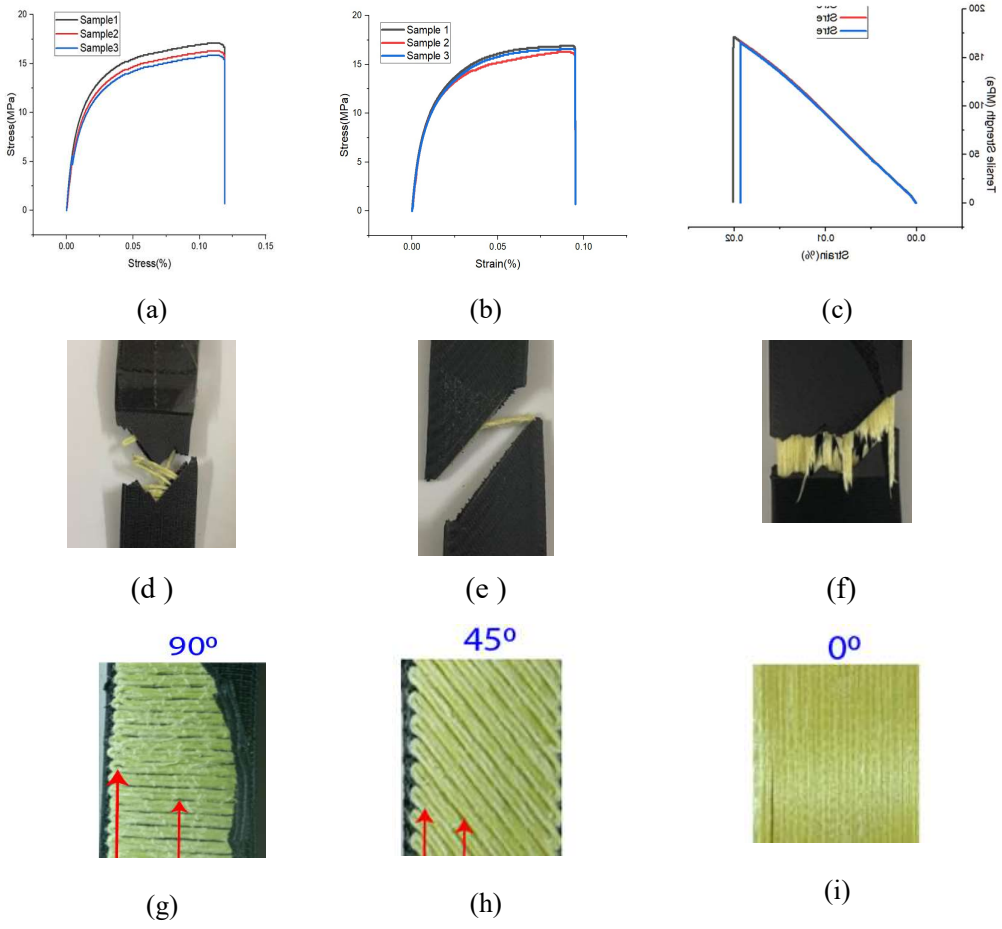


Figure 4.7 Schematic showing (a), (b) and (c) represents stress strain diagram of 90° , 45° and 0°, (d), (e) and (f) represents stress strain diagram of 90° , 45° and 0° , (g), (h) and (i) represents void in case of 3D printed specimen .

considering and optimizing fiber orientation to achieve the tailored mechanical performance of 3D printed parts. There is a strong correlation between tensile strength and degree of fiber rotation at different fiber angles. Smaller fiber angles result in smaller force component causing fiber rotation.A smaller fiber angle results in a lower force component inducing fiber rotation, as evidenced by the stiffness behaviour in Fig. 9. However, a smaller fiber angle also leads to a shorter rotation duration, facilitating an earlier transition to the plateau region in the stress-strain curve.Fiber orientation have strong impact on 3D printed composites Table 4.1 compares the experimental results

with the data available in literature. It may be noted that the volume fraction of the fiber reinforcement is not same in this comparison. The work reported by Shi et al., 2021a have 10% fiber volume fraction and that reported by (Dong et al., 2018) have 50% volume fraction. The experimental results in this chapter consists of 22.6% fiber volume fraction.

Table 4.1 Comparison of Experimental tensile strength obtained vs obtained in literature by changing fiber direction

| **Matrix** | **Fiber Orientation (Unidirectional)** | **Volume Fraction** | **Tensile Strength (MPa))** | **Standard Deviation** | **Reference** |
|---|---|---|---|---|---|
| Nylon | 30° | *10%* | 47 | - | Shi et al., 2021a |
| Nylon | 45° | *10%* | 42 | - | Shi et al., 2021a |
| Nylon | 60° | *10%* | 39 | - | Shi et al., 2021a |
| Nylon | 0° | *50%* | 296 | - | (Dong et al., 2018) |
| Nylon | ±45° | *50%* | 13.14 | - | (Dong et al., 2018) |
| Nylon | 90° | *50%* | 7.213 | - | (Dong et al., 2018) |
| *Onyx* | *0°* | *22.6%* | *171* | ±9.7 | *This Work* |
| *Onyx* | *45°* | *22.6%* | *16.3* | ±2.4 | *This Work* |
| *Onyx* | *90°* | *22.6%* | *16.2* | ±2.6 | *This Work* |

Fiber orientation is crucial in determining the strength and stiffness of the composite. When fibers are aligned with the load direction (0°), they effectively carry the load, resulting in higher tensile strength and modulus. This is because fibers oriented in this direction can efficiently bear the applied tensile stresses.

At 90° orientation (transverse direction), the fibers are perpendicular to the load, making the composite rely more on the matrix for load bearing. Since the matrix is typically weaker than the fibers, this results in lower tensile strength and stiffness.

At 45°, fibers are subject to shear stresses when loaded longitudinally. The composite's response here is governed by both the fibers and the matrix, leading to a complex stress distribution and often lower strength and modulus than in the 0° configuration. These differences underscore the anisotropic nature of fiber-reinforced composites, where

mechanical properties are highly directional due to fiber alignment. Fiber orientation is key to the tensile properties of composite materials. Fibers aligned at 0° (parallel to loading) offer the highest tensile strength, efficiently transferring load along their length. However, when fibers are oriented transversely (90° or 45°), they provide less tensile resistance due to lower alignment with the applied force, reducing reinforcement efficiency. Higher raster angles (further from 0°) can weaken interfacial adhesion between fibers and matrix, compromising load transfer. These orientations may also introduce voids, further diminishing mechanical strength. 3D printing builds structures layer-by-layer, introducing an additional source of anisotropy. The bonding between layers is generally weaker than within a single layer due to the sequential deposition process as shown in (figure 4.7). As a result, the printed specimen often has different mechanical properties along the layer stacking direction compared to within a layer. This is often evident in lower strength and stiffness perpendicular to the printed layers, which can create preferred planes for crack propagation under stress. The strength and quality of the bond between the continuous fiber and the surrounding matrix material (e.g., Onyx) are critical.

In a 3D-printed composite, the interface between fiber and matrix layers can act as a point of weakness if bonding is insufficient, especially in alternating fiber and matrix layers. Poor bonding between the fiber and matrix can prevent effective load transfer, especially under bending or impact loading. This leads to anisotropic behavior as the material may perform well along fiber directions but poorly across layers, where fiber-matrix bonds are weaker.The 3D printing process can introduce porosity or gaps between layers, especially in the areas where fiber and matrix are layered together .These pores can act as stress concentrators, making the material more prone to failure along certain directions. Such porosity can reduce the energy absorption capacity of the composite, as micro-cracks can initiate and propagate more easily in directions where bonding is weaker or where gaps are present. In anisotropic 3D-printed specimens, failure often initiates along the weaker bonding interfaces. For instance, during impact testing, fractures may follow paths with poor bonding (e.g., along inter-layer interfaces), highlighting the anisotropic nature of failure .Fiber orientation also affects the failure modes observed. For example, 0° fiber orientations may resist tensile loads well but may fail under shear loading, while 45° orientations provide better shear

resistance but might be less effective under direct tensile loads. Variations in temperature during the printing process can lead to differential cooling rates in different parts of the material, further impacting anisotropy. Faster cooling layers may lead to residual stresses or even micro-cracking in certain directions, affecting the material's properties in a way that depends on orientation and bonding.Anisotropy in 3D-printed specimens is largely due to the directionally-dependent fiber orientation, the layer-by-layer nature of the FDM process, and variations in bonding quality. Together, these factors create a composite material that responds differently to stress along different axes. A detailed understanding of these mechanisms aids in optimizing print settings for desired mechanical performance and can guide future improvements in the design of 3D-printed composites for enhanced isotropy and strength. bonding (e.g., along inter-layer interfaces), highlighting the anisotropic nature of failure .Fiber orientation also affects the failure modes observed. For example, 0° fiber orientations may resist tensile loads well but may fail under shear loading, while 45° orientations provide better shear resistance but might be less effective under direct tensile loads. Variations in temperature during the printing process can lead to differential cooling rates in different parts of the material, further impacting anisotropy. Faster cooling layers may lead to residual stresses or even micro-cracking in certain directions, affecting the material's properties in a way that depends on orientation and bonding.Anisotropy in 3D-printed specimens is largely due to the directionally-dependent fiber orientation, the layer-by-layer nature of the FDM process, and variations in bonding quality. Together, these factors create a composite material that responds differently to stress along different axes. A detailed understanding of these mechanisms aids in optimizing print settings for desired mechanical performance and can guide future improvements in the design of 3D-printed composites for enhanced isotropy and strength.

### 4.1.2 Effect of Fiber Pattern on Tensile Properties

Apart from unidirectional fiber orientation for composite fabrication, another important fiber deposition pattern is concentric. This fiber pattern may significantly influence the tensile properties of the 3D printed FRCP. In order to investigate the effect of this fiber pattern and to compare it with the unidirectional fiber tensile specimens were fabricated and tested as per the ASTM standards.

The concentric pattern is shown in Fig 4.8, where the fibers follow a spiral and angular trajectory, gradually forming concentric rings toward the center, resulting in a ring-like structure. A total of 15 rings were incorporated to entirely fill the specimen to avoid void formation. This pattern can be realized as the outer wall or boundary of the specimen geometry. On offsetting these walls, moving inward will create a circular pattern.

The tensile testing revealed that the concentric arrangement, wherein the layering of the pattern converges toward the central region demonstrated tensile strength little lower than the 0° fiber pattern. However, the strength was significantly more the other unidirectional pattern of 90° and 45°. The experimental stress determined in this configuration registers at 121 MPa.

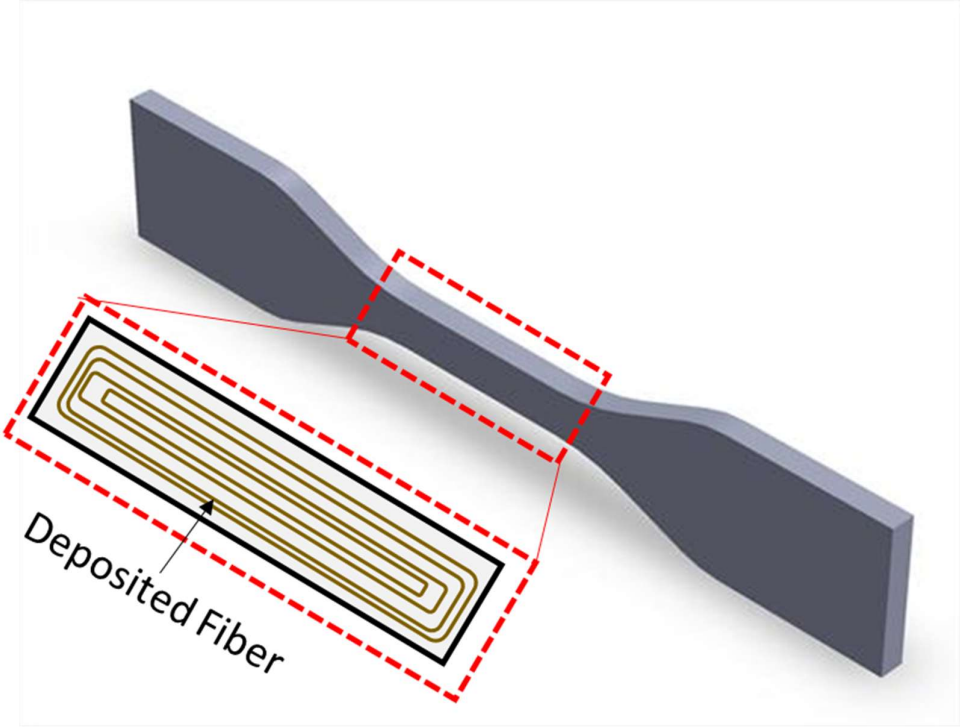


Figure 4.8 Schematic diagram showing concentric fiber pattern in the gauge length of tensile specimen

The stress-strain graph for the specimens fabricated by depositing the fiber in concentric pattern as illustrated in figure 4.9. It must be realized that the onyx material was also deposited in the similar manner for polymer layers. The tensile strength achieved for the specimens was 121 MPa. On comparing the strength with 0° oriented

fiber specimens a reduction of 29% was observed. However, on comparing the concentric patterned specimens' strength with that of 90° and 45° fiber oriented specimens an increment of 86.6% and 86.5% respectively was achieved. The comparison is depicted in figure 4.10.

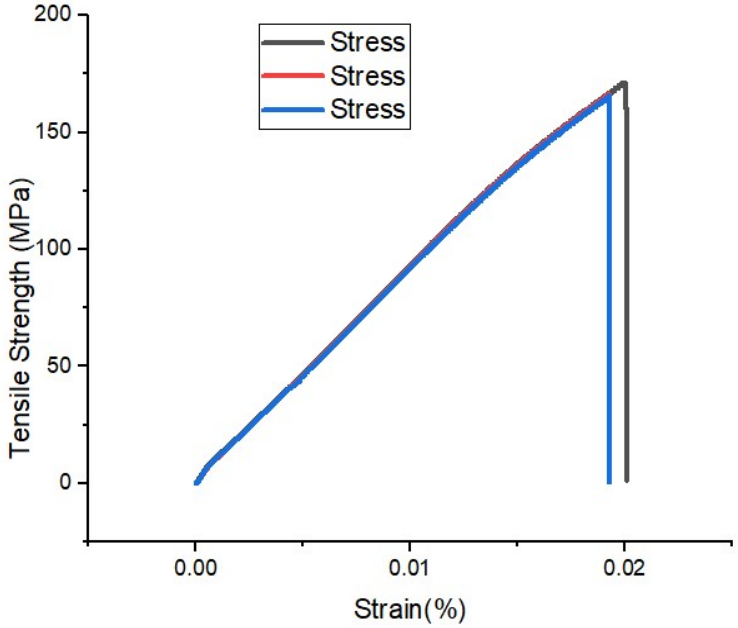


Figure 4.9 Stress-strain plot for concentric patterned fiber composites

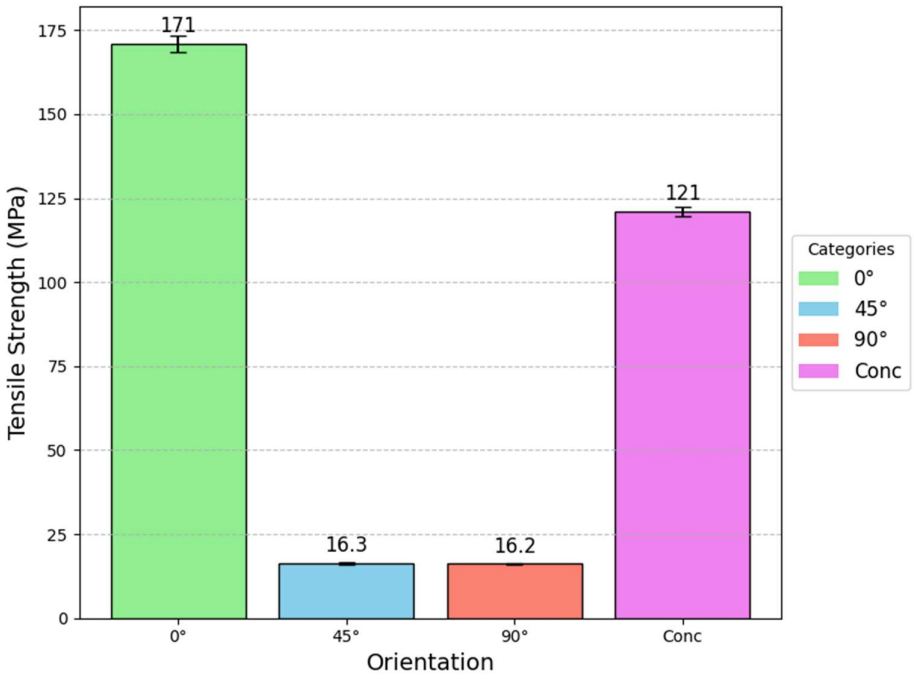


Figure 4.10 Comparison of tensile strength of concentric fiber patter with unidirectional fiber orientations

The obtained trend of the results is in line with the reported literature of 3D printed continuous fiber specimens with different stacking sequence (Hetrick *et al.*, 2021). Table 4.2 shows the comparison of fiber deposited in concentric pattern of the present work with other reported literature. It needs to be realized that the fiber volume fraction is different, for serial number 1 and 2 the fiber volume fraction is 10 and 11%. For third the volume fraction is 43%. These are compared with the present work in which 22.6% volume fraction of fiber is used.

Table 4.2 Comparison of experimental tensile strength vs reported in literature for concentric pattern

| S.No. | Matrix | Fiber pattern | Tensile Strength (MPa) | Reference |
|---|---|---|---|---|
| 1 | Nylon | Concentric | 110 | (Dickson, Barry, Dickson, et al., 2017) |
| 2 | Nylon | Concentric | 161 | (Dickson, Barry, Dickson, et al., 2017) |
| 3 | Nylon | Concentric | 259.7 | (Mohammadizadeh et al., 2019) |
| *4* | *Onyx* | *Concentric* | *121*±1.67 | *This Work* |

### 4.1.3 Fiber Alignment of 3D Printed Composites

On observing the tensile strength of various fiber orientation and pattern, it is evident that the 0° and concentric yields better performance compared to other orientations. Further comparison of fiber alignment between concentric and 0° provides insights on the achieved 3D printed structures. In concentric pattern, the fiber structure exhibit irregular alignment. Furthermore, a discernible void is observable at the central region of the concentric configuration as shown in Figure 4.11. Owing to the absence of homogeneity in this structural arrangement, discontinuities manifest leading to a diminished tensile strength relative to isotropic 0° pattern. In case of isotropic pattern the fiber demonstrate a consistent uniform alignment encompassing the entire surface area. However, when subjected to loading scenario where the fiber is loaded in transverse direction of the print bed they are incapable of sustaining the load. Concentric ring leads to discontinuity, delamination and due to improper bonding between matrix and reinforcement tensile strength decreases compared to 0° oriented fibers (Fidan *et al.*, 2020).

For unidirectional 0° and concentric fiber composites stress-strain graph it can be inferred that the graphs are linear in nature which indicates their brittle nature. However, for 90° and 45° oriented fibers the strain was more compared to the 0°and concentric indicating a shift towards the ductile nature.

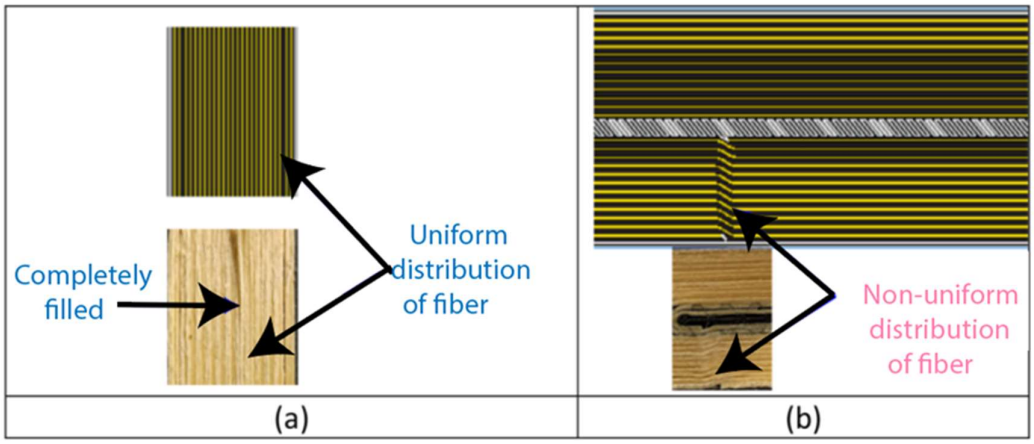

Figure 4.11 Schematic diagram comparing alignment of fiber in case of unidirectional 0° vs concentric.

Experimental results attest that fibers achieve their maximum load bearing capacity when printed along the print bed which previously stated that the fiber must printed along the direction of loading to withstand maximum tensile strength. The tensile performance for concentric was followed by the 0°. However, when subjected to a loading scenario where the fibers are oriented 90° to the direction of applied force, they prove incapable of sustaining the load. Experimental findings substantiate and corroborate previous research (Dickson, Barry, Dickson, et al., 2017). Indeed the variation of stress was not linear as can be observed in stress strain graph. An increase in angle let to an decrease in overall resistance against external loading. Two type of rupture has been observed Shear rupture and tensile rupture. Shear rupture in damage occurred in the direction of fiber loading. Shear rupture leads fiber pull put, debonding and delamination. Tensile rupture damage is in the transverse to the direction of the loading. The strain in 90° oriented fibers was more and stress strain graph was not linear that indicates the failure was ductile in nature. 3D printed specimen is stronger when the surface area covered by fiber is more. The maximum surface area can be achieved if the longest dimension of the specimen is along the direction of print bed. When surface area is more there is a proper adhesion between the fiber and thermoplastic material leading to stronger part. Even the concentric pattern also needs to be deposited along the print bed as shown in figure 4.12.

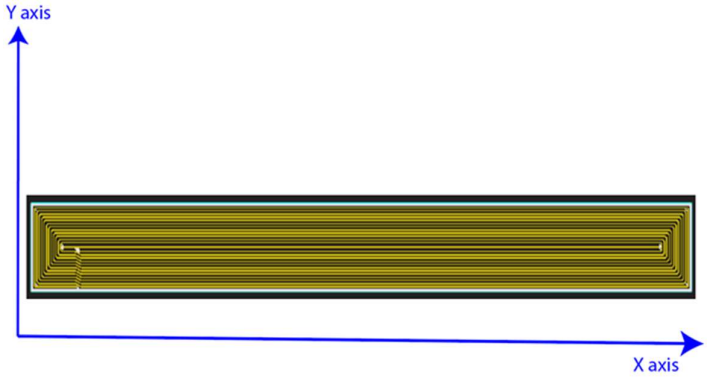


Figure. 4.12 Schematic illustrating the concentric tensile specimen printed along the print bed direction

4.1.4 Anisotropy Due to Fiber Orientation

It is evident that the strength of 3D printed parts varies in build direction (Z direction) compared to properties in XY plane. Due to this behavior the parts need to be printed flat on the bed instead of on edge or upright in order to achieve better mechanical performance. Figure 4.13 illustrates the three build orientations for 3D printed specimens. This anisotropic behavior of 3D printed specimens greatly affects the tensile behavior. Moreover, in case of 3D printed continuous fiber reinforced polymer composite, fiber orientations/pattern contribute to this anisotropy. The section discusses the anisotropy caused by deposited fiber orientations.

The literature reveals that for investigation of anisotropy caused by ZXY (upright) specimens can be replaced by the XYZ (flat) in which raster's are laid in transverse direction (90°) as the obtained results are comparable.

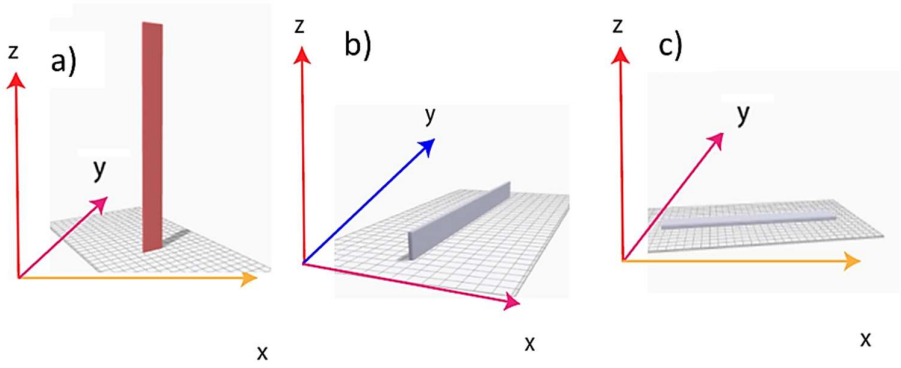


Figure 4.13 Build orientations a) upright b) on edge and c) flat

It underscores the fact that tensile strength is influenced by the fiber direction and subsequent alignment of polymer molecules, indicating the presence of an anisotropic property. Even when the composites are printed flat on the bed even though due to variation in fiber orientation, the tensile properties can vary and cause anisotropy. The same can be seen on comparing the printed specimens with longitudinal and transverse orientations of fiber.

3D printed parts are strong when the fiber is aligned in the direction of loading and is weak other two planes. The change in the properties can be observed on comparing the longitudinal and transverse oriented fibers. Since the fiber deposition strategy differ for both the cases the inter and intra layer adhesion also varies. The fiber deposition strategy is depicted in figure 4.14.

As it can be seen from the figure that the nozzle deposits the fibers along the length of the specimen causing the fiber orientation in the loading direction. However, the transverse move for fiber deposition in this case is very small comparatively to longitudinal direction. This aligns the fibers and exposes the printed sample in such a way that the load has to overcome the strength of the fiber along with the polymer matrix. Moreover, the intra layer bonded areas, which is the weakest region, is also parallel to the loading direction. Due to this the specimens will possess greater strength. On the other hand, when the fibers are laid in transverse direction to the loading, the longitudinal moves of the nozzle are very less for deposition of the fibers compared to the transverse movement. This causes the fibers to be aligned perpendicular to the loading direction. In this scenario the exposed bonded area (intra layer bonding) is very high and these weakest regions are exposed to the load. Now the load applied needs to overcome the bonding between the fibers and polymer matrix. This causes a significant variation in the load bearing capacity of the 3D printed continuous FRCPs.

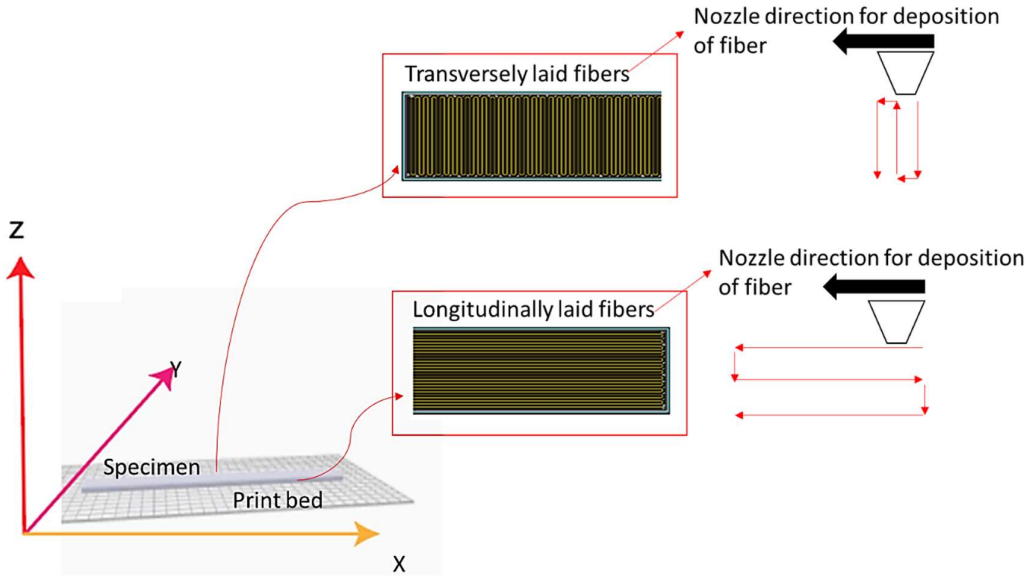


Figure 4.14 Fiber deposition variation in longitudinal and transverse directions

It can be seen that the variation caused by the fiber direction is much more significant when compared with the volume fraction of fiber. This shows the importance of selection of fiber orientation in 3D printed continuous FRCPs. To provide a comprehensive understanding of the anisotropic behavior observed in 3D-printed specimens, it's crucial to explain the mechanisms that cause directional variations in properties. In 3D-printed composites, anisotropy arises due to factors like fiber orientation, layer-by-layer deposition, and bonding quality between the fiber and matrix. Here is a deeper look into these mechanisms:

In 3D-printed composites, fibers can be aligned in specific directions (e.g., 0°, 45°, 90°) based on the printing pattern. The orientation of these fibers creates anisotropic behavior because the properties of the material vary with the fiber alignment.Fibers aligned along the load direction (e.g., 0°) generally enhance tensile strength and stiffness in that direction, as load transfer is more efficient. Conversely, fibers oriented perpendicular (e.g., 90°) or at an angle (e.g., 45°) to the load may not contribute as much to strength in the primary load direction, as they do not support the load as effectively.

3D printing builds structures layer-by-layer, introducing an additional source of anisotropy. The bonding between layers is generally weaker than within a single layer due to the sequential deposition process. As a result, the printed specimen often has

different mechanical properties along the layer stacking direction compared to within a layer. This is often evident in lower strength and stiffness perpendicular to the printed layers, which can create preferred planes for crack propagation under stress. TheStrength and quality of the bond between the continuous fiber and the surrounding matrix material (e.g., Onyx) are critical. In a 3D-printed composite, the interface between fiber and matrix layers can act as a point of weakness if bonding is insufficient, especially in alternating fiber and matrix layers. Poor bonding between the fiber and matrix can prevent effective load transfer, especially under bending or impact loading. This leads to anisotropic behavior as the material may perform well along fiber directions but poorly across layers, where fiber-matrix bonds are weaker.

The 3D printing process can introduce porosity or gaps between layers, especially in the areas where fiber and matrix are layered together (Figure 4.7). These pores can act as stress concentrators, making the material more prone to failure along certain directions. Such porosity can reduce the energy absorption capacity of the composite, as micro-cracks can initiate and propagate more easily in directions where bonding is weaker or where gaps are present.In anisotropic 3D-printed specimens, failure often initiates along the weaker bonding interfaces. For instance, during impact testing, fractures may follow paths with poor bonding (e.g., along inter-layer interfaces), highlighting the anisotropic nature of failureFiber orientation also affects the failure modes observed. For example, 0° fiber orientations may resist tensile loads well but may fail under shear loading, while 45° orientations provide better shear resistance but might be less effective under direct tensile loads.Variations in temperature during the printing process can lead to differential cooling rates in different parts of the material, further impacting anisotropy. Faster cooling layers may lead to residual stresses or even micro-cracking in certain directions, affecting the material's properties in a way that depends on orientation and bonding.

Anisotropy in 3D-printed specimens is largely due to the directionally-dependent fiber orientation, the layer-by-layer nature of the FDM process, and variations in bonding quality. Together, these factors create a composite material that responds differently to stress along different axes. A detailed understanding of these mechanisms aids in optimizing print settings for desired mechanical performance and can guide future

improvements in the design of 3D-printed composites for enhanced isotropy and strength.

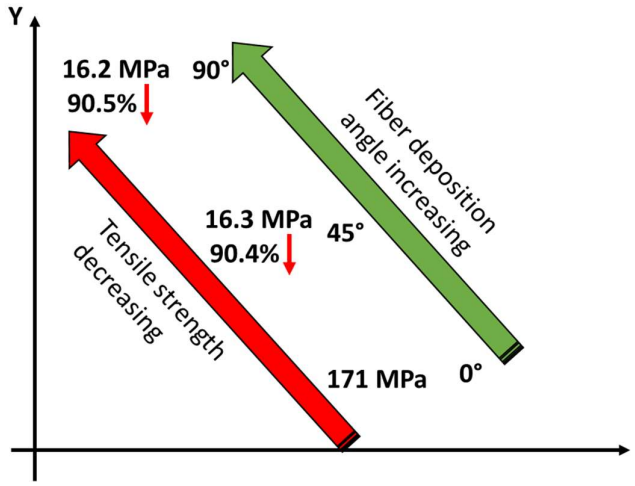


Fig 4.15 Shows Relation between fiber deposition angle and tensile strength

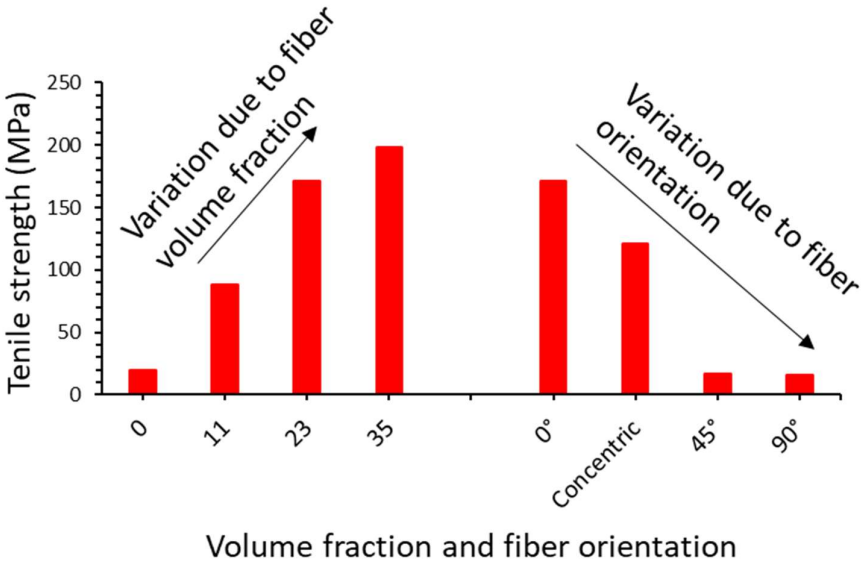


Figure 4.16 Fig shows the variation in tensile strength due to fiber orientation and volume fraction

### 4.2. Impact Strength of FRCPs

To study the effect fiber orientations and pattern on impact properties of the composites. Impact testing was performed on the 3D printed specimens. Remarkably there exist less research work pertaining to the impact energy absorption characteristics of continuous fiber reinforced 3D printed composites. The primary aim of this study is to investigate the effects of varying fiber patterns (unidirectional and concentric) on the impact properties of 3D printed continuous Kevlar fiber-reinforced Onyx composites. A comparative analysis was conducted between unreinforced impact specimens and their reinforced counterparts. In this present section of the chapter, impact specimens were printed by varying the fiber orientation/pattern. Solid filling was used as this ensures that the specimen's internal structure is completely filled with material and it avoids formation of voids. A total of three specimen for each configuration as per ASTM D256 was printed.

The main purpose of impact test is to measure resistance against fracture and toughness. Impact test is used to determine the resistance of composites by using standardized type pendulum with hammers to break the specimen. Essential factors which determine impact properties are plastic deformation, crack initiation, crack growth, crack length, and the capability to absorb energy without fracture. It is the summation of all the energy required to initiate fracture, propagate fracture, bend, provide vibration, and indent plastic deformation in the specimen. Impact properties will be determined. The notch is a stress concentration zone, which increases the probability of fracture due to brittle rather than ductile. The specimen failure is categories as complete break, hinge break, partial break, or non-break. Notch when reversed or is in the opposite direction of the load the breakage is due to flexural shock. All test methods measure energy per unit area absorbed to break the sample. In this work, only complete break has been used. The specimen is a cantilever beam with a fixed support at one end and load acting on the other end. The top part where load acts is the compression region, and bottom part is the tension region (figure 4.16). A complete fracture and separation are observed in the entire specimen.

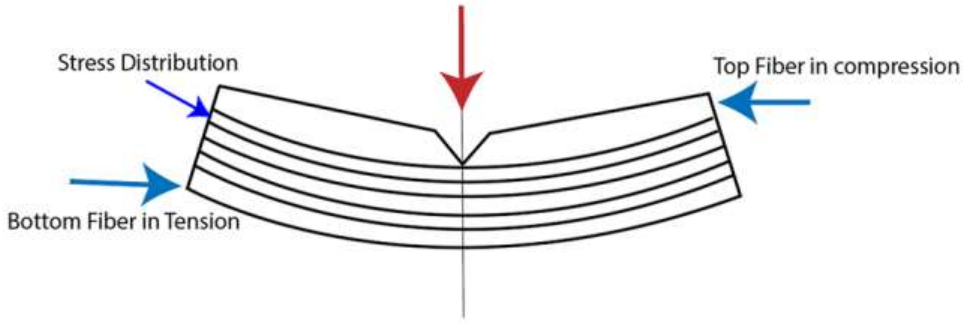


Figure 4.17 Schematic diagram representing tension and compression condition in testing

### 4.2.1 Impact Properties with Varying Fiber Orientation

The specimens with varying unidirectional fiber orientation were 3D printed and impact testing was performed on them in order to observe the effect of the fiber orientation on impact strength. Figure 4.18 demonstrates the build orientation of the specimens and the deposited fiber orientations/pattern. The fibers were laid in 0°, 45°, 90° and concentric pattern for fabrication of impact specimens.

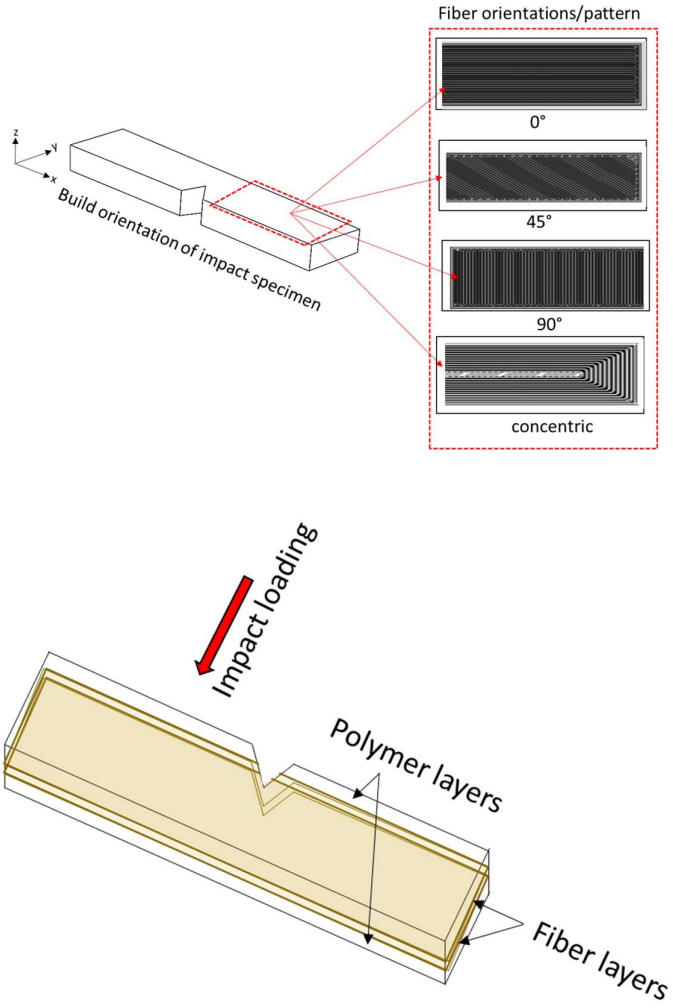


Figure 4.18 Build orientation and fiber orientations/pattern for impact specimen fabrication and fiber layering strategy

### 4.2.2. Effect of Unidirectional Fiber Orientation on Impact Properties

Impact specimens were printed as per the ASTM D256 and three different fiber orientations (unidirectional) were selected. The fiber direction was varied from 0° to 90° with an increment of 45°. Apart from fiber orientation the selection of build direction or orientation of specimen itself was selected to ensure maximum impact strength of 3D printed specimens. The volume fraction of the Kevlar fiber was kept constant for this investigation.

The results of the impact testing revealed that the impact energy was highest for 0° (74.78 KJ/$m^2$ + 1.3), followed by 45° (49.36 KJ/$m^2$ 1.41) and 90° (39.91 KJ/$m^2$ + 1.66). Experimental result correlated that significant change in impact strength is obtained with change in fiber orientation. The impact strengths of the three fiber orientations showed a strong correlation with the tensile strength results also. Figure 4.19 illustrates the comparison of impact strength obtained for the investigated fiber orientation.

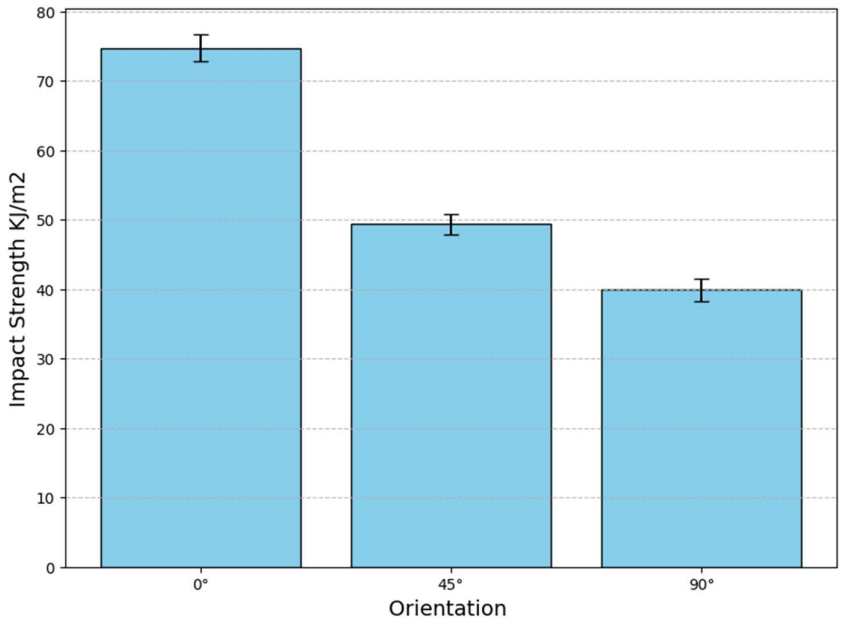


Figure 4.19 Impact strength with varying unidirectional fiber orientation

Significant increment in impact strength can be achieved by varying the fiber orientation. Figure 4.18 illustrates the percentage increment achieved in impact strength when the fiber orientation was changed from 90° to 45° and further to 0°. It can be seen that 87.38% increment was achieved when the fibers were changed from 90° to 0° and 22.6.69% increment was achieved for the case of fiber change from 90° to 45°. This highlights the importance of fiber deposition strategy for achieving improved impact properties. If the specimen is assumed to be cuboid-shaped specimen with 'l' representing the length and 'a' and 'b' representing the other two sides (where 'l' is greater than 'a' and 'b'), it is advantageous to align the fibers in the longest dimension, which is

'l' as shown in Fig 4.21. This strategy is suggested to be effective in enhancing the mechanical properties of the composite. Aligning the fibers with the longest dimension is a common approach in composite materials engineering. This strategy is employed to increase the surface area of the reinforcement, which is often the fiber component. When the fibers are aligned with the longest dimension, it means that they are oriented along the direction in which the material is most likely to experience mechanical loads. This alignment maximizes the load-carrying capacity of the fibers and, consequently, the overall mechanical properties of the composite material. The increased surface area of the fibers in this alignment can lead to improved tensile and impact strength, making the material more suitable for applications where mechanical performance is crucial.

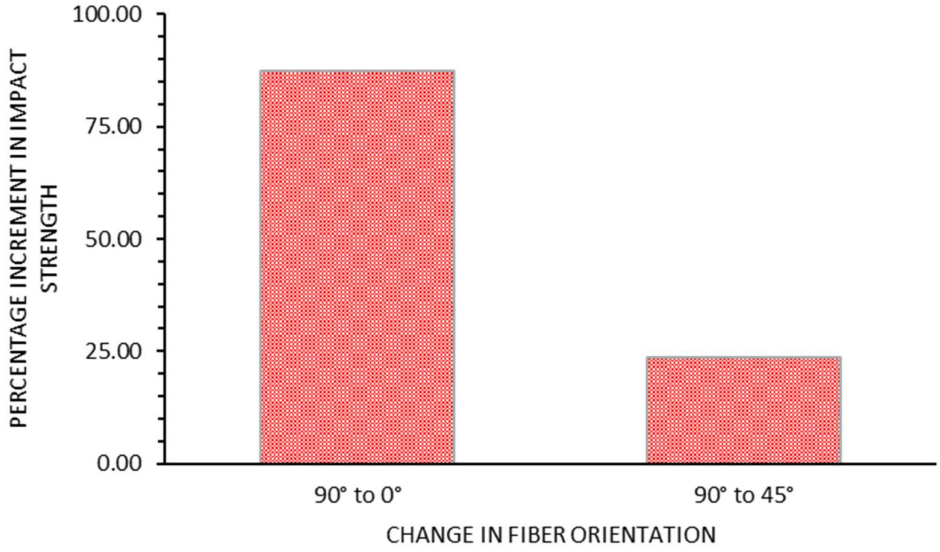


Figure 4.20 Percentage increment in impact strength

Conversely if the impact specimen is printed vertically the fiber is laid in the transverse direction of the print bed hence it will not perform mechanically as compared to the specimen when kept it in the vertical direction.

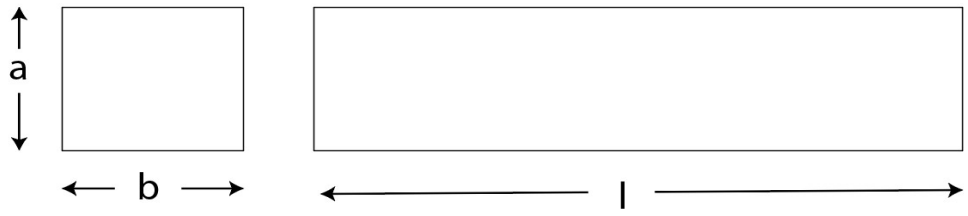


Figure 4.21 Schematic diagram showing two-dimensional representation of cube where l is the length and a, b are the two sides

### 4.2.3 Effect of Fiber Pattern on Impact Properties

To understand the effect of fiber pattern on impact strength, samples with concentric pattern were tested and compared with the 0° and 90° oriented fibers. Figure 4.22 illustrates the schematic view of the fiber patterns used for the study along with 3D printed samples.

Among these patterns, the concentric pattern, demonstrated the highest effectiveness in enhancing the impact resistance of samples. Concentric pattern exhibited an impact strength of 76.95 KJ/$m^2$ 1.3 while the 0° displayed 74.78 KJ/$m^2$ +1.2. It is important to note that in both fiber orientation/pattern same volume fraction of fiber was used. The observed values are approximately similar however, when comparing the concentric pattern with 45° and 90° fiber orientation the change is significant. Concentric pattern exhibited maximum impact strength. Figure 4.22 shows the comparison of impact strength of various fibers orientations.

The impact strength of concentric patterned samples was higher as compared to 0° pattern since it properly shields the outer layer. Increase in concentric ring around the wall increases impact strength of the material. The experimental result is validated by earlier researchers (Prajapati et al., 2020) .When fibers align with the direction of stress, they exhibit superior resistance to impacts. In both the pattern, the fibers align with the stress direction, rendering both patterns suitable for creating anti-impact specimens. The impact samples feature notches with sharp contours. In cases involving sharp corners or holes, the concentric pattern is justified, as it uniformly covers the entire surface, ensuring continuity. Impact specimen with no reinforced undergone angled crack with complete break and total failure. The matrix layer teared along the path of the print. In case of concentric pattern partial break was observed.

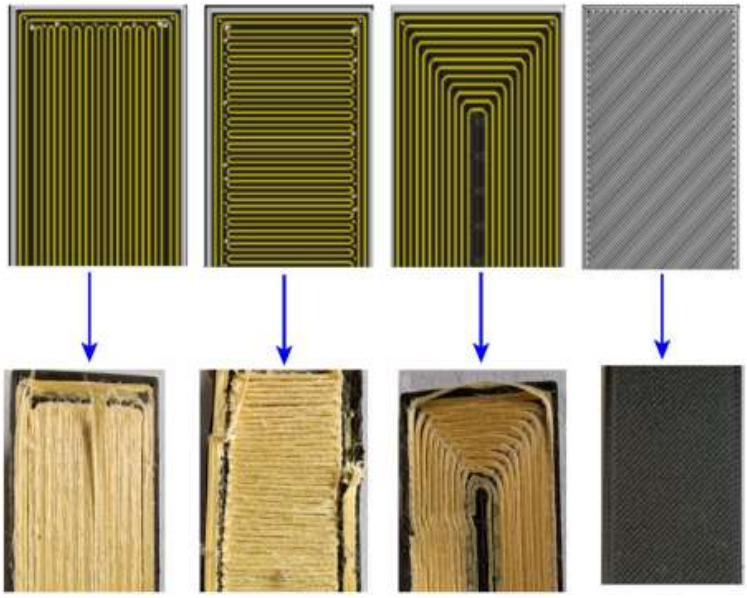

Figure 4.22 Schematic diagram and fabricated samples showing 0°, 90°, concentric pattern and unreinforced sample

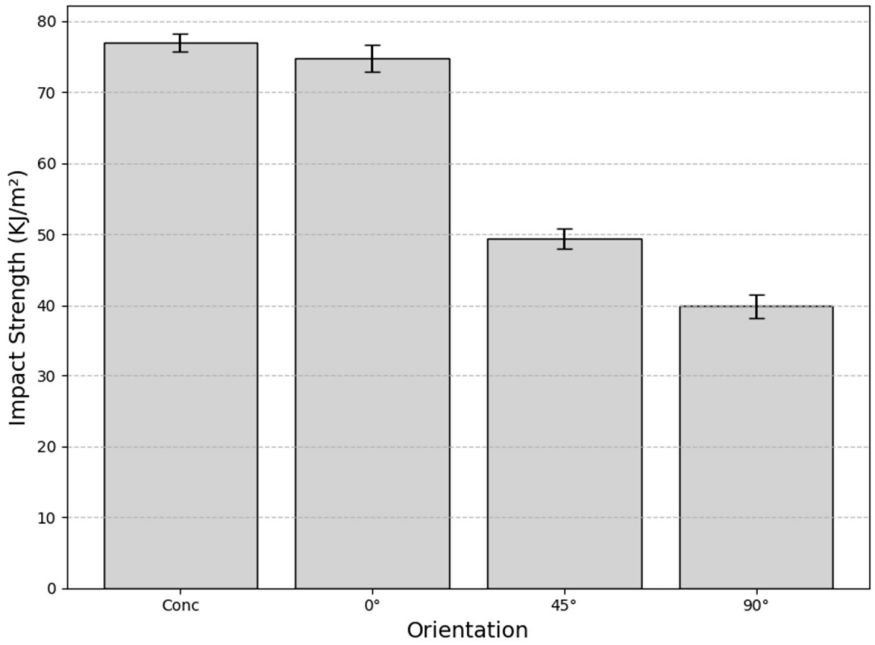


Figure 4.23. Comparison of impact strength for different fiber orientations

Impact test is an extreme case of compression and tension, as shown in Fig. 4.24. The anvil when strikes other end creates a plastic deformation which ultimately leads to final deformation (Figure 4.24 a and b). The types of failure are characterized as complete break in which the specimen separates into more than two pieces (figure 4.25 b , c and d). Hinge, partial, and non-break are the incomplete break where the specimen does not separate away. In this type of failure, complete break of the 3D-printed parts was observed in all the specimen. As compared to tensile specimen, it is found that all impact specimen is having same types of failure, as shown in Fig. 4.22.6. Impact test is only useful to calculate toughness of the sample. It only shows the effect of reinforcement on toughness. The type of crack was angled in nature. Hence, impact test can only tell the effect of change in reinforcement on change in toughness. It does not answer the effect of change in reinforcement on delamination and different types of failure encountered by impact specimen with change in toughness.

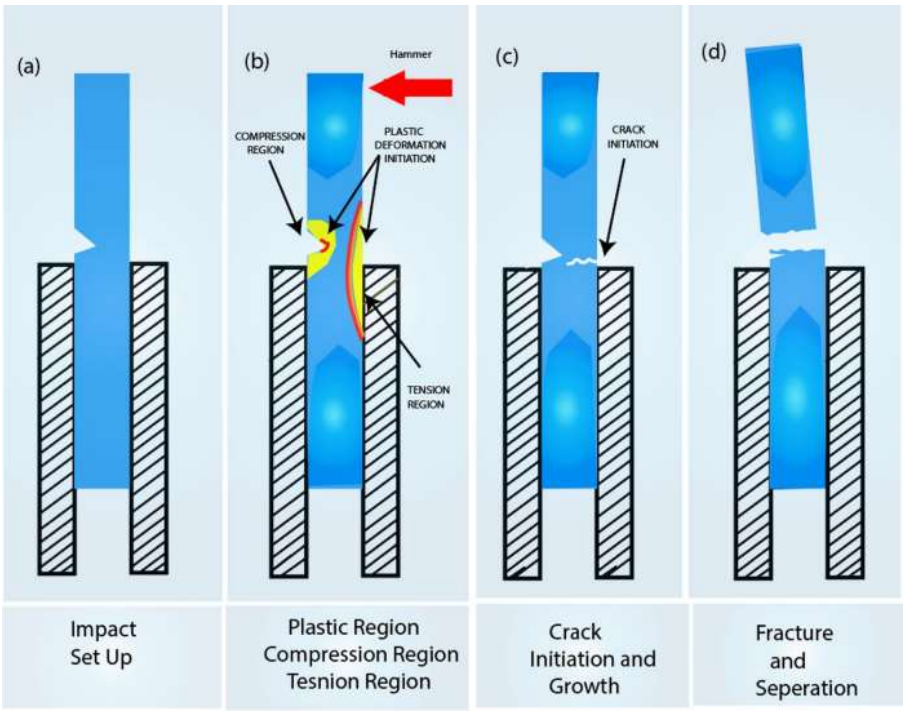


Figure 4.24 Schematic diagram for different types of fracture in specimen

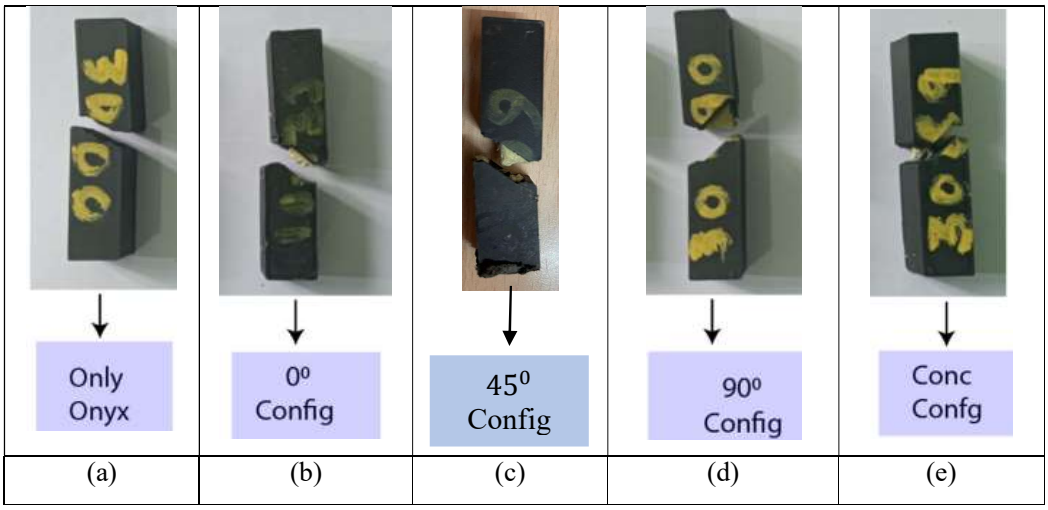


Figure 4.25 Fractured specimens after impact test (a) represent only onyx, (b)zero degree configuration (c) forty five degree configuration (d) ninety degree configuration and (e) Concentric configuration

| | |
|---|---|
| 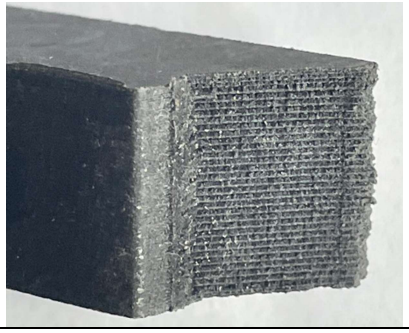 | 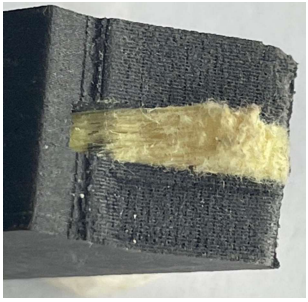 |
| (a) Only Onyx | (b) Zero degree Reinforcement |
| 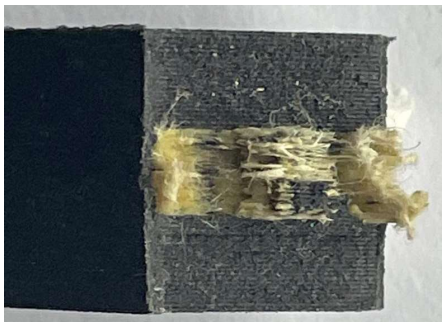 | 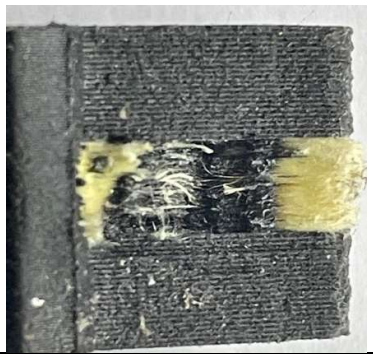 |
| (c)Forty five degree Reinforcement | (d) Ninety degree Reinforcement |
| 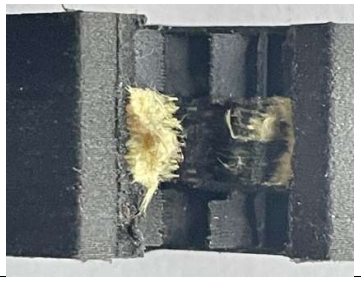 | |
| (e) Concentric Reinforcement | |

Figure 4.26 Macroscopic view of fractured specimens after impact test (a) represent only onyx, (b) Zero degree configuration (c) Forty five degree configuration (d) Ninety degree reinforcement and (e) Concentric configuration

The study of crack behaviour in unreinforced 3D-printed specimens reveals variations based on the printing patterns and orientations. In case of Isotropic Ninety and Isotropic Forty-Five Orientations the fibers within the printed matrix were not fully detached from the surrounding material during fracture as seen from fig 4.6 (b) and (c). This indicates that while the crack propagated, the fibers maintained some adhesion with the matrix, thereby preventing complete load transfer across the fracture plane. This behaviour suggests that the bonding between the fiber and the matrix was sufficient to sustain partial structural integrity despite crack initiation and propagation. In case Isotropic Zero figure 4.6 a and Isotropic Concentric Orientations figure 4.6 e , specimens printed in these orientations exhibited complete fiber pull out during fracture. This indicates a lower level of interfacial bonding between the fibers and the matrix material. As a result, the fibers were entirely disengaged from the matrix, leading to a failure mechanism dominated by fiber pullout rather than crack propagation through the matrix. This complete pull out suggests that the load transfer mechanism was severely compromised, resulting in a more abrupt failure. The observed differences in fracture behaviour across orientations underline the critical role of printing patterns and interfacial adhesion in the mechanical performance of 3D-printed materials. Orientations that promote stronger fiber-matrix bonding exhibit greater resistance to complete load transfer disruption, while weaker bonding leads to dominant fiber pullout mechanisms. This analysis emphasizes the importance of optimizing printing parameters to enhance the fracture resistance of 3D-printed structures.

The impact performance of 3D-printed composite materials is strongly influenced by fibre orientation and build configuration. Effective fibre-matrix bonding is critical for enhanced impact resistance; however, this bonding is often limited in porous regions of 3D-printed composites. Fibre orientation and build configuration play pivotal roles, with concentric fibre patterns and isotropic zero-degree orientations exhibiting superior impact performance compared to ninety-degree and forty-five-degree configurations. These results underscore the importance of optimizing fibre type, orientation, and volume fraction to enhance the mechanical properties of 3D-printed composites. The

addition of fibres introduces a dual effect on the structural integrity of the composite. While an increase in fibre content may elevate defect density—thereby promoting crack initiation and potentially compromising the material's integrity—fibres aligned perpendicular to the direction of crack propagation effectively inhibit crack propagation. This mechanism significantly enhances the material's resistance to fracture. When fibre content is increased to an optimal threshold, the crack-arresting capability of the fibres surpasses the negative effects of increased defect density, resulting in a net improvement in impact strength (Caminero et al., 2018).

### 4.3. Uncertainty Analysis

Uncertainty analysis is essential in experimental research to quantify variability in measured values due to inherent errors in fabrication, measurement, and testing processes. In this study, uncertainty analysis is performed on the tensile strength measurements of continuous fiber-reinforced polymer (CFRP) composites produced by 3D printing. This analysis ensures the reliability of the results by accounting for uncertainty sources such as dimensional variations in printed samples and variability in tensile test data (Shamsuri et al., 2016).$C_w$ = Sensitivity coefficients of width, $C_t$ = sensitivity coefficients of thickness as per equation 4.1, TS = tensile strength, w is the width of the sample and t is the thickness of the sample the uncertainty contribution ($u_{con}$) of each parameter is given by: $u_{con}$ = c x u, where u is the standard uncertainty of the measured parameter and c is the Sensitivity Coefficient of parameter or equipment S.

$$C_t = \frac{TS}{t} \qquad 4.1$$

The combined standard uncertainty is calculated as equation 4.2

$$u_c = \sqrt{\sum {u_{con}}^2} \qquad 4.2$$

Which considers the uncertainty contributions from width and thickness .The expanded uncertainty (U) is determined by applying a coverage factor (k) at 95% confidence level .For small sample sizes , k = 2.306 (based on Student's t-distribution ) as per equation 4.3 .

$$U = \mathrm{k} \times \mathrm{u}_c \qquad 4.3$$

Measurement uncertainty expresses the likely range within which the true value of a measured parameter is likely to exist. In tensile testing, uncertainties occur from variations in the dimensions of specimens, testing apparatus, and measuring procedures. The analysis adheres to the method outlined in the reference document and includes uncertainty contributions from sample variability and measuring instruments, such as micrometers. The uncertainty of measurement for tensile strength was estimated by using standard uncertainty, contributions to uncertainty, combined uncertainty, and expanded uncertainty at 95% confidence level. The sources of uncertainty addressed below include:

- Tensile strength measurements variability across a number of specimens.
- Dimensional measurement uncertainty from calibrated micrometers.
- The calculated uncertainties for tensile strength measurements in various fiber orientations are as below:

The standard uncertainty (u) is as per equation 4.4 for tensile strength (TS) is determined using:

$$\mathrm{u} = \frac{s}{\sqrt{n}} \qquad 4.4$$

Where:

- s is the standard deviation of tensile strength values,
- n is the number of specimens tested.

For dimensional measurements, the sensitivity coefficients were calculated using

$$C_w = \frac{TS}{w} \qquad 4.5$$

Table 4.3 Uncertainty Contribution due to fiber orientation

| **Fiber Orientation** | **Mean Tensile Strength (MPa)** | **Standard Uncertainty (MPA)** | **Expanded Uncertainty (MPa, 95 % Confidence)** |
|---|---|---|---|
| $0^0$ | 171 | 5.60 | 12.91 |
| $45^0$ | 16.3 | 1.39 | 3.20 |
| $90^0$ | 16.2 | 1.50 | 3.46 |
| Concentric | 121 | 0.96 | 2.22 |

The outcome reveals that increased uncertainty is fiber orientation-dependent. Maximum uncertainty in the 0° orientation results from greater variation in tensile strength. Concentric orientation reported the minimum uncertainty, possibly a result of a more even material distribution.

The computed expanded uncertainties as per Table 4.2 provide confidence in the provided tensile strength values as per standard deviation from Table 4.1, which is necessary for material characterization and assessment of mechanical performance. Future research can include other factors like environmental variations and operator variability to further improve the level of uncertainty estimation.

Table 4.4 Uncertainty in fiber orientation Width, thickness for the PC samples

| **Fiber Orientation** | **Vf** | **X-dimension (mm)** | | | **Mean** | **Dev.** | **Y-dimension (mm)** | | | **Mean** | **Dev.** | **Z-dimension (mm)** | | | **Mean** | **Dev** |
|---|---|---|---|---|---|---|---|---|---|---|---|---|---|---|---|---|
| | | **X1** | **X2** | **X3** | | | **Y1** | **Y2** | **Y3** | | | **Z1** | **Z2** | **Z3** | | |
| $0^0$ | 22.6 | 251.4 | 253.6 | 252.4 | 251.8 | 1.105 | 24.93 | 25.01 | 25.03 | 25.25 | 0.053 | 3.14 | 2.77 | 3.31 | 3.1 | 0.3 |
| $45^0$ | 23 | 249.601 | 249.86 | 250.13 | 249.86 | 0.265 | 26.33 | 24.83 | 24.82 | 25.33 | 0.869 | 2.83 | 3.40 | 3.23 | 3.2 | 0.3 |
| $90^0$ | 23 | 248.9 | 252.6 | 250.3 | 250.61 | 1.899 | 25.43 | 25.83 | 24.72 | 25.33 | 0.562 | 3.23 | 3.83 | 3.13 | 3.4 | 0.4 |
| Conc | 23 | 253.3 | 250.0 | 251.7 | 251.67 | 1.685 | 25.13 | 24.78 | 25.353 | 25.09 | 0.288 | 2.99 | 2.987 | 3.029 | 3.0 | 0.0 |

## CHAPTER 5

## ANALYSIS OF MECHANICAL PROPERTIES IN RELATION TO KEVLAR VOLUME FRACTION

In the previous chapter the effect of fiber orientation and pattern on the mechanical properties of the 3D printed composite was studied. Fiber orientation plays an important role in determining the mechanical performance of the FRCPs and even is responsible for anisotropy. However, the other significant parameter in FRCPs is the volume fraction of the fiber. There is a direct relation between the mechanical properties and the fiber volume fraction. In this chapter discussion about the effect of fiber volume fraction is presented and important findings have been elaborated related to a threshold value of fiber volume fraction for 3D printed samples. The control of reinforcement volume in Markforged 3D printers is meticulously managed through the adjustment of the matrix-to-fiber ratio and the utilization of fiber usage settings within the Eiger software. By specifying the fiber layout and fill density, users can precisely determine the amount of matrix material (thermoplastic) that remains in the part relative to the continuous fiber reinforcement, effectively controlling the matrix-to-fiber ratio. Furthermore, Eiger provides detailed metrics on the amount of fiber material used, which aids in planning and adjusting the reinforcement volume fraction. The effective composite volume fraction is calculated by considering the fiber volume in each layer, which is influenced by the fill density, patterns, and coverage, in relation to the total part volume, which includes both reinforced and non-reinforced layers of the thermoplastic matrix. By adjusting the relative proportion of reinforced to unreinforced layers, users can increase or decrease the overall fiber volume fraction, enabling precise tailoring of the composite's mechanical properties to meet specific application requirements.

Effective design methodology is essential for optimizing mechanical strength, incorporating factors such as fiber orientation, fiber pattern, and reinforcement levels. Notably, 3D printed Kevlar fiber-reinforced composites exhibited maximum load-bearing capabilities when printed in alignment with the direction of the print bed. The study observed that laying the fiber along the print bed orientation yielded superior

strength compared to laying the fiber in the transverse direction of loading. Moreover, enhanced impact properties were noted when the outside contour was shielded. Experimental findings also revealed a notable threefold increase in impact strength with an increase in the volume fraction of the reinforcement material.

### 5.1 Tensile Properties with Varying Fiber Reinforcement

This section delves into correlation of fiber reinforcement on tensile strength and Young's modulus of 3D printed composites. The study incorporated varying the Kevlar fiber reinforcement from 0% to 35%. The fiber orientation was kept as 0° as this yield better results compared to other orientations as discussed in the previous chapter. The other parameters were fixed for the samples. During tensile testing the specimen was continuously monitored up to fracture. Stress-strain curve was recorded and analyzed using Origin Pro 2022.6 student version. Since there is no direct control of weight or volume fraction of the fiber in the 3D printer. Therefore, an indirect method was used to calculate the volume fraction. It was calculated by the controlling the numbers of fiber layers in the sample. Since the dimensions are fixed as per the ASTM standards, the volume fraction was calculated as per the deposited fiber layers.

There is a strong correlation between varying reinforcement of fiber and tensile strength of the composite. The maximum tensile strength of 198.6 MPa is attained with a 12-layers (35% volume fraction) fiber configuration using continuous Kevlar fiber. The samples demonstrated a significant increment of 918.4% in tensile strength compared to unreinforced composite. Figure 5.1 shows the stress-strain plot of onyx sample (without fiber reinforcement). Unreinforced specimens showed a ductile failure pattern with significant plastic deformation and high tensile strain compared to reinforced samples. The ultimate tensile strength in case of thermoplastic onyx was found to be 19.5 MPa.

With increase in reinforcement the strain of 3D printed composite samples reduced, and slope of the graph increased resulting in an increase in Young's modulus and tensile strength. The graphs of 3D printed composite are linear in nature which shows they exhibit brittle behavior. Figure 5.2 to 5.4 shows the stress-strain plot for 11%, 22.6% and 35% fiber reinforcement respectively. In case of 3D printed composite, the tensile property is being governed by fiber so increase in fiber content increases tensile

property. Percentage elongation started to decrease with increase in reinforcement and least was found in case of 35% volume fraction of reinforcement. The strain for unreinforced samples was found to be 0.125 on the other hand, on introducing Kevlar fibers the strain decreased and was found to be 0.012 for 11% (sample2) volume fraction. 22.6% (sample 3) volume fraction of fiber reinforcement demonstrated strain value of 0.02. For reinforcement of 35 % (sample 4) volume fraction the strain was comparable to that of 22.6% and it was recorded as 0.02

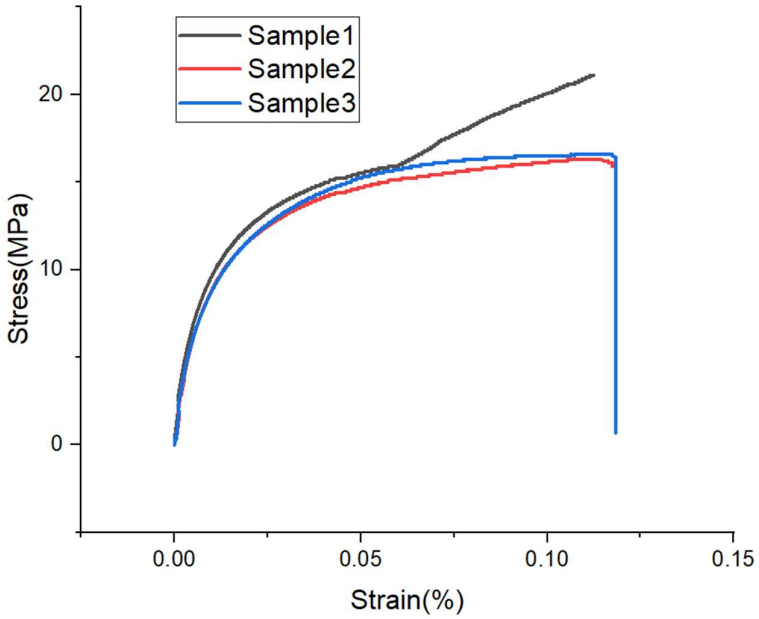


Figure 5.1 Stress strain plot for onyx specimens sample (1)

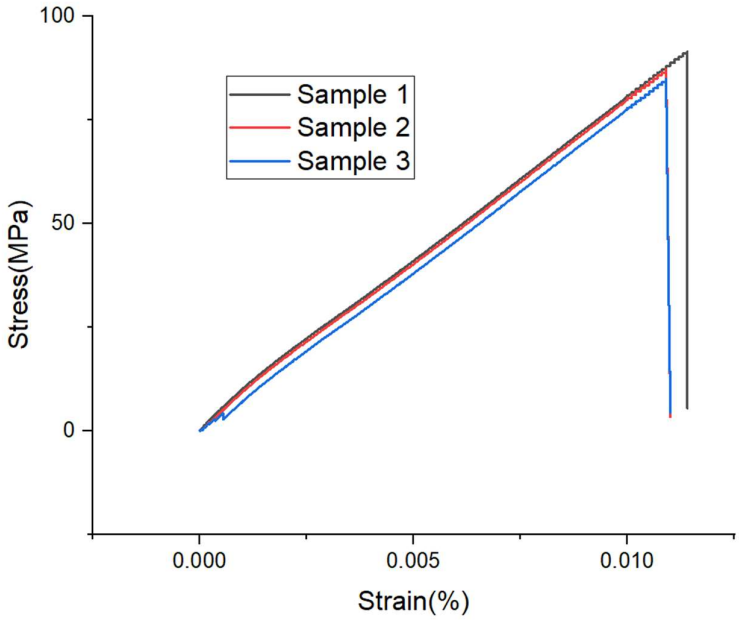


Figure 5.2. Stress strain diagram with Volume fraction of 11 % sample (2).

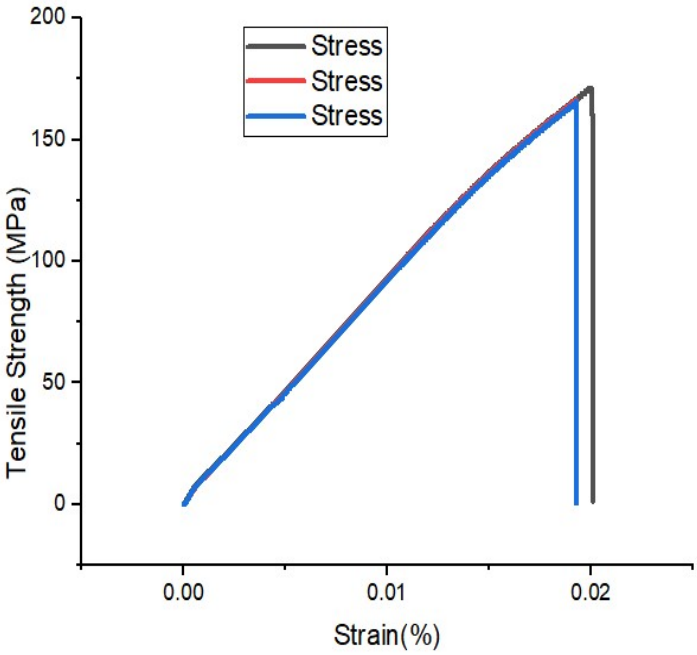


Figure 5.3. Stress strain diagram with fiber volume fraction of 22.6 % sample (3).

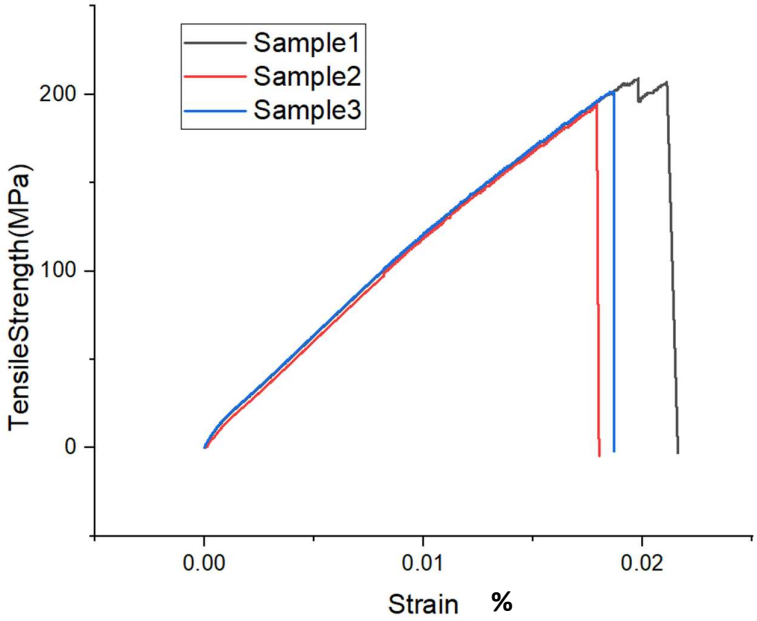


Figure 5.4. Schematic diagram showing stress strain diagram with volume fraction of 35 % sample (4).

The effect of fiber reinforcement on tensile strength and strain is illustrated in figure 5.5. It can be seen form the graph that the as fiber reinforcement increases, the tensile strength also increases and strain decreases. Notably, the introduction of a 35% volume fraction fiber (sample 4) reinforcement led to a significant increase of about 10.8/12.5 times in the tensile strength of composite compared to unreinforced samples. This strengthening effect can be attributed to the consistent alignment of continuous fibers along the load-bearing axis. The notable strength enhancement arises from the combination of amplified reinforcement, precise alignment of fibers along the load direction, and uniform fiber distribution within the onyx matrix. The unidirectional fibers withstand higher tensile stress due to the distribution of stresses along the axis on which the fibers are deposited, having minimal or no significant shear stresses to affect tensile performance (González-estrada & Pertuz, 2018). If perfect bonding is assumed between fiber and matrix and fiber and matrix are elastic then stress in matrix is always less than the stress in the reinforcement since Young's modulus of the matrix is always less than the modulus of the reinforcement. In 3D printed composite, continuous fiber has more tensile strength and elastic modulus as compared to the matrix material. In laying Kevlar fiber in longitudinal direction overall strength of the

3D printed composite is due to Kevlar fiber alone rather than onyx matrix, which plays the role of holding the matrix and transferring entire load to Kevlar fiber which is evident from the stress strain graph which shows high strength and stiffness and less strain. Tensile strength of the composites is primarily influence by contribution of fiber and surpasses matrix component because of superior property of the fiber. The mechanical performance of the composite is governed by the fiber as it withstands the external loads. Inclusion of fibers increases the stiffness of the matrix and restricts the movement of polymer chain at microscopic level. That is the reason that by adding fibers along the printing direction eradicates plasticity, reduces strain and makes it brittle (P.K. Mallick, n.d.)

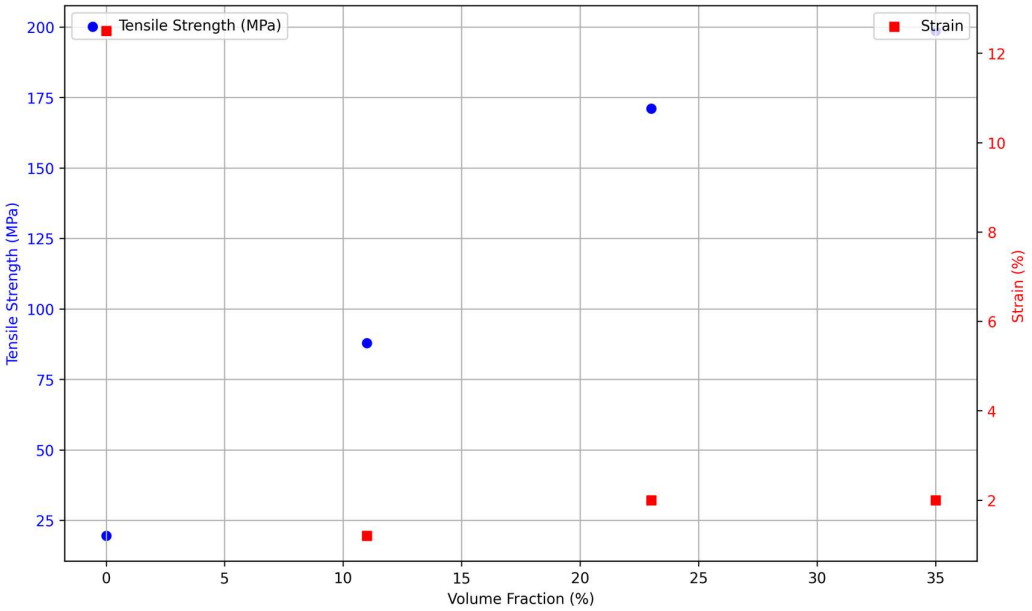


Figure 5.5 Comparison of tensile strength and strain with varying fiber volume fraction

In the context of KFRCP the fibers play a dominant role in bearing the load, the onyx matrix's contribution is pivotal, onyx matrix serves multiple purposes, including conferring directional attributes, encapsulating the reinforcement, and facilitating load transmission.

Ductile fracture in 3D-printed specimens occurs due to mechanisms involving void nucleation, growth, and coalescence. In ductile materials, microvoids typically form at imperfections, such as weakly bonded areas between printed layers, and the absence of reinforcements allows these voids to grow and coalesce freely under stress. Except the onyx sample others failed near the grip area. In sample with volume fraction between 11-22.6% the composite failed due to fiber pull off. This indicates good bonding between fiber and the matrix. In sample with 35% delamination was observed and the layers of the matrix and reinforcement was peeled off (Figure 5.6 a). Reinforced samples were observed to have a brittle type fracture and all failed with strong sound of energy release. Strength and ductility of 3D printed part is correlated to reinforcement level with higher increase in reinforcement ductility was decreased. The strength and ductility of each specimen was found dependent on their Kevlar fiber volume fraction levels. An angled crack was observed in unreinforced onyx specimen. In case of thermoplastic onyx impregnated with 11-22.6% of continuous Kevlar fiber complete fiber pull out was observed in Fig 5.6 b and c. 3D printed KFRCP with approximately 35 % volume fraction delamination was observed. Reinforcement layer was peeled off from the matrix layer due to poor bonding between the matrix and the reinforcement, leaving all load to the reinforcement. During delamination an explosive sound is observed.

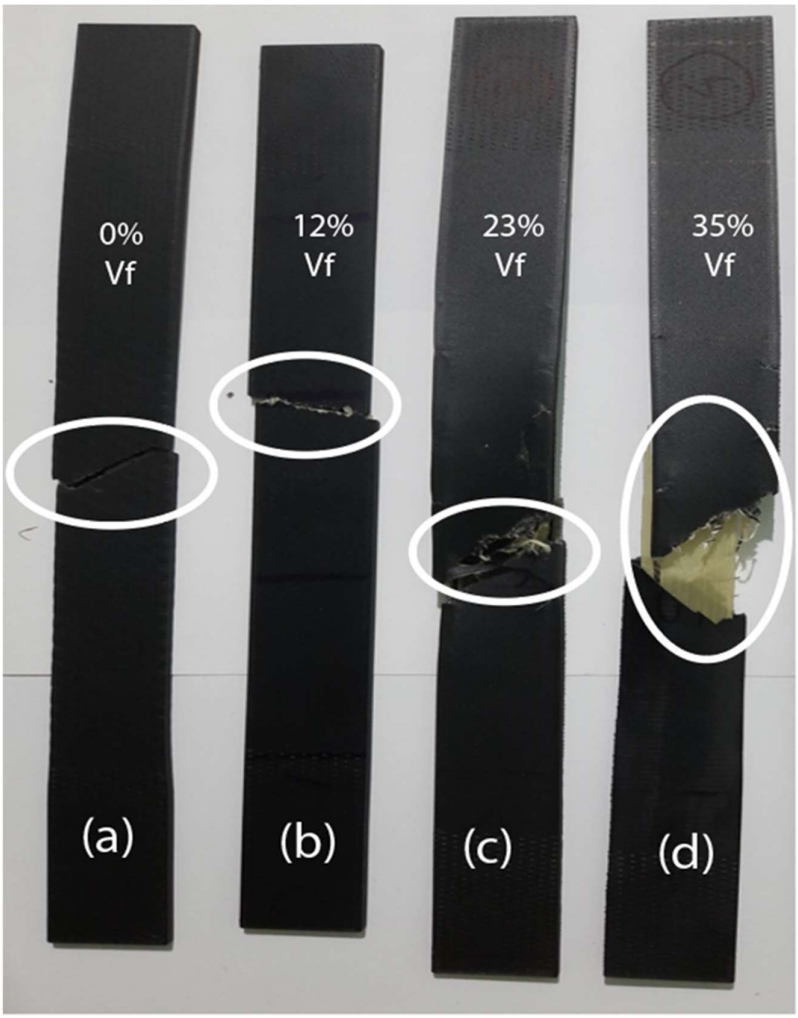


Figure 5.6 Schematic diagram showing Different types of failure in 3D printed KFRCP (a) Unreinforced thermoplastic onyx material (b) 11% (c) 22.6% and 35% volume fraction

Three types of failure have been observed in tensile testing of fiber reinforced specimens. Samples having zero layers of Kevlar fiber (onyx specimens) is observed to have an angled middle crack. Specimens reinforced with 11% volume fraction of fibers are found to have angled middle failure. As the volume fraction was increased beyond this value the specimens showed delamination behavior. In 3D-printed fiber reinforced samples, the role of onyx (matrix) is to transfer load to reinforcement (Kevlar). The overall strength is achieved if there is proper synergy between matrix and reinforcement. The bonding strength between fiber and matrix is weak as compared to

the strength of the fiber. In case samples with fiber reinforcement, if there is angled middle crack, then it shows that the matrix is able to wet the fiber properly. In uniaxial loading, complete load is being transferred from onyx to Kevlar fiber. However, after 8 layers, delamination was observed. When the matrix is unable to wet the fiber, the onyx (matrix) and Kevlar (reinforcement) layers separate. Delamination is a major issue in case of 3D-printed continuous fiber composites where the matrix material is unable to hold the fiber during external loading and the layer between fiber and the matrix peels off. This is due to weak bonding between the matrix and the fiber interface. Visual inspection was used to identify different types of failure, as shown in figure 5.7. Figure 5.7b, shows that there is an angled crack in the specimens. However, in case of delamination phenomenon, the bundled fibers are pulled off, as shown in Fig. 5.7c. The pulled out bundled fiber is at the interface between the matrix and the fiber. Delamination between the fiber and matrix was evident as the fiber volume fraction is increased as depicted in figure 5.7d. This information provides insight into the crucial factor of selecting the threshold value of the fiber in 3D printed continuous fiber composites. Table 5.1 shows a comparison of achieved tensile properties of FRCPs with elsewhere reported work.

### 5.1.1. Comparison of the Enhanced Mechanical Properties at Maximum Fiber Loading with Those of Unreinforced 3D-Printed Samples.

The composite material's modulus is a weighted combination of the modulus of the reinforcement and the matrix, as described by models like the rule of mixtures. The reinforcement provides a high surface area for stress transfer through the matrix-reinforcement interface. As the percentage of reinforcement increases, the effective load-transfer area increases, improving strength. Strong interfacial bonding (e.g., through adhesion or mechanical interlocking) ensures efficient stress transfer. The shear stresses at the interface resist relative motion between the matrix and reinforcement, preventing failure. Higher reinforcement content can optimize the microstructure by, reducing voids and flaws in the matrix. Providing uniform stress distribution. Enhancing thermal and mechanical properties due to a more interconnected structure. The stiffness of the material is dictated by the matrix material, often resulting in lower stiffness values that may not suffice for load-bearing

applications. Reinforced Samples with high fiber loading results in the introduction of fibres typically results in a marked increase in stiffness. The modulus of elasticity can increase by 20-60%, depending on the fiber type and orientation. This enhances the composite's overall structural performance, making it suitable for applications requiring rigidity. Unreinforced Samples typically exhibit lower tensile strength due to the absence of continuous fibres. The matrix alone bears the load, which can lead to earlier failure under tensile stress. The inclusion of continuous fibres significantly enhances tensile strength. Fibers aligned in the load direction improve load transfer efficiency, resulting in higher resistance to deformation and fracture. 3D-printed composites with high fiber loading demonstrate significantly improved mechanical properties over unreinforced samples across various metrics. The physics behind the improved tensile strength in fiber-reinforced materials revolves around the way fibers interact with the matrix material under stress. Fibers generally have a much higher tensile strength and modulus than the matrix, so they can bear a larger portion of the load. This load-sharing effect means that the fibers handle the bulk of the applied stress, resulting in an overall increase in tensile strength. In unreinforced materials, cracks can spread quickly under tensile stress, leading to material failure. In fiber-reinforced composites, however, fibers act as barriers to crack propagation. When a crack encounters a fiber, the fiber can stop or redirect the crack, thus increasing the energy required to propagate it further. This slows down or halts the crack growth, enhancing the material's overall resistance to fracture under tensile loads. Fibers within the matrix help to distribute stress more evenly throughout the material. In an unreinforced matrix, stress tends to concentrate at weak points, which can lead to localized failure. With reinforcement, the fibers help dissipate the applied force, reducing these stress concentrations and making the composite less likely to fail at any single point. Fibers are typically stiffer than the matrix material, meaning they have a higher modulus of elasticity. This stiffness limits the strain (deformation) that the composite undergoes when under tension. As a result, the entire composite becomes less prone to stretching, which improves its tensile strength and rigidity. These mechanisms combine to make fiber-reinforced materials much stronger in tension than their unreinforced counterparts. The physics behind these interactions—load transfer, crack resistance, even stress distribution, and strain limitation—creates a synergistic effect that boosts

the tensile strength and makes fiber-reinforced materials highly effective in structural and load-bearing applications. Stress distribution becomes more homogeneous, reducing weak points. Up to a certain percentage, increasing reinforcement improves properties. Beyond this point Reinforcement may agglomerate, causing stress concentrations. The matrix may no longer fully bind the reinforcement, reducing efficiency. Ductility decrease as the material becomes brittle due to weak interlayer adhesion between the fiber and the matrix (Tóth et al., 2024).

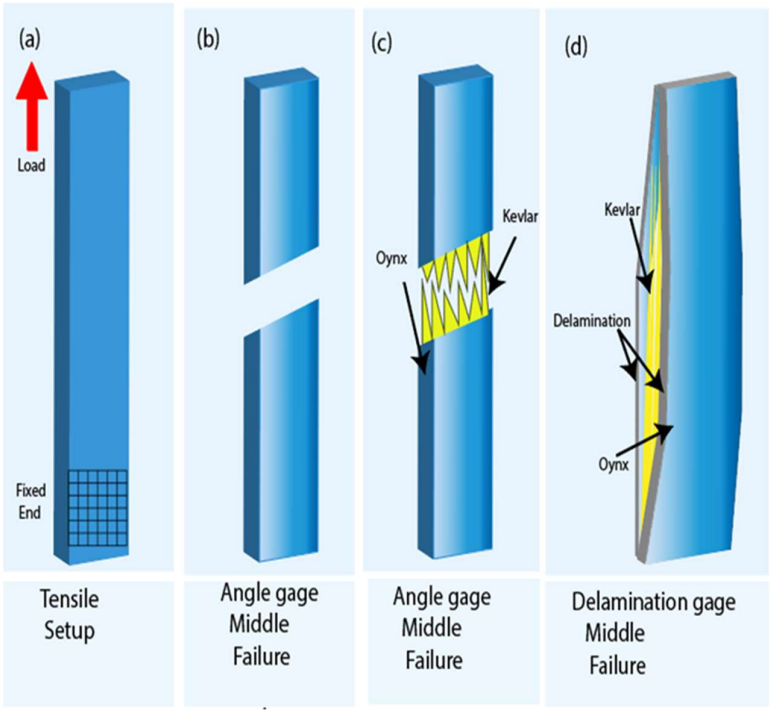


Figure 5.7 Schematic diagram showing different types of failure in 3D printed KFRCP (a) Unreinforced thermoplastic onyx material (b) 11% beyond which delamination was observed (c) 22.6% and 35% volume fraction

Table 5.1 Comparison of tensile properties

| Matrix | Volume Fraction (%) | Mean Tensile Strength (MPa) | Mean Young' Modulus (G Pa) | Reference |
|---|---|---|---|---|
| Nylon | 10 | 161 | 4.26 | (Dickson et al., 2017) |
| Nylon | 18 | 35.57 | 9.57 | (Melenka et al., n.d.) |
| Nylon | 41 | 305.2 | 25.5 | (Mohammadizadeh & Fidan, 2021a) |
| Nylon | 43 | 309.14 | - | (Mohammadizadeh & Fidan, 2021a) |
| Nylon | 57 | 261.95 | - | (Araya-Calvo et al., 2018) |
| Nylon | 90 | 305.2 | - | (Chacón et al., 2017) |
| *Onyx* | *0* | 19.5± 2.2 | 1.81 | *This Work* |
| *Onyx* | *11* | 87.9±5 .6 | 7.86 | *This Work* |
| *Onyx* | *22.6* | 171± 9.7 | 8.64 | *This Work* |
| *Onyx* | *35* | 198.6± 10.6 | 10.52 | *This Work* |

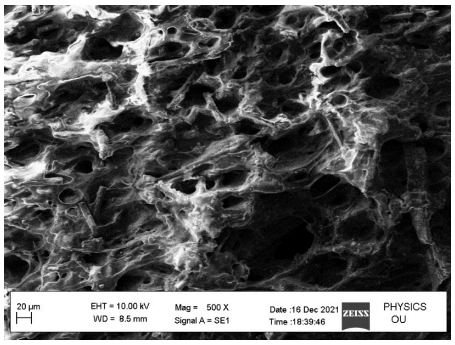


(a) 0 %

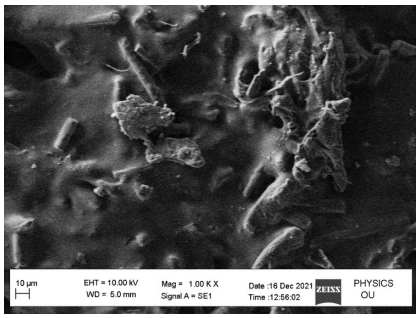


(b) 11 %

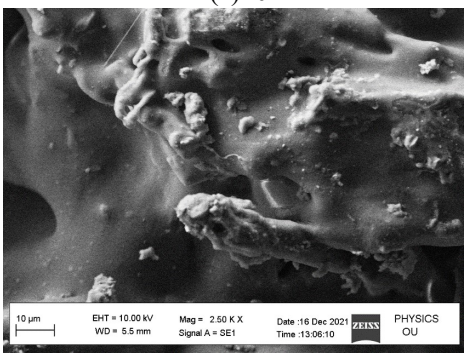


(c)22.6 %

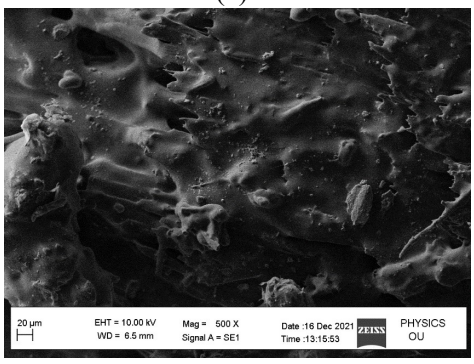


(d) 35 %

Figure 5.8 Sem Image of Fractured surface (a) Unreinforced thermoplastic onyx material (b) 11% beyond which delamination was observed (c) 22.6% and (d)35% volume fraction

Ductile matrix deformation was observed in Onyx specimens due to the presence of voids in 3D-printed Kevlar fiber-reinforced composite polymers (K.F.R.C.P.), as illustrated in (figure 5.8a) Regions exhibiting ductile fracture were characterized by dimples formed via micro-void coalescence, indicating extensive plastic deformation preceding failure. In specimens with 0% fiber reinforcement, failure behaviour was dominated by gradual fiber failure accompanied by plastic deformation. A correlation between the observed fracture morphology and the mechanical properties of the composite matrix revealed that ductile behaviour was primarily governed by reinforcement followed by substantial plastic deformation before ultimate failure. The morphology, size, and distribution of the dimples provided critical insights into the composite matrix's ductility and deformation behaviour. Microscopic analysis of 3D-printed K.F.R.C.P. specimens revealed distinct failure characteristics influenced by material composition and processing parameters. Brittle fracture modes, predominantly associated with Kevlar fibers or interfacial failures, were identified by features such as fiber pull-out, fiber breakage, and matrix cracking (figure 5.8b). In specimens with 22.6% fiber reinforcement, failure mechanisms included fiber-matrix debonding and delamination, indicating potential process-induced defects brittle fiber breakage was the predominant failure mechanism, highlighting the trade-off between reinforcement and structural integrity in 3D-printed composite systems (figure 5.8c).For specimens with 35% fiber reinforcement, delamination was observed, attributed to weak interlayer adhesion. Additionally, mixed failure modes, including fiber breakage, pull-out, and splitting, were evident. The presence of brittle features such as fiber cleavage and pull-outs suggested the intrinsic limitations of Kevlar fibers in accommodating significant deformation (figure 5.8d).

### 5.2 Delamination Behavior of Composite

In order to critically examine the delamination behavior, the continuous FRCP, the fiber volume fraction was increased further from 35%. The issue of delamination was initially observed during the 3D printing process itself as the fiber volume fraction was increased. In cases where the fiber content exceeded 20 layers (58% volume fraction), as illustrated in figure 5.8, the interface between the matrix and reinforcement was pulled away. The peeling off of the interface indicated a failure mechanism where the matrix was unable to transfer any load, leading to the ultimate failure of the composite due to a lack of proper bonding between the matrix and fiber.

Three distinct failure modes were identified in as discussed in the previous section of the chapter. For composites having 0-11% volume angled cracks were observed. In case of angled cracks all fibers were observed to be pulled out, indicating a cohesive synergy between the matrix and the reinforcement. When the volume fraction was in the range of 22.6% - 58%, partial delamination was observed. Delamination manifested as bundles of fibers being pulled out together, indicating a weakened bond between the matrix and fiber interface. Delamination occurs when the matrix fails to adequately wet the fibers, resulting in insufficient synergy between the two components. However, beyond this threshold value of continuous Kevlar fiber reinforcement in onyx matrix the delamination was dominated. It was observed experimentally that fiber layer can take maximum load up to 58% volume fraction of fiber beyond which (64%.) it resulted in complete delamination. However, in case of composites with 64% the failure was due to delamination. In this case the matrix completely peeled of and it was unable to do testing further. Figure 5.9 illustrates the fiber pull out and delamination of samples in terms of increasing volume fraction range.

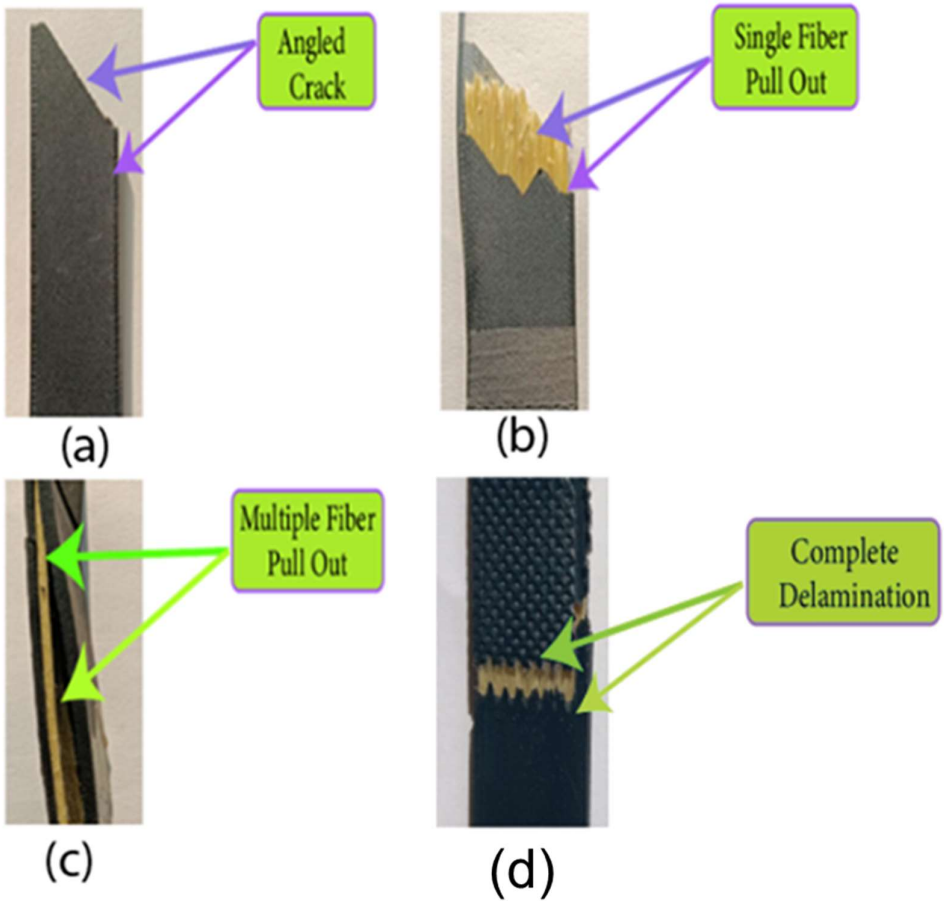


Figure 5.9: Fracture, delamination and fiber pull out in 3D printed FRCPs (a) Unreinforced thermoplastic onyx material, fiber reinforcement of: (b) 11%, (c) 22.6% -58 % and (d) 64% (complete delamination)

Table 5.3 Maximum tensile strength before delamination

| Matrix | Volume Fraction (%) | Mean Tensile Strength (MPa) | Standard Deviation | Reference |
|---|---|---|---|---|
| *Onyx* | 0 | 19.5 | ±2.2 | *This Work* |
| *Onyx* | 5.8 | 56.1 | ±4.3 | *This Work* |
| *Onyx* | 11 | 87.9 | ±5.6 | *This Work* |
| *Onyx* | 17.44 | 150 | ±8.2 | *This Work* |
| *Onyx* | 22.6 | 171 | ±9.7 | *This Work* |
| *Onyx* | 29.06 | 183.18 | ±12.4 | *This Work* |
| *Onyx* | 35 | 198.6 | ±10.6 | *This Work* |
| *Onyx* | 40.69 | 280.5 | ±19.5 | *This Work* |
| *Onyx* | 46.50 | 313.5 | ±13.6 | *This Work* |
| *Onyx* | 52.32 | 356.7 | ±11.6 | *This Work* |
| *Onyx* | 58.13 | 405.7 | ±17.8 | *This Work* |

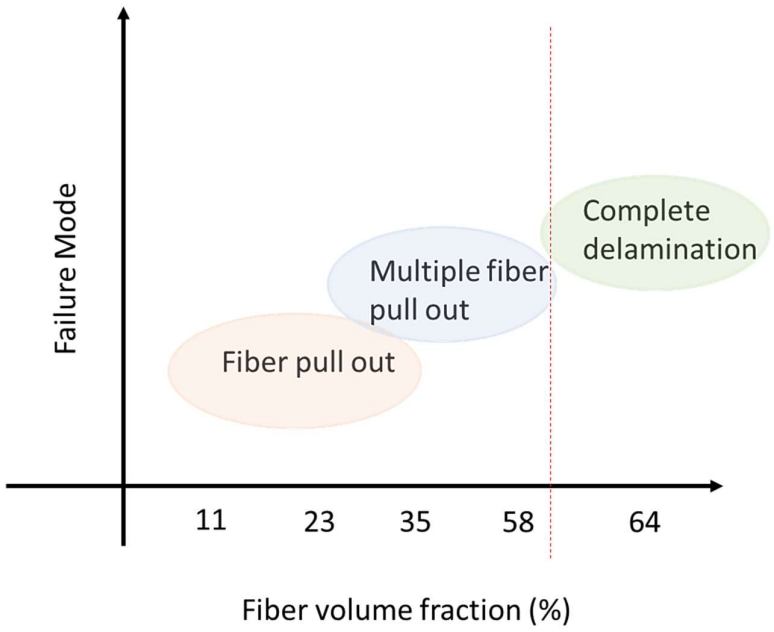


Figure 5.10 Delamination with respect to volume fraction

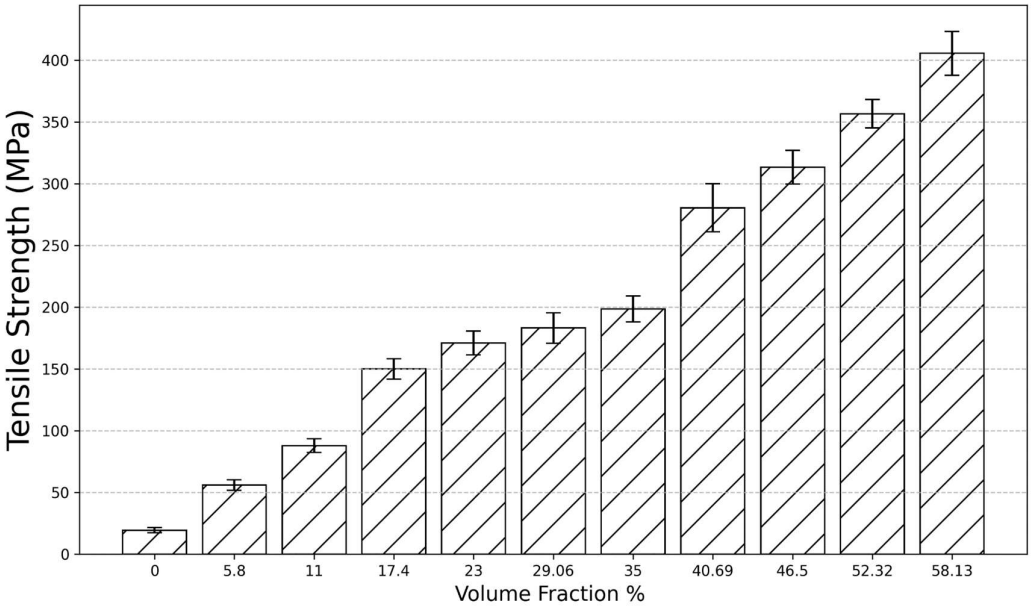

Figure 5.11 Experimental tensile strength with change in volume fraction

Considering continuous Kevlar FRCP to be a square array as shown in Figure 5.10 having length l and radius of Kevlar fiber in unit cell to be $r_{kf}$.

Area of the fiber in the unit cell is $A_{kfrcp}$. Area of the unit cell is $A_{uc}$. Fiber volume fraction is $v_f$. Length of the unit cell of the cube is considered to be l. Interspacing between middle fiber and each side fiber is given by R. If the 3D printed composite is arranged in an array of square as shown in figure 5.10. In order to calculate the fiber volume fraction that can be added in the matric for development of continuous fiber composites the following equation were used:

The maximum theoretical volume fraction of reinforcement that can be obtained is approximately 78.5 % as per equation 5.6. As observed in experimentation it becomes apparent that up to 34% there is a significant increase in tensile strength. However, beyond which the strength becomes marginal which suggest that further impregnating more reinforcement does not result in substantial increase in tensile strength. The effective fiber content for 3D printed composite is up to 30%. This conclusion is also supported by previous research work (P.K. Mallick, 2007).

The number of fibers within one unit cell can be calculated by:

Number of fibers in a one-unit cell = (4) (1/4) + 1 = 2

The cross-sectional area occupied by the fibers, $A_{kfrcp}$is: $A_{kfrcp}$= (2) ( $\pi r_{kf}^2$) (5.1)

The area of the unit cell, $A_{uc}$ , is given by: $A_{uc} = l^2$ (5.2)

The volume $v_f$ fraction then becomes: $v_f = \frac{(2)\,(\pi r_{kf}^2)}{l^2}$ (5.3)

The length lll in terms of volume fraction $v_f$ and fiber radius $r_{kf}$ can be derived as: $l = \frac{\sqrt{2\pi}}{v_f^{1/2}} r_{kf}$ (5.4)

To maximize the volume fraction, we consider RRR (the radius of the cell's effective volume):$R = \frac{l}{\sqrt{2}} - 2r_{kf} = r_{kf}\left[ \left(\frac{\pi}{v_f}\right)^{1/2} - 2\right]$ (5.5)

SettingR=0 leads to the maximum volume fraction, where: For maximum volume fraction, R = 0, $v_{fmax}$ = 78.5% (5.6)

$R_f = \frac{F_r}{F_t}$ Finally, the reinforcement factor, $R_f$ which is the ratio of tensile strength of the reinforced composite $F_r$ to that of the unreinforced matrix $F$ , is expressed as (5.7)

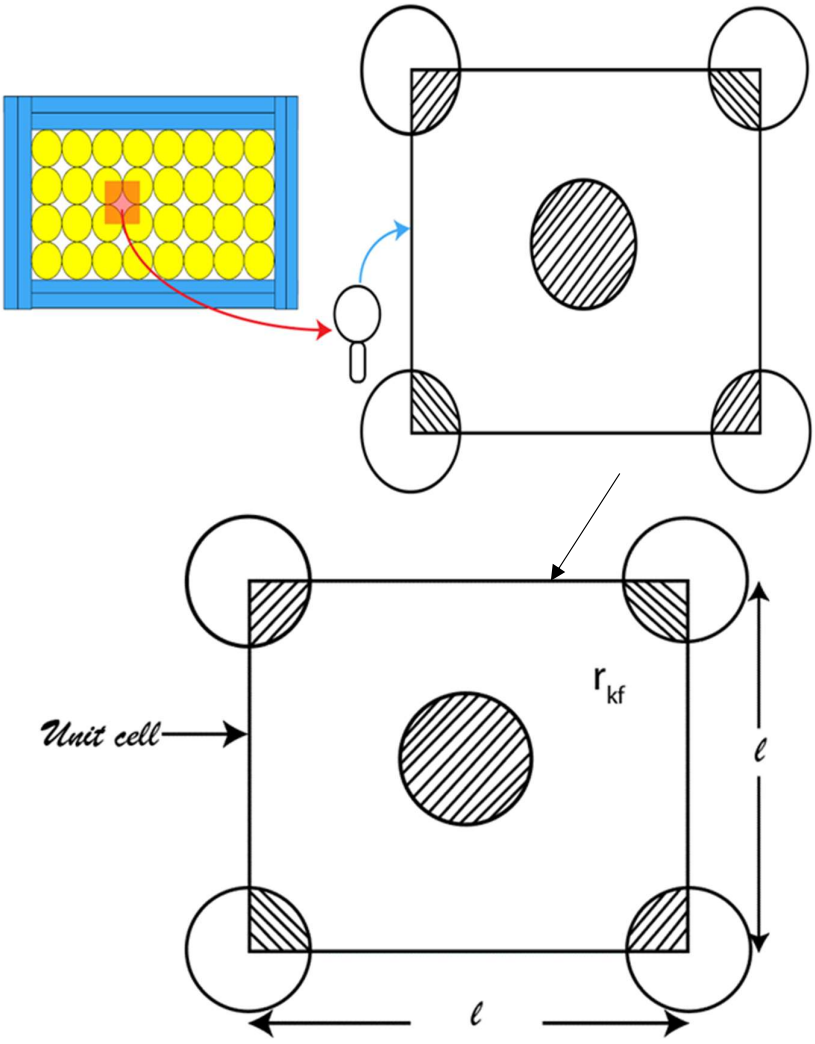


Figure 5.12 Schematic diagram representing detailed 3D printed part as square array and nomenclature used in square array

### 5.3 Impact Properties with Varying Fiber Reinforcement

The total energy absorbed during impact tests is closely correlated with the total volume fraction of reinforcing fibers. This section investigates into a comprehensive analysis of the impact strength exhibited by 3D printed Kevlar FRCP plastics. The scope of investigation encompasses a spectrum of fiber layer variations, ranging from 0 to 50 layers, corresponding to volume fractions of 0 %, 5.81%, 8.09%, 16.41%, 25%, 33.81%, and 42.79%. Parameters fixed in this study are feed rate fill density, matrix, reinforcement material and fiber angle (0°). Empirical observations elucidate a discernible and direct correlation, as anticipated, between the reinforcement level and the impact properties of the fiber material. Notably, the highest level of impact strength, approximately 90.675 KJ/m2, is attained when the Kevlar volume fraction reaches 42.79%. Conversely, samples composed exclusively of onyx or devoid of any Kevlar layers exhibit the lowest impact strength at 30.837 KJ/m2. The increase in volume fraction causes a remarkable threefold amplification in the impact strength of composite. Impregnated Kevlar fiber withstood maximum load imparting an impact property to 3D printed composites. This enhanced impact strength can be principally ascribed to the consistent alignment of continuous fibers along the load-bearing axis. Within the framework of continuous FRCPs, the onyx matrix fulfills several pivotal roles, encompassing the provision of directional attributes, encapsulation of the reinforcement fibers, and facilitation of load transmission. While the fibers play a primary role in bearing the load, the contribution of the onyx matrix holds equal significance. The substantial augmentation in strength arises from a synergistic amalgamation of heightened reinforcement, precise alignment of fibers along the load-bearing direction, and uniform dispersion of fibers within the onyx matrix. The increase in fiber content restricts the polymer flow and prevents the propagation of crack resulting in impact strength. It is noteworthy that no external pressure was applied during printing process which play a crucial role on manufacturing conventional composites which otherwise create void. Void is one of the predominate phenomenon which occurs while 3D printing.

Thermoplastic material with less reinforcement has more void and weak bonding. With increase in reinforcement void is reduced resulting in an increase in impact strength. All specimen breaks due to delamination. Breakage was observed at the layer. Table 5.2 shows the comparison of impact strength on increasing the fiber volume fraction. The data illustrates the impact strength of a composite material at various fiber volume fractions. As the fiber volume fraction increases from 0% to 42%, there is a clear trend of improvement in impact strength. A substantial increase of 190% was observed on comparing unreinforced samples with the 42% volume fraction of fibers as depicted in figure 5.12. At the lowest fiber volume fraction of 0%, the impact strength stands at 30.837 KJ/m2, suggesting the material's vulnerability to impact. However, as the fiber volume fraction increases, so does the impact strength, indicating enhanced resistance to mechanical forces. Notably, there is a substantial increase in impact strength with increase in fiber volume fraction, where the strength increases from 30.83 KJ/ m2 to 90.675 KJ/m2 more than 100%. Beyond this, the rate of improvement in impact strength becomes more gradual, with smaller increments in strength observed at higher fiber volume fractions. This data underscores the importance of fiber reinforcement in enhancing the mechanical properties of composite materials, providing valuable insights for materials engineering and structural design applications.

Table 5.4: Experimental results of Impact strength obtained by increasing reinforcement

| **Fiber volume fraction (%)** | **Impact strength KJ/m2** | **Standard Deviation** |
|---|---|---|
| 0 | 30.84 | ± 0.29 |
| 5 | 39.91 | ±0.79 |
| 8 | 62.16 | ±1.21 |
| 16 | 67.27 | ±1.21 |
| 25 | 74.72 | ±0.77 |
| 33 | 84.48 | ±1.06 |
| 42 | 90.68 | ±1.07 |

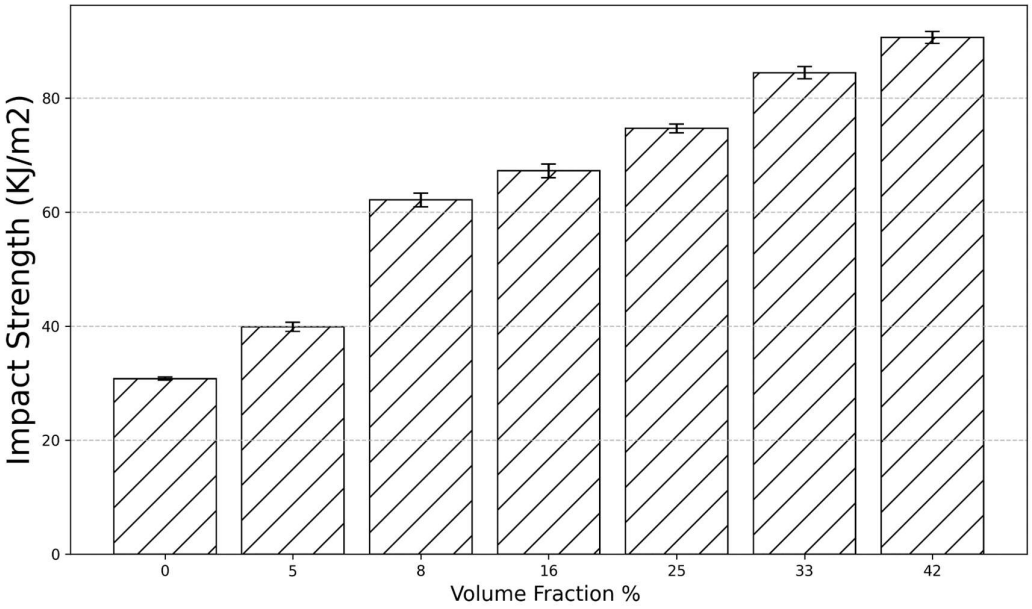


Figure 5.13 Increment in impact strength of composite compared to unreinforced samples

### 5.3.1. Comparison the improved mechanical properties achieved by the highest fiber loading with unreinforced 3D Printed sample

The enhanced impact performance of fiber-reinforced 3D-printed composite materials is governed by the interaction between reinforcing fibers and the matrix under dynamic loading. When subjected to impact forces, the matrix transfers stress to the reinforcing fibers through shear stresses at the fiber-matrix interface. Fibers, with their higher modulus of elasticity and tensile strength, absorb a significant portion of the applied energy, reducing the stress on the matrix and delaying failure. In unreinforced materials, the matrix alone absorbs the energy, leading to localized plastic deformation, crack initiation, and rapid failure due to its limited toughness. In reinforced composites, the fibers bear most of the load, mitigating strain on the matrix and enhancing resilience. Furthermore, fibers improve crack resistance through mechanisms such as crack path redirection, which increases crack length and energy dissipation, and bridging crack faces to slow crack growth. These mechanisms contrast with unreinforced materials, where cracks propagate unhindered, resulting in brittle failure. Fibers also distribute stress more uniformly, minimizing localized concentrations that lead to crack initiation. Their high stiffness limits overall deformation, preventing excessive strain in the matrix

and further improving impact resistance. The impact strength of fiber-reinforced composites is significantly influenced by fiber orientation and material properties. Aligned fibers maximize energy absorption and deformation resistance in the load direction, while randomly oriented fibers provide multidirectional reinforcement. High-modulus fibers, like carbon fibers, enhance performance by resisting deformation under sudden forces. The bond at the fiber-matrix interface is critical, with strong bonding ensuring efficient stress transfer and poor bonding leading to weak points that compromise impact resistance. Techniques like surface treatments and optimized printing parameters enhance this bonding and overall performance. The synergistic effects of load sharing, crack resistance, stress distribution, and strain limitation result in higher energy absorption, reduced failure probability, and improved durability under repeated or high-magnitude impacts. These mechanisms make fiber-reinforced composites significantly tougher, more resilient, and capable of withstanding dynamic loads, making them ideal for demanding applications in aerospace, automotive, and structural engineering industries. The enhanced impact performance of fiber-reinforced 3D-printed composite materials is governed by the interaction between reinforcing fibers and the matrix under dynamic loading. When subjected to impact forces, the matrix transfers stress to the reinforcing fibers through shear stresses at the fiber-matrix interface. Fibers, with their higher modulus of elasticity and tensile strength, absorb a significant portion of the applied energy, reducing the stress on the matrix and delaying failure. In unreinforced materials, the matrix alone absorbs the energy, often leading to localized plastic deformation, crack initiation, and rapid failure due to its limited toughness. Additionally, unreinforced samples tend to have higher void content, a result of the inherent limitations in layer bonding during the 3D printing process. These voids act as stress concentrators and crack initiation sites, significantly reducing the material's impact resistance.In reinforced composites, the addition of fibers reduces the void content by improving the packing density and interfacial bonding between layers (figure 5.11). The fibers fill gaps within the matrix, minimizing defects and creating a more uniform and compact structure. This reduction in voids enhances the material's structural integrity and prevents the rapid propagation of cracks that often originate from voids in unreinforced materials. Furthermore, the fibers bear most of the load in reinforced composites, mitigating strain on the matrix and enhancing overall resilience.

Fibers also improve crack resistance through mechanisms such as crack path redirection, which increases crack length and energy dissipation, and bridging crack faces to slow crack growth. These mechanisms contrast sharply with unreinforced materials, where voids exacerbate crack propagation and lead to brittle failure. Fibers distribute stress more uniformly, minimizing localized concentrations that contribute to void collapse and crack initiation. Their high stiffness limits overall deformation, preventing excessive strain in the matrix and further improving impact resistance.

The impact strength of fiber-reinforced composites is significantly influenced by fiber orientation and material properties. Aligned fibers maximize energy absorption and deformation resistance in the load direction, while randomly oriented fibers provide multidirectional reinforcement. High-modulus fibers, like carbon fibers, enhance performance by resisting deformation under sudden forces. The bond at the fiber-matrix interface is critical, with strong bonding ensuring efficient stress transfer and poor bonding leading to weak points that compromise impact resistance.

The synergistic effects of load sharing, crack resistance, stress distribution, strain limitation, and void reduction result in higher energy absorption, reduced failure probability, and improved durability under repeated or high-magnitude impacts. These mechanisms make fiber-reinforced composites significantly tougher, more resilient, and capable of withstanding dynamic loads, making them ideal for demanding applications in aerospace, automotive, and structural engineering industries.

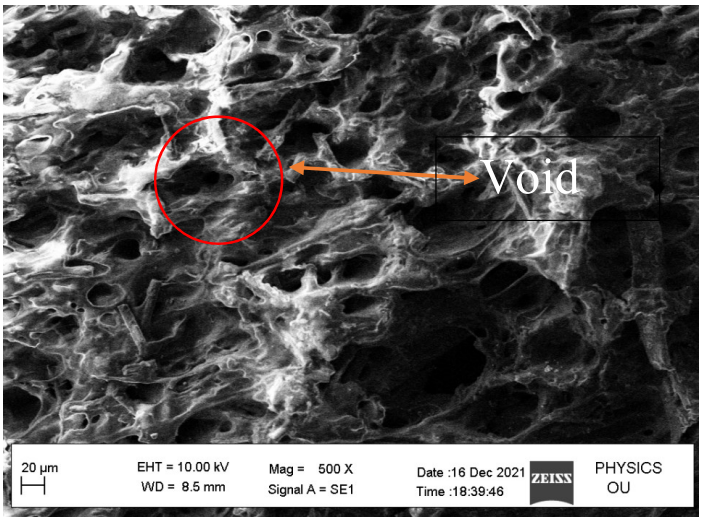


Fig.5.14 Schematic showing 3D printed specimen with 0 % reinforcement with void

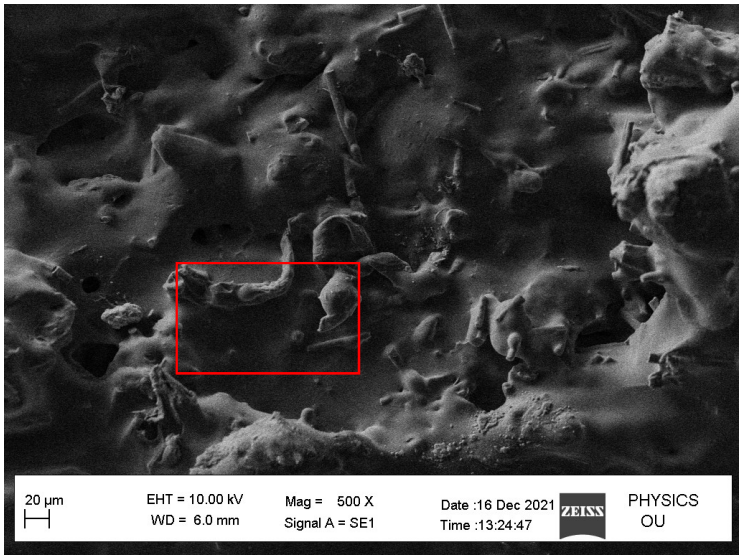


Fig.5.15 Schematic 3D printed specimen with 5% reinforcement representing absence of void

# CHAPTER 6

# COMPARATIVE ANALYSIS OF FIBER REINFROCED COMPOSITE

In the previous chapter's discussion was made related to the effect of fiber orientations and volume fraction on mechanical properties of the continuous FRCPs fabricated by 3D printing process. In this chapter investigations are carried out to study the effect of manufacturing process on the mechanical properties of the FRCPs. A comparative analysis is carried out further, conventional manufacturing technique is compared with the 3D printing process in respect to their mechanical performance.

The aim is to identify the mechanical behavior of composite materials as part of their manufacturing processes. The tensile samples were manufactured using 3D printing method. Additionally, their counterparts were made using a traditional process in which Kevlar fibers were manually placed between layers of onyx fibers using hand-layering techniques and then compression moulded. Through this comparison information on the effectiveness of various manufacturing techniques in optimizing the mechanical properties of Kevlar fiber-reinforced composites is obtained, thereby making a valuable contribution to materials science and engineering.

## 6.1 Manufacturing Process

The fabrication process of samples using the conventional technique involved careful attention to detail to ensure uniformity and consistency in the fiber-reinforced composites. Initially, Kevlar fibers were manually laid up between layers of Onyx filaments, a process known as hand layup. This method ensured placement of the Kevlar fibers within the composite structure. The Onyx filaments served as the matrix material, providing a supportive framework for the Kevlar fibers. Subsequently, the composite structure underwent compression moulding, where pressure and heat were applied to consolidate the materials and promote bonding between the fibers and the matrix. This step may enhance the structural integrity and mechanical properties of the composite.

In parallel, tensile specimens as per the standard were fabricated using additive manufacturing through 3D printing. Two layers of Kevlar were strategically sandwiched between layers of Onyx matrix material during the printing process. The use of 3D printing allowed for precise control over the placement and orientation of the

fibers within the composite, ensuring consistency and reproducibility across samples. Throughout the fabrication process, proper measures were taken to maintain identical percentages and locations of fiber content in both the 3D printed and conventionally manufactured samples. This attention to detail minimized variations in the material composition and structure, facilitating a meaningful comparison of the mechanical properties between the two fabrication methods.

In the conventional technique employed for fabricating composites, several key parameters were carefully selected to ensure optimal processing conditions and the attainment of desired material properties. The machine capable of applying load of 5 tones was used to apply a pressure of 25 kg/cm$^2$ during the fabrication process, aiding in the compaction of the composite materials and promoting intimate contact between the reinforcing fibers and the matrix material. A temperature of 145 degrees Celsius was maintained throughout the fabrication process, a critical factor in facilitating the curing and bonding of the composite constituents while ensuring minimal thermal degradation of the materials involved. Additionally, a time frame of 20 minutes was designated for the fabrication process, allowing sufficient duration for the curing reaction to occur and for the consolidation of the composite structure. Table 6.1 shows the parameters selected for fabrication of samples by conventional process. Figure 6.1b, illustrate the specimen fabrication process via conventional manufacturing technique.

The specimens were molded using a mold to attain the specified specimen dimensions as per ASTM standards. The fabrication process began by layering Onyx material at the bottom of the mold, followed by the deposition of Kevlar filament layers in accordance with the predetermined volume fraction of fiber used in the 3D printed samples. To maintain consistency for comparison purposes, filaments of Onyx and Kevlar were utilized instead of Kevlar woven matte, ensuring that the same grade of material was employed as in the 3D printed samples. Both Onyx and Kevlar are proprietary materials of the machine manufacturer, necessitating their use in the conventional fabrication technique.

The fabrication process continued by layering Onyx material at the top of the composite structure, thus creating a sandwiched arrangement with the Kevlar fibers positioned in the middle. This configuration was designed to ensure the optimal distribution and alignment of the fibers within the composite matrix. Subsequently, the mold containing

the composite specimen was placed in a compression molding machine where it was heated to around its softening point, and pressure was applied to facilitate proper fusion of the polymer matrix and ensure a homogeneous internal structure.

After the molding process, the samples were carefully removed from the mold and allowed to cool to room temperature for 24 hours. Once cured, the samples were used to perform the tensile testing to evaluate their tensile properties. Figure 6.1 illustrates the comparison of 3D printing process and conventional process for composite fabrication. For preparation of samples by 3D printing process same procedural steps were utilized as discussed in previous chapters. The fibers were deposited at 0° orientations.

Table 6.1 Parameters for conventional composite fabrication

| **Parameters** | **Values** |
|---|---|
| Temperature (°C) | 145 |
| Time (min) | 20 |
| Pressure (kg/cm2) | 25 |

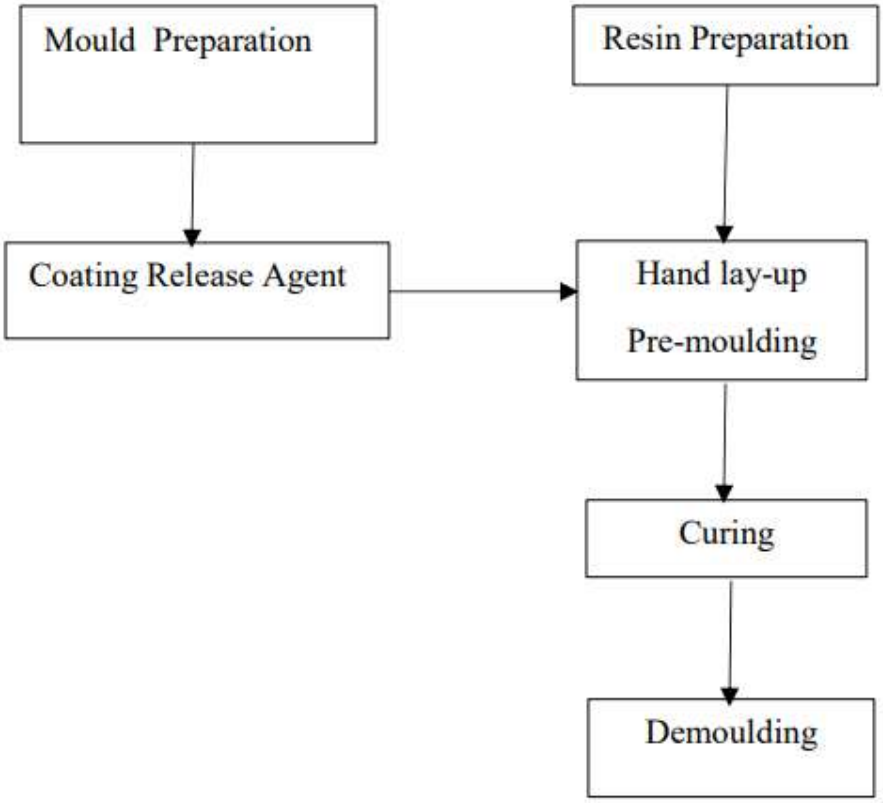


Figure 6.1: Schematic representing Flow chart for Composite fabrications by conventional technique

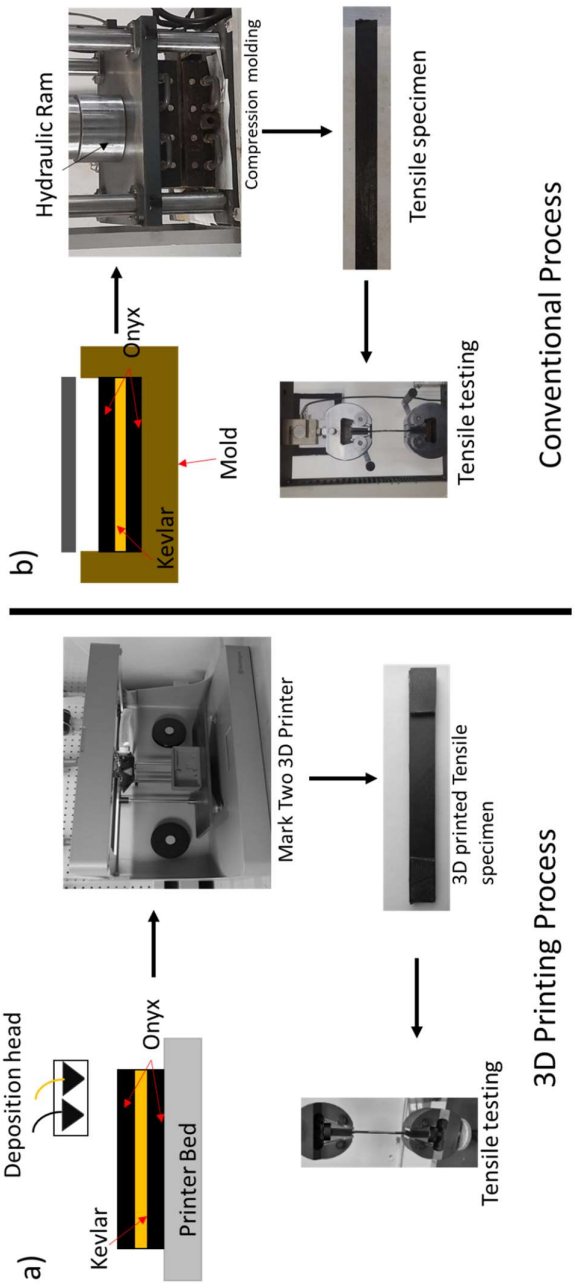


Figure 6.2 Composite fabrications by conventional technique

## 6.2 Comparison of tensile strength

Figure 6.2 shows the stress-strain graph obtained from testing 3D printed samples of continuous Kevlar fiber reinforced Onyx composites. The graph demonstrates a linear relationship between stress and strain, indicating the absence of plastic deformation, suggesting brittle failure. The high slope of the linear portion of the graph suggests that the composite possesses excellent stiffness and resistance to deformation under applied loads. This high slope indicates that small changes in strain result in significant changes in stress, highlighting the material's ability to withstand external forces with minimal deformation. The presence of continuous Kevlar fibers within the composite likely contributed to the observed strength, as Kevlar fibers are known for their exceptional tensile strength and resistance to deformation.

The stress-strain graph obtained from testing samples fabricated by conventional techniques, in contrast to 3D printed samples, exhibits notable differences in mechanical behaviour as shown in figure 6.3. Unlike the steep slope observed in the 3D printed samples, the stress-strain curve for the conventionally fabricated specimens shows a lower slope. This lower slope indicates a lower stiffness and modulus of elasticity compared to the 3D printed samples, suggesting that the conventional fabrication method may result in a less rigid composite structure. Moreover, the graph illustrates a higher strain recorded in the conventionally fabricated samples before failure compared to the 3D printed counterparts. This increased strain implies that the conventional samples can deform to a greater extent before reaching their breaking point, indicating a higher level of ductility in the material. However, it's worth noting that despite the higher strain, the conventionally fabricated samples exhibited a lower peak value of stress compared to the 3D printed samples. This suggests that while the conventionally fabricated samples may deform more before failure, they ultimately have a lower ultimate tensile strength compared to the 3D printed samples.

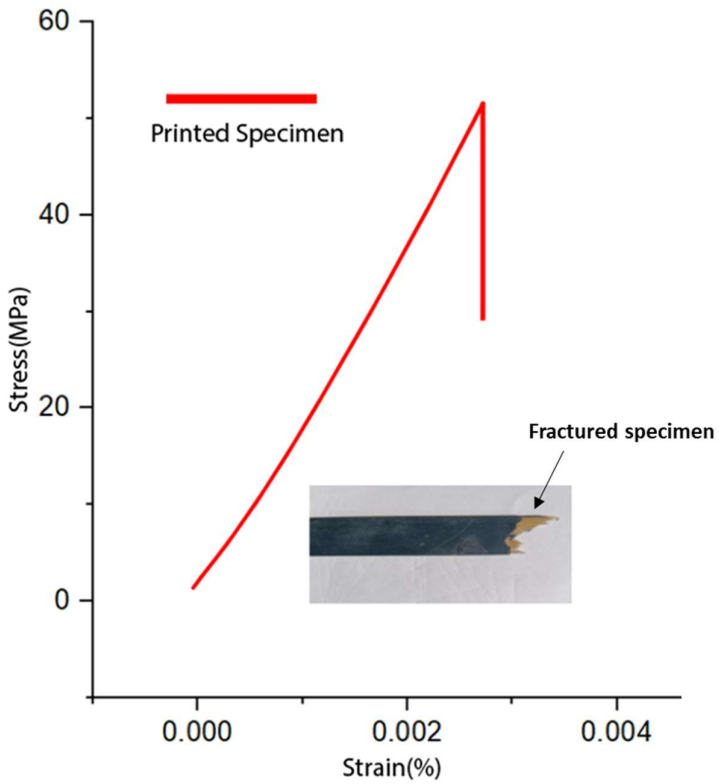


Figure 6.3 Stress-strain plot for 3D printed sample

The comparison of ultimate tensile strength and strain values between samples fabricated by 3D printing and conventional techniques reveals significant differences in mechanical performance. The ultimate tensile strength of the 3D printed specimens was measured at 56.1 MPa, indicating a high level of structural integrity and resistance to applied forces. In contrast, the ultimate tensile strength of specimens fabricated using conventional techniques was notably lower, at 31.38 MPa. This difference underscores the superior mechanical properties achieved through 3D printing, likely attributed to the precise fiber alignment and uniform distribution of materials facilitated by additive manufacturing processes.

Similarly, the strain values further emphasize the differences between the two fabrication methods. The strain exhibited by the 3D printed specimens was recorded at 0.0035, suggesting limited deformation before failure. In contrast, the conventional specimens demonstrated a higher strain of 0.025, indicating greater ductility and

deformation capacity under tensile loading. Figure 6.4 illustrates the comparison of ultimate tensile strength and strain for 3D printed and conventionally manufactured samples.

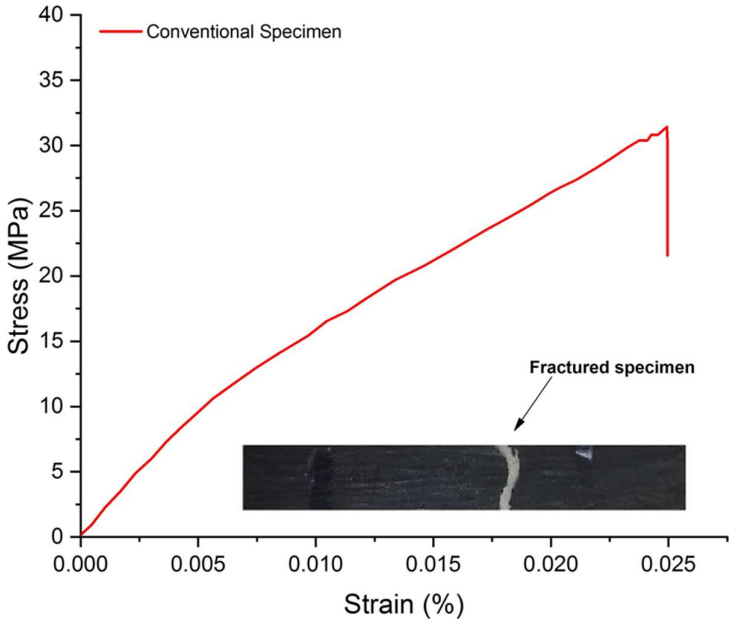


Figure 6.4 Stress-strain plot for conventionally manufactured sample

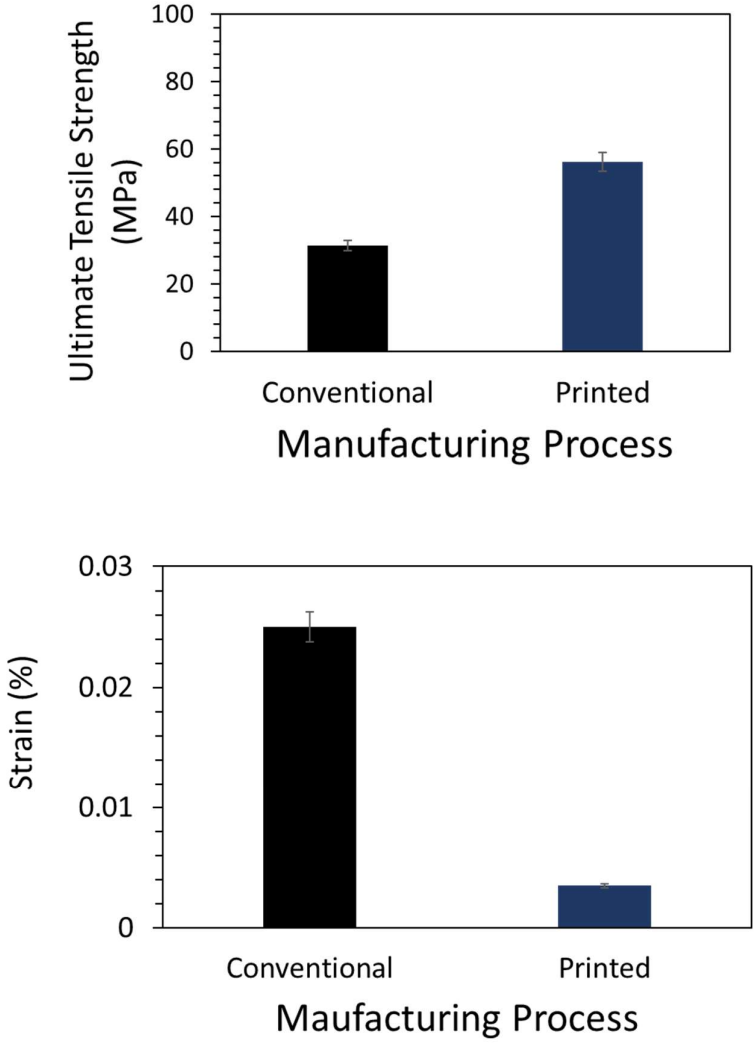


Figure 6.5 Comparison of ultimate tensile strength and strain of 3D printed and conventionally manufactured samples

The obtained results, particularly the difference in tensile strength between the specimens fabricated by conventional techniques and those by 3D printing, can be justified through several observations. Firstly, the reduced tensile strength of the conventional specimens compared to the printed specimens can be attributed to inherent differences in the fabrication processes. In conventional techniques, such as compression moulding, the possibility of fiber entanglement and uneven distribution within the composite matrix is higher. This could lead to areas of weakness and susceptibility to failure under applied loads, resulting in reduced tensile strength. On

the other hand, 3D printing allows for precise control over fiber alignment and distribution, resulting in a more uniform and optimized composite structure, hence the higher tensile strength observed in the printed specimens.

Moreover, the observation of fiber pull-outs on the conventional specimens further supports the notion of uneven distribution and inadequate bonding between the fibers and the matrix material (figure 6.5). These pull-outs weaken the overall structure of the composite, contributing to the lower tensile strength observed.

The possibility of improved strength has been documented in prior literature. The findings of Wickramasinghe et al., for instance, support the notion that conventional fabrication methods may result in inferior mechanical properties compared to continuous fiber composites fabricated by additive manufacturing techniques (figure 6.6).

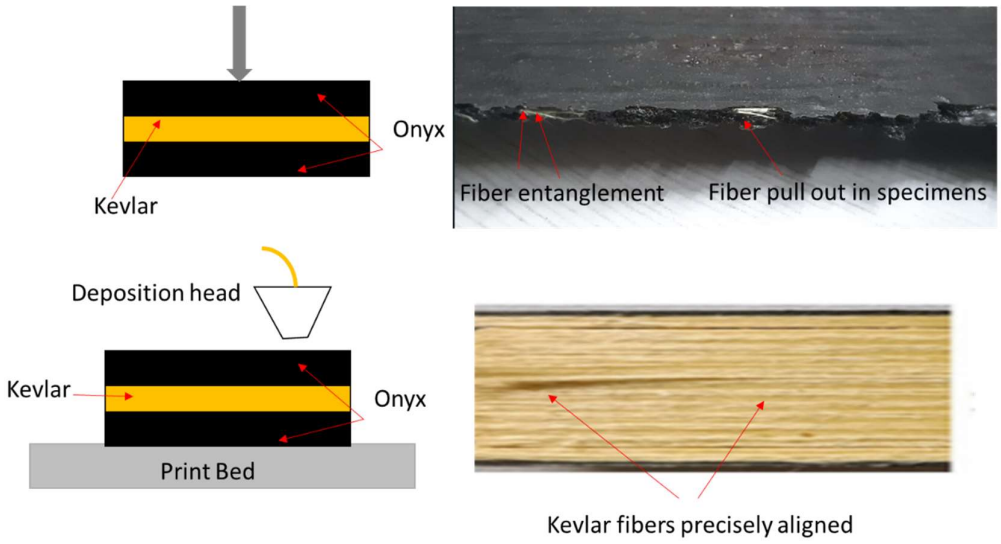


Figure 6.6 Precise deposition of continuous fiber in 3D printing and issue of fiber entanglement in conventional method

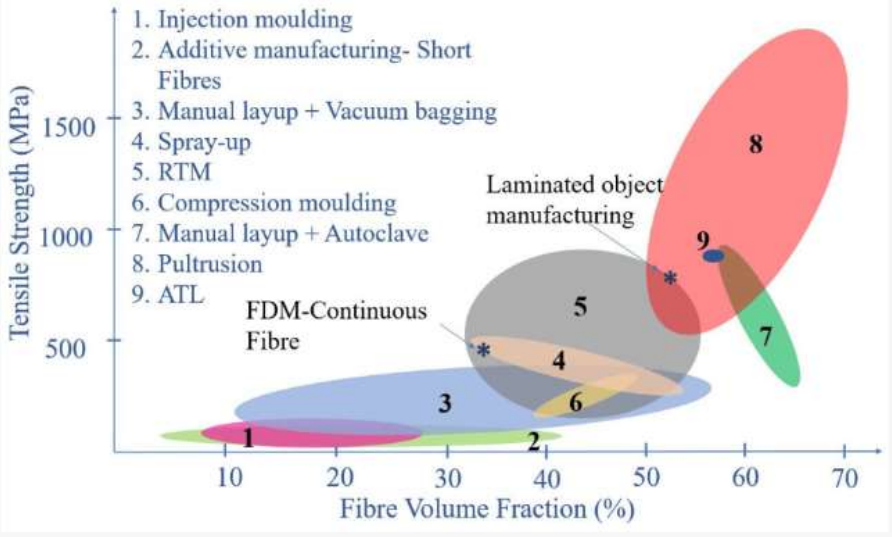


Figure 6.7 Comparison of various manufacturing processes with FDM based continuous fiber composites (MacDonald & Wicker, 2016)

### 6.3 Micromechanical Modelling

This study evaluates the applicability of micromechanical models—Voigt, Reuss, and Halpin–Tsai—for predicting the modulus and strength dependency on fiber volume fraction in 3D-printed composites. Unidirectional fibers were aligned at 0°, 45°, and 90° to assess longitudinal, shear, and transverse properties. The Voigt model demonstrated high accuracy for predicting longitudinal tensile strength and provided a reasonable approximation for longitudinal modulus. However, the Reuss model as well as Halpin Tsai failed to capture transverse modulus trends. 3D printed fiber-reinforced composites exhibit microscopically inhomogeneous and orthotropic behaviour, leading to complex mechanical responses that are analysed using micromechanics. This approach models interactions between constituents to predict the elastic, thermal, and failure properties of the composite lamina. Several assumptions simplify this analysis: fibers are uniformly distributed in the matrix with perfect bonding, and the matrix is void-free. The applied load is assumed to act either parallel or perpendicular to the fiber direction. Additionally, the composite is considered stress-free before loading, with no residual stresses in fibers or the matrix. Both the fibers and the matrix are treated as

linearly elastic materials, enabling a simplified yet effective study of composite responses under tensile loading. (P.K. Mallick, n.d.).

Three models are used to predict the properties of the composites. Voigt, Ruess and Halpin-Tsai model were utilized in this section for prediction. The Voigt model is employed to predict the longitudinal modulus under the assumption that there is equal strain distributed among the matrix, fiber, and composite in the longitudinal direction .It is a rule of misturs approach, giving an upper-bound estimates of the composite stiffness.The model assumes that the strain throughout the composite material is same equation [1-3]. $E_{cx}$ and $E_{cy}$ is the Longitudinal and Transverse Young's modulus of the composite, $E_r$ and $E_m$ is the Young's modulus of the reinforcement and the matrix respectively. In the similar fashion $\sigma_{cx}$ , $\sigma_{cy}$ $\sigma_r$ and $\sigma_m$ are the Longitudinal and Transverse stress in the composite, reinforcement and the matrix. $\varepsilon_c$ , $\varepsilon_r$ and $\varepsilon_m$ are the strains in composite, reinforcement and matrix respectively.The Ruess model or the inverse rule of mixture, is a widely utilized approach for predicting the transverse and shear modulus of composites material. It is derived based on the assumption that the stresses experienced by the individual constituents within the composite are equal in the transverse direction. The model assumes uniform stress distribution across the constituents in the transverse direction. This model is useful in evaluating shear modulus as well as transverse elastic modulus. The Reuss model is given by the equation 7.Halpin-Tsai model is a widely used semi-empirical approach to predict effective mechanical properties of composite materials. It is particularly helpful in estimating properties like modulus of elasticity (stiffness) for composite systems with different reinforcement geometries and volume fractions. (Hetrick et al., 2021) .$\zeta$ fitting parameter ranging from 1 to 2 for continuous fiber and $\eta$ is given by the following equations 8, 9 .

Voigt model forecast for longitudinal tensile strength and Young's modulus closely approximates experimental outcomes (figure 14 and 15). Ruess Model and Halpin-Tsai model does not fit the trend and over fit the model (figure 16 and 17). The underlying causes of this discrepancy are multifaceted and encompass factors such as limited interfacial bonding between fibers and the matrix arising from deficient infiltration, and inherent micro cracks prevalent in 3D printed components, among others. These

observations imply that the composite material, consisting of continuous Kevlar fiber despite its elevated fiber volume fraction in transverse direction, demonstrates a detrimental impact on its mechanical properties due to an insufficient degree of infiltration. Table 5, 6 shows the Experimental vs Micro modeling Results.

| | |
|---|---|
| $\varepsilon_r = \varepsilon_m = \varepsilon_c$ | 6.1 |
| $\sigma_r = E_r\varepsilon_r = E_r\varepsilon_c$ | 6.2 |
| $\sigma_m = E_m\varepsilon_m = E_m\varepsilon_c$ | 6.3 |
| $\sigma_c = V_r\sigma_r + (1\text{-}V_r)\,\sigma_m$ | 6.4 |
| $E_{cx} = V_rE_r + (1\text{-}V_r)\,E_m$ | 6.5 |
| $\sigma_{cx} = V_r\sigma_r + (1\text{-}V_r)\,\sigma_m$ | 6.6 |
| $E_{cy} = \left(\frac{V_r}{E_r} + \frac{1-V_r}{E_m}\right)^{-1}$ | 6.7 |
| $E_{cy} = E_m\left(\frac{1+\zeta*\eta*V_r}{1-\zeta*\eta*V_r}\right)$ | 6.8 |
| $\eta = \frac{\left(\frac{E_r}{E_m}\right)-1}{\frac{E_r}{E_m}+\zeta}$ | 6.9 |

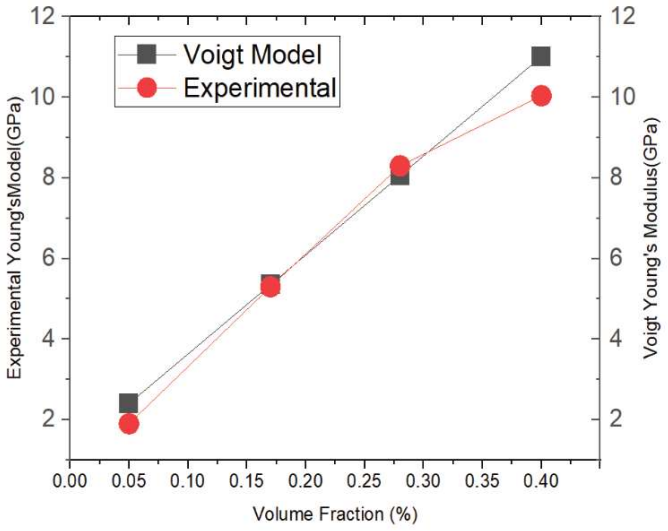


Figure 6.8: Comparison of predicted tensile strength using Voigt vs experimental values

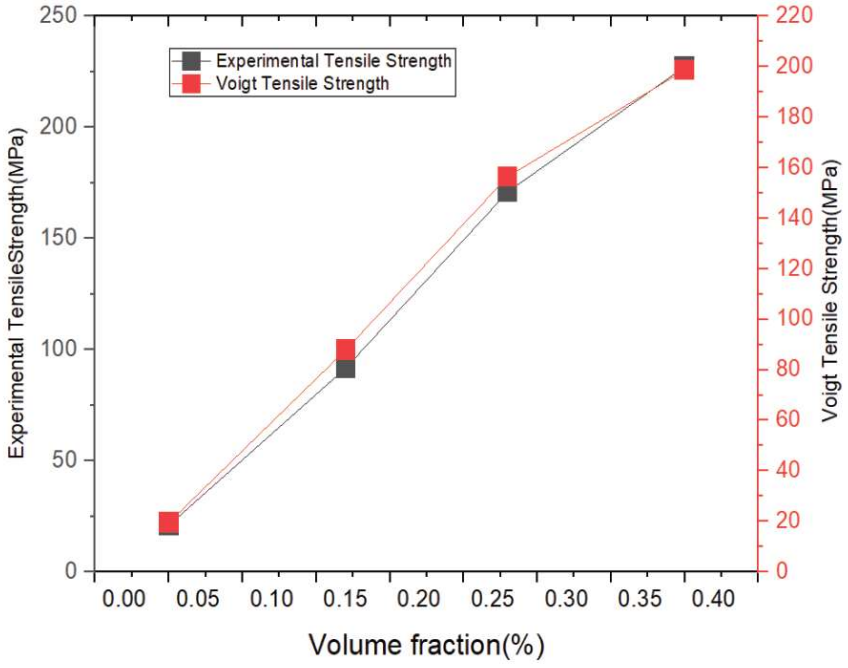


Figure 6.9 Schematic diagram represents comparison of predicted Young's modulus Voigt vs experimental values

Table 6.2 Comparsion of Experimental results vs Predcited modeling thorugh Micromdelling technique

| Mechanical Property | Modelling Technique | Volume Fraction | Predicted Values | Experimental Values |
|---|---|---|---|---|
| **Longitudinal Tensile Strength (MPa)** | **Voigt Model** | 0 | 21 | 19.5 |
| | | 0.12 | 91.68 | 87.9 |
| | | 0.22.6 | 156.47 | 171 |
| | | 0.35 | 227.15 | 198.6 |
| **Longitudinal Elastic strength (GPa)** | **Voigt Model** | 0 | 2.4 | 1.81 |
| | | 0.12 | 5.352 | 5.3 |
| | | 0.226 | 8.058 | 8.3 |
| | | 0.35 | 11.01 | 10.04 |

Table 6.3 Comparsion of Experimental results vs Ruess model

| Mechanical Property | Modelling Technique | Volume Fraction | Predicted Values | Experimental Values |
|---|---|---|---|---|
| Transverse Tensile Strength (MPa) | Ruess Model | 0 | 40 | 19.5 |
| | | 0.12 | 45.05 | 11.7 |
| | | 0.226 | 50.95 | 16.3 |
| | | 0.35 | 59.43 | 20.2 |
| Transverse Elastic Modulus (GPa) | Ruess Model | 0 | 2.4 | 1.81 |
| | | 0.12 | 2.69 | 1.65 |
| | | 0.226 | 3.036 | 1.93 |
| | | 0.35 | 3.52 | 2.15 |

Table 6.4 Comparsion of Experimental results vs Halpin Tsai model

| Mechanical Property | Modelling Technique | Volume Fraction | Predicted Values | Experimental Values |
|---|---|---|---|---|
| Transverse Tensile Strength (MPa) | Halpin Tsai Model | 0 | 40 | 19.5 |
| | | 0.12 | 52.21 | 11.7 |
| | | 0.226 | 65.82 | 16.3 |
| | | 0.35 | 84.27 | 20.2 |
| Transverse l Elastic Modulus (GPa) | Halpin Tsai Model | 0 | 2.4 | 1.81 |
| | | 0.12 | 3.13 | 1.65 |
| | | 0.226 | 3.94 | 1.93 |
| | | 0.35 | 5.05 | 2.15 |

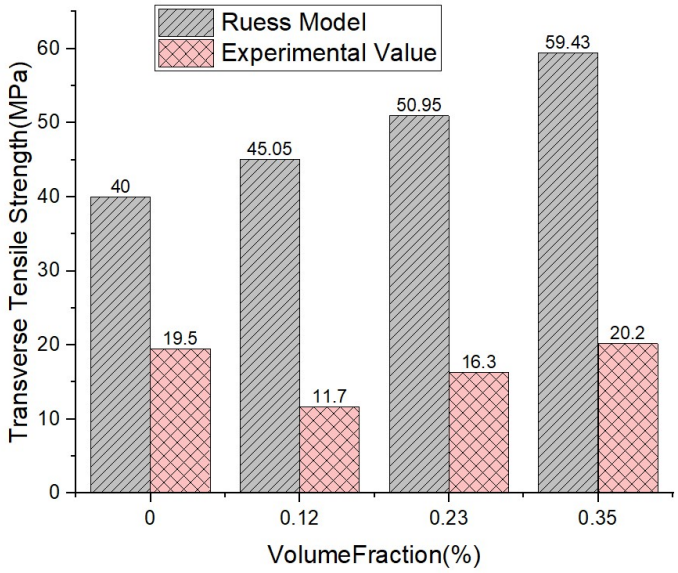


Figure 6.9 Schematic diagram represents comparison of predicted Tensile Strength Ruess vs experimental values

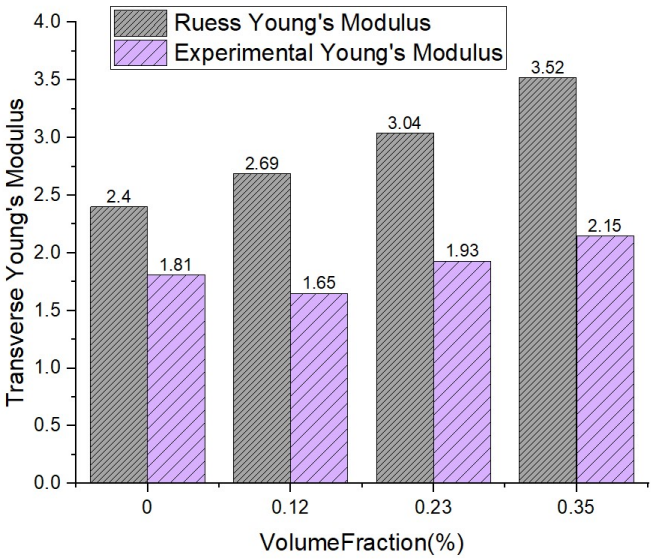


Figure 6.10 Schematic diagram represents comparison of predicted Young's modulus Ruess vs experimental values

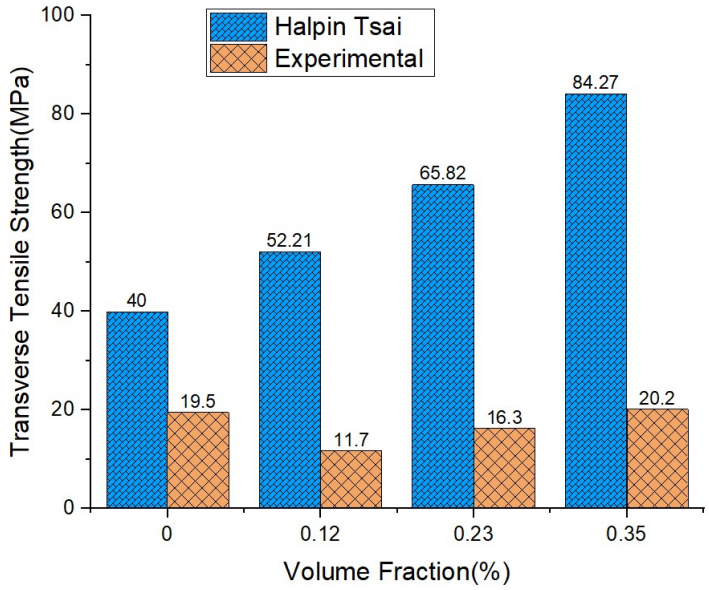


Figure 6.11 Schematic diagram represents comparison of predicted Young's modulus Halpin Tsai vs experimental values

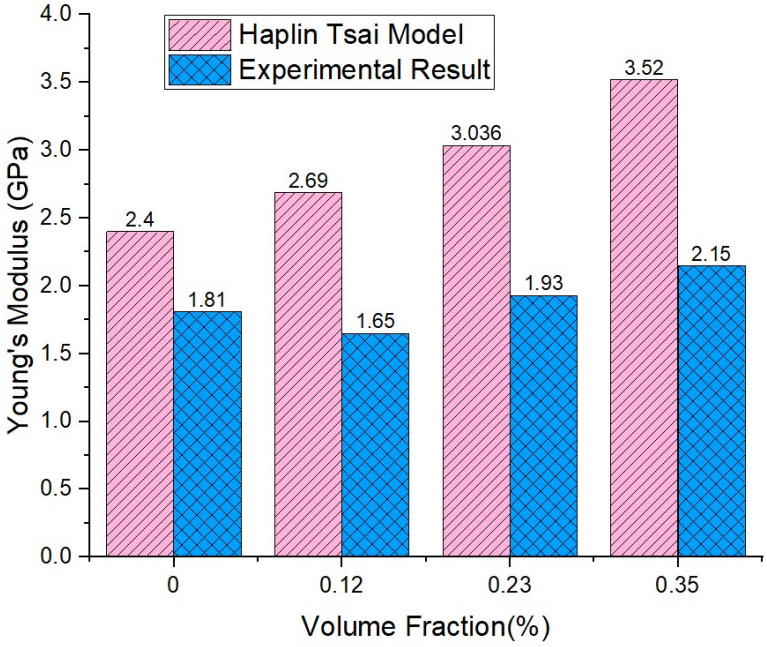


Figure 6.12 Schematic diagram represents comparison of predicted Young's modulus Halpin Tsai vs experimental values

This study investigates the accuracy of mixture rules in predicting the mechanical properties of 3D-printed continuous carbon fiber composites, focusing on the effects of fiber orientation, volume fraction, and printing-related factors. Continuous, unidirectional fibers were printed at orientations of 0°, 90°, or 45° relative to the loading direction, with fiber volume fractions varied by adjusting the number of fiber layers in the specimens. The Rule of Mixtures accurately predicted the longitudinal tensile strength and provided reasonable approximations for the longitudinal modulus across different fiber contents. However, for transverse properties, the Halpin–Tsai model showed moderate accuracy in predicting the transverse modulus, while the Reuss model was less reliable. Despite variations in fiber volume fraction, mechanical property variability did not correlate strongly with it, suggesting that other factors, such as material quality and printing parameters, significantly influence performance. The lack of compression inherent to the 3D printing process likely resulted in macroscopic internal voids, weakening the material and introducing inconsistencies. These voids were assumed negligible during micromechanical modelling, limiting its accuracy. The mechanical properties of these 3D-printed composites cannot be directly compared to conventional composites due to their combination of high-strength carbon fibers with low-strength matrix materials and the unique defects associated with 3D printing. Consequently, while the Rule of Mixtures effectively models longitudinal properties, more advanced approaches are needed to account for transverse and off-axis behavior, as well as void effects, to improve predictive accuracy and performance. The observed outcomes and limitations in predicting the mechanical properties of 3D-printed continuous carbon fiber composites arise from a combination of material, manufacturing, and modelling factors .The mechanical properties of fiber-reinforced composites are inherently anisotropic, meaning they vary depending on the fiber orientation relative to the loading direction. Fibers aligned with the load direction (0°) efficiently bear stress, leading to higher longitudinal strengths and moduli. Conversely, fibers oriented at 90° or 45° contribute less effectively, resulting in weaker transverse or off-axis properties. The Rule of Mixtures assumes idealized conditions such as perfect bonding, uniform stress transfer, and void-free materials, which align closely

with the longitudinal behaviour where fibers dominate the load-bearing. However, for transverse properties, these assumptions fail to capture the complexities of the fiber-matrix interface, resulting in less accurate predictions. The lack of compression during the 3D printing process can lead to internal voids and defects. These voids reduce the effective load-bearing area, act as stress concentrators, and weaken the composite, particularly in the matrix-dominated transverse direction. Such imperfections deviate from the idealized assumptions used in micromechanical models. In 3D-printed composites, the matrix material often has significantly lower strength compared to conventional composite matrices. This reduces the matrix's ability to distribute stress effectively, especially in the transverse and off-axis directions where it plays a more prominent role. While fiber volume fraction significantly affects the stiffness and strength of composites, the observed variability in mechanical properties did not directly correlate with it. This suggests that factors like fiber alignment accuracy, interface quality, and layer bonding dominate the mechanical response more than the volume fraction alone. Assumptions like negligible void effects and linear elastic behaviour of constituents simplify the models but overlook the real-world complexities introduced by the 3D printing process. These oversights limit the applicability of conventional models such as the Rule of Mixtures, Halpin–Tsai, and Reuss for accurately predicting properties under non-ideal conditions.In summary, the mismatch between model predictions and experimental results is rooted in the simplifications inherent in the models, combined with the unique imperfections introduced by 3D printing processes and the material limitations of printed composites.

.

# CHAPTER 7
# CONCLUSION AND FUTURE WORK

In this study, the mechanical analysis of 3D printed KFRCP components was investigated. Experimental data validate that the inclusion of continuous fiber in the direction of the print bed exhibits superior mechanical properties compared to another configuration.

## 7.1 Tensile Properties of 3D Printed KFRCP

Fiber orientation plays a crucial role in determining the mechanical properties of composite materials, particularly in tension. When fiber are oriented at 0° (parallel to the direction of loading), they provide the maximum reinforcement and alignment with the applied force, resulting in the highest tensile strength. This configuration allows for efficient load transfer along the length of the fibers, maximizing the material's resistance to stretching. Conversely, when fibers are loaded in the transverse direction, such as at 90° or 45°, they offer less resistance to tensile forces. This is because fibers at these angles are less aligned with the applied force, leading to lower reinforcement efficiency and reduced tensile strength. The change in raster angle towards higher values (away from 0°) can indeed lead to poor interfacial adhesion between the matrix and reinforcement. This poor adhesion results in decreased load transfer between the matrix and fibers, leading to compromised mechanical strength. Additionally, higher raster angles may also introduce more voids or gaps between fibers and the matrix, further reducing the material's overall strength. A higher raster angle means that filaments do not align well with the previous layer, leading to reduced contact between layers.When the raster is nearly perpendicular (e.g., 90°), the mechanical bonding relies mostly on weak Van der Waals forces rather than strong polymer entanglement.

Thermal Gradients: Steeper angles may result in non-uniform cooling and residual stresses, leading to delamination or weak bonding. Markforg offers two types of patterns: concentric and isotropic. Experimental findings reveal that the isotropic 0° pattern exhibits superior tensile strength compared to the concentric pattern. Furthermore, the presence of voids in the central region of the concentric configuration

compromises uniformity, leading to diminished tensile strength in contrast to the isotropic 0° pattern. The incorporation of concentric rings reduces overall isotropic filling, consequently lowering mechanical strength. Additionally, inadequate bonding between the matrix and reinforcement material contributes to the decrease in tensile strength. In contrast, the isotropic pattern demonstrates consistent and uniform fiber alignment across the entire surface area, oriented in the direction of loading, resulting in maximized tensile strength as evidenced by experimental observations. The anisotropic behaviour observed in 3D printed specimens significantly influences their tensile behaviour. Furthermore, within 3D printed continuous fiber reinforced polymer composites, the orientations and patterns of fibers actively contribute to this characteristic anisotropy. This underscores the influence of fiber direction and the resulting alignment of polymer molecules on tensile strength, highlighting the inherent anisotropic property. Even when composites are printed flat on the bed, variations in fiber orientation can lead to differing tensile properties and induce anisotropy. This observation is further evident when comparing printed specimens with longitudinal and transverse fiber orientations.

Delamination occurs when the matrix fails to adequately wet the fibers, leading to insufficient synergy between the two components. However, beyond the threshold volume fraction of continuous Kevlar fiber reinforcement in the Onyx matrix, delamination becomes predominant. Within the volume fraction range of 22.6% to 58%, partial delamination occurs, characterized by bundles of fibers being pulled out together, indicating a compromised bond between the matrix and fiber interface. Experimental findings demonstrate that fiber layers can withstand a maximum load up to a 58% volume fraction of fiber. Beyond this threshold, at 64%, complete delamination ensues. Consequently, in composites with a 64% volume fraction, failure is attributed to delamination, resulting in the complete peeling off of the matrix, thereby rendering further testing unfeasible.

As reinforcement levels increase, a decrease in ductility is observed. Experimental findings establish a correlation between the strength and ductility of specimens and the extent of reinforcement. Notably, heightened reinforcement results in increased

strength but decreased ductility. The linear stress-strain graph of 3D printed KFRCP illustrates its brittleness. The impregnation of Continuous Kevlar into the thermoplastic Onyx substantially enhances the tensile strength of Onyx, elevating it from 21 MPa to 405 MPa with a 50% volume fraction of reinforcement.

This study shows that mixture rules can predict longitudinal tensile strength and approximate longitudinal modulus in 3D-printed continuous carbon fiber composites. However, transverse property predictions remain limited, particularly with the Reuss model. The observed variability in mechanical properties, independent of fiber volume fraction, may stem from factors unique to the printing process, such as internal voids due to the absence of compression. While mathematical models can approximate tensile strength for fibers oriented in a specific direction, they fail to account for mechanical properties across varied fiber orientations due to voids observed at the macroscopic level. Differences in tensile strength between 3D-printed and conventionally fabricated specimens can be attributed to fabrication variations.

### 7.2 Impact Properties of 3D Printed KFRCP

Significant improvements in impact strength can be achieved by altering the fiber orientation. This underscores the pivotal role of fiber deposition strategy in enhancing impact properties. When fibers align with the longest dimension, they orient along the direction most likely to encounter mechanical loads. This alignment optimizes the load-carrying capacity of the fibers and consequently enhances the overall mechanical properties of the composite material. The increased surface area of fibers in this alignment can result in improved tensile and impact strength, rendering the material.
The higher impact strength observed in concentric patterned samples compared to those with a 0° pattern can be attributed to the former's ability to effectively shield the outer layer. The addition of concentric rings around the wall further enhances the impact strength of the material. When fibers align with the direction of stress, they demonstrate superior resistance to impacts. Both the concentric and 0° patterns align the fibers with the stress direction, making them suitable for creating anti-impact specimens. Notably, the impact samples feature notches with sharp contours. In cases involving sharp

corners or holes, the concentric pattern is justified as it uniformly covers the entire surface, ensuring continuity.

When fibers align with the direction of stress, they demonstrate superior resistance to impacts. In both patterns, the fibers align with the stress direction, making them suitable for creating anti-impact specimens. The impact samples feature notches with sharp contours. In cases involving sharp corners or holes, the concentric pattern is justified as it uniformly covers the entire surface, ensuring continuity.

During impact testing, specimens without reinforcement experienced angled cracks with complete breakage and total failure, with the matrix layer tearing along the path of the print. In the case of the concentric pattern, partial breakage was observed, indicating its ability to mitigate the extent of damage during impact events.

During impact testing, specimens without reinforcement experienced angled cracks with complete breakage and total failure, with the matrix layer tearing along the path of the print. In contrast, specimens with the concentric pattern exhibited partial breakage, highlighting the pattern's ability to mitigate the extent of damage during impact events.

Empirical observations elucidate a discernible and direct correlation, as anticipated, between the reinforcement level and the impact properties of the fiber material The increase in volume fraction results in a remarkable threefold amplification in the impact strength of the composite. Impregnated Kevlar fiber withstands maximum load, imparting impactful properties to 3D printed composites. The substantial augmentation in strength arises from a synergistic amalgamation of heightened reinforcement, precise alignment of fibers along the load-bearing direction, and uniform dispersion of fibers within the Onyx matrix. The increase in fiber content restricts polymer flow and prevents crack propagation, resulting in enhanced impact strength.

The increase in volume fraction results in a remarkable threefold amplification in the impact strength of the composite. Impregnated Kevlar fiber withstood the maximum load, imparting an impact property to 3D printed composites. This enhanced impact strength can be primarily attributed to the consistent alignment of continuous fibers along the load-bearing axis.

The increase in fiber content restricts polymer flow and prevents the propagation of cracks, resulting in improved impact strength. Notably, no external pressure was applied during the printing process, which plays a crucial role in manufacturing conventional composites, mitigating the occurrence of voids. Void formation is a predominant phenomenon during 3D printing. Thermoplastic material with less reinforcement tends to have more voids and weaker bonding. With an increase in reinforcement, voids are reduced, resulting in an increase in impact strength.

# 7.3 FUTURE WORK

- More experimental testing by changing fiber orientation like on flat surface on edge surface
- More experimental impact test .
- FEM modelling to predict the mechanical performance on 3D printed parts.
- Developing mathematical modelling technique to predict tensile properties

# PUBLICATION

KK.Ojha,,SChowdarpally,VishalFrancis Additive manufacturing of FRCP: material, methods challenges and future works Recent Advancements in Mechanical Engineering pp 473–483.( kamal kumar Ojha, 2008)

KK Ojha, G Gugliani, V Francis Tensile properties and failure behavior of continuous kevlar FRCPs fabricated by additive manufacturing processAdvances in Materials and Processing Technologies ,Page1-5 (K. K. Ojha *et al.*, 2022b).

KK Ojha, G Gugliani, V Francis Impact and tensile performance of continuous 3D-printed Kevlar fiber-reinforced composites manufactured by Fused deposition modeling International Journal of Materials and Product Technology Volume 57, Page 1-3, Pages 20-42 (K. K. Ojha *et al.*, 2022a).

KK Ojha, G Gugliani, V Francis Mechanical behavior analysis of KFR Taylor & Francis publication (CRC Press). ISBN No 9781032740713Composites (Chapter 16) titled " Mechanical Behaviour Analysis of Additive Manufactured KFR Composites,".

**CONFERENCE PRESENTATIONS**

KK Ojha, G Gugliani, V Francis Tensile Properties and Failure behavior Of Continuous Kevlar FRCPs Fabricated by Additive Manufacturing Process" (CIMS-2021). Nov 11-13, 2021

KK.Ojha, SChowdarpally,Vishal Francis Additive manufacturing of FRCP: material, methods challenges and future works ICRAME(2021) Oct 11-13, 2021

# REFERENCE


1. Akhoundi, B., Behravesh, A. H., & Bagheri Saed, A. (2019). Improving mechanical properties of continuous fiber-reinforced thermoplastic composites produced by FDM 3D printer. *Journal of Reinforced Plastics and Composites*, *38*(3), 99–116. https://doi.org/10.1177/0731684418807300
2. Araya-Calvo, M., López-Gómez, I., Chamberlain-Simon, N., León-Salazar, J. L., Guillén-Girón, T., Corrales-Cordero, J. S., & Sánchez-Brenes, O. (2018). Evaluation of compressive and flexural properties of continuous fiber fabrication additive manufacturing technology. *Additive Manufacturing*, *22*, 157–164. https://doi.org/10.1016/j.addma.2018.05.007
3. Caminero, M. A., Rodríguez, G. P., & Muñoz, V. (2016). Effect of stacking sequence on Charpy impact and flexural damage behavior of composite laminates. *Composite Structures*, *136*, 345–357. https://doi.org/10.1016/j.compstruct.2015.10.019
4. Cersoli, T., Yelamanchi, B., MacDonald, E., Carrillo, J. G., & Cortes, P. (2021). 3D printing of a continuous fiber-reinforced composite based on a coaxial Kevlar/PLA filament. *Composites and Advanced Materials*, *30*, 263498332110000. https://doi.org/10.1177/26349833211000058
5. Chacón, J. M., Caminero, M. A., García-Plaza, E., & Núñez, P. J. (2017). Additive manufacturing of PLA structures using Fused deposition modeling: Effect of process parameters on mechanical properties and their optimal selection. *Materials and Design*, *124*, 143–157. https://doi.org/10.1016/j.matdes.2017.03.065
6. Chacón, J. M., Caminero, M. A., Núñez, P. J., García-Plaza, E., García-Moreno, I., & Reverte, J. M. (2019). Additive manufacturing of continuous fiber reinforced thermoplastic composites using Fused deposition modeling: Effect of process parameters on mechanical properties. *Composites Science and Technology*, *181*. https://doi.org/10.1016/j.compscitech.2019.107688
7. Chaudhry, F. N., Butt, S. I., Mubashar, A., Naveed, A. Bin, Imran, S. H., & Faping, Z. (2022). Effect of carbon fiber on reinforcement of thermoplastics using FDM and RSM. *Journal of Thermoplastic Composite Materials*, *35*(3), 352–374. https://doi.org/10.1177/0892705719886891
8. Chen, W., Zhang, Q., Cao, H., & Yuan, Y. (2021). Process evaluation, tensile properties, mathematical models, and fracture behavior of 3D printed continuous fiber reinforced thermoplastic composites. *Journal of Reinforced Plastics and Composites*, *40*(21–22), 845–863. https://doi.org/10.1177/07316844211016091
9. Chen J, Yu Z and Jin H (2022), Nondestructive testing and evaluation techniques of defects in fiber-reinforced polymer composites: A review. Front. Mater. 9:986645.
10. Dickson, A. N., Barry, J. N., Dickson, A. N., Barry, J. N., Mcdonnell, K. A., & Dowling, D. P. (2017). Fabrication of Continuous Carbon , Glass and Kevlar fiber reinforced polymer composites using Additive Manufacturing Fabrication of continuous carbon , glass and Kevlar fiber reinforced polymer composites using additive manufacturing. *Additive Manufacturing*, *16*(June), 146–152. https://doi.org/10.1016/j.addma.2017.06.004

11. Dong, G., Tang, Y., Li, D., & Zhao, Y. F. (2018). *Mechanical Properties of Continuous Kevlar Fibre Reinforced Composites Fabricated by Fused Deposition Modeling Process*. *26*, 774–781. https://doi.org/10.1016/j.promfg.2018.07.090
12. Es-Said, O. S., Foyos, J., Noorani, R., Mendelson, M., Marloth, R., & Pregger, B. A. (2000). Effect of layer orientation on mechanical properties of rapid prototyped samples. *Materials and Manufacturing Processes*, *15*(1), 107–122. https://doi.org/10.1080/10426910008912976
13. Farina, I., Singh, N., Colangelo, F., Luciano, R., Bonazzi, G., & Fraternali, F. (2019). High-Performance Nylon-6 Sustainable Filaments for Additive Manufacturing. *Materials*, *12*(22.6), 3955. https://doi.org/10.3390/ma1222.63955
14. Ferreira, R. T. L., Amatte, I. C., Dutra, T. A., & Bürger, D. (2017). Experimental characterization and micrography of 3D printed PLA and PLA reinforced with short carbon fibers. *Composites Part B: Engineering*, *124*, 88–100. https://doi.org/10.1016/j.compositesb.2017.05.013
15. Fidan, I., Russell, N., Imeri, A., Ortiz Rios, C., & Chen, Y. (2020). Investigation of the Tensile Properties in Fiber-Reinforced Additive Manufacturing and Fused Filament Fabrication. *International Journal of Rapid Manufacturing*, *9*(3), 1. https://doi.org/10.1504/ijrapidm.2020.10019313
16. Florin Cofaru, N., Pascu, A., Oleksik, M., & Petruse, R. (2021). Tensile Properties of 3D-printed Continuous-Fiber-Reinforced Plastics. *Mater. Plast*, *58*(4), 271–282. https://doi.org/10.37358/Mat.Plast.1964
17. Garrett W. Melenkaa, Benjamin K.O. Cheunga, Jonathon S. Schofielda, Michael R. Dawsonb, J. P. C. (2016). *Title: Evaluation and Prediction of the Tensile Properties of Continuous Fibre-Reinforced 3D Printed Structures Authors: Garrett W. Melenka*.
18. Ghebretinsae, F., Mikkelsen, O., & Akessa, A. D. (2019). Strength analysis of 3D printed carbon fiber reinforced thermoplastic using experimental and numerical methods. *IOP Conference Series: Materials Science and Engineering*, *700*(1). https://doi.org/10.1088/1757-899X/700/1/012024
19. Goh, G. D., Dikshit, V., Nagalingam, A. P., Goh, G. L., Agarwala, S., Sing, S. L., Wei, J., & Yeong, W. Y. (2018). Characterization of mechanical properties and fracture mode of additively manufactured carbon fiber and glass fiber reinforced thermoplastics. *Materials and Design*, *137*, 79–89. https://doi.org/10.1016/j.matdes.2017.10.021
20. González-estrada, O. A., & Pertuz, A. (2018). *Evaluation of Tensile Properties and Damage of Continuous Fibre Reinforced 3D-Printed Parts*. *774*, 161–166. https://doi.org/10.4028/www.scientific.net/KEM.774.161
21. González-Estrada, O. A., Pertuz, A., & Quiroga, J. (2018). Evaluation of tensile properties and damage of continuous fiber reinforced 3D-printed parts. *Key Engineering Materials*, *774 KEM*, 161–166. https://doi.org/10.4028/www.scientific.net/KEM.774.161
22. Hao, W., Liu, Y., Zhou, H., Chen, H., & Fang, D. (2018). Preparation and characterization of 3D printed continuous carbon fiber reinforced thermosetting composites. *Polymer Testing*, *65*, 29–34. https://doi.org/10.1016/j.polymertesting.2017.11.004

23. Hetrick, D. R., Sanei, S. H. R., Ashour, O., & Bakis, C. E. (2021). Charpy impact energy absorption of 3D printed continuous Kevlar reinforced composites. *Journal of Composite Materials*, *55*(12), 1705–1713. https://doi.org/10.1177/0021998320985596
24. Hetrick, D. R., Sanei, S. H. R., Bakis, C. E., & Ashour, O. (2021). Evaluating the effect of variable fiber content on mechanical properties of additively manufactured continuous carbon fiber composites. *Journal of Reinforced Plastics and Composites*, *40*(9–10), 365–377. https://doi.org/10.1177/0731684420963217
25. James Sauer, M., & James, M. (2018). *Evaluation of the Mechanical Properties of 3D Printed Carbon Fibre Composites*.
26. Jatti, V. S., Jatti, S. V, Patel, A. P., & Jatti, V. S. (2019). A Study On Effect Of Fused Deposition Modeling Process Parameters On Mechanical Properties. *INTERNATIONAL JOURNAL OF SCIENTIFIC & TECHNOLOGY RESEARCH*, *8*(11). www.ijstr.org
27. Kabir, S. M. F., Mathur, K., & Seyam, A. F. M. (2021a). Maximizing the performance of 3d printed fiber-reinforced composites. *Journal of Composites Science*, *5*(5). https://doi.org/10.3390/jcs5050136
28. Kabir, S. M. F., Mathur, K., & Seyam, A. F. M. (2021b). Maximizing the performance of 3d printed fiber-reinforced composites. *Journal of Composites Science*, *5*(5). https://doi.org/10.3390/jcs5050136
29. Letcher, T., & Waytashek, M. (2014). Material property testing of 3D-printed specimen in pla on an entry-level 3D printer. *ASME International Mechanical Engineering Congress and Exposition, Proceedings (IMECE)*, *2A*. https://doi.org/10.1115/IMECE2014-39379
30. Liao, G., Li, Z., Cheng, Y., Xu, D., Zhu, D., Jiang, S., Guo, J., Chen, X., Xu, G., & Zhu, Y. (2018). Properties of oriented carbon fiber/polyamide 12 composite parts fabricated by fused deposition modeling. *Materials and Design*, *139*, 283–292. https://doi.org/10.1016/j.matdes.2017.11.027
31. Maqsood, N., & Rimašauskas, M. (2021). Characterization of carbon fiber reinforced PLA composites manufactured by fused deposition modeling. *Composites Part C: Open Access*, *4*(November 2020). https://doi.org/10.1016/j.jcomc.2021.100112
32. Melenka, G. W., Cheung, B. K. O., Schofield, J. S., Dawson, M. R., Carey, J. P., Carey, J. P. R., Melenka, G., & Cheung, B. K. (n.d.). *Title: Evaluation and Prediction of the Tensile Properties of Continuous Fibre-Reinforced 3D Printed Structures*.
33. Mohammadizadeh, M., & Fidan, I. (2020). Experimental Evaluation of Additively Manufactured Continuous Fiber Reinforced Nylon Composites. In *Minerals, Metals and Materials Series*. Springer International Publishing. https://doi.org/10.1007/978-3-030-36296-6_30
34. Mohammadizadeh, M., & Fidan, I. (2021). Tensile performance of 3d-printed continuous fiber-reinforced nylon composites. *Journal of Manufacturing and Materials Processing*, *5*(3). https://doi.org/10.3390/jmmp5030068
35. Mohammadizadeh, M., Imeri, A., Fidan, I., & Elkelany, M. (2019). 3D printed fiber reinforced polymer composites - Structural analysis. *Composites Part B: Engineering*, *175*. https://doi.org/10.1016/j.compositesb.2019.107112
36. Naranjo-Lozada, J., Ahuett-Garza, H., Orta-Castañón, P., Verbeeten, W. M. H., & Sáiz-González, D. (2019). Tensile properties and failure behavior of chopped and continuous

carbon fiber composites produced by additive manufacturing. *Additive Manufacturing*, *26*, 227–241. https://doi.org/10.1016/j.addma.2018.12.020

37. Nikiema, D., Balland, P., & Sergent, A. (2022.6). Study of the Mechanical Properties of 3D-printed Onyx Parts: Investigation on Printing Parameters and Effect of Humidity. *Chinese Journal of Mechanical Engineering: Additive Manufacturing Frontiers*, *2*(2), 100075. https://doi.org/10.1016/j.cjmeam.2022.6.100075
38. Ning, F., Cong, W., Hu, Z., & Huang, K. (2017). Additive manufacturing of thermoplastic matrix composites using fused deposition modeling: A comparison of two reinforcements. *Journal of Composite Materials*, *51*(27), 3733–3742. https://doi.org/10.1177/0021998317692659
39. Ojha, K. K., Gugliani, G., & Francis, V. (2022). Impact and tensile performance of continuous 3D-printed Kevlar fiber-reinforced composites manufactured by Fused deposition modeling. *Progress in Additive Manufacturing*. https://doi.org/10.1007/s40964-022-00374-8
40. Patterson, A. E., Pereira, T. R., Allison, J. T., & Messimer, S. L. (2021). IZOD impact properties of full-density fused deposition modeling polymer materials with respect to raster angle and print orientation. *Proceedings of the Institution of Mechanical Engineers, Part C: Journal of Mechanical Engineering Science*, *22.65*(10), 1891–1908. https://doi.org/10.1177/0954406219840385
41. P.K. Mallick. (2007). *FIBRE- REINFORCED*.
42. Prajapati, A. R., Dave, H. K., & Raval, H. K. (2020). INFLUENCE OF FIBER RINGS ON IMPACT STRENGTH OF 3D PRINTED FIBER REINFORCED POLYMER COMPOSITE. In *International Journal of Modern Manufacturing Technologies: Vol. XII* (Issue 1).
43. Pyl, L., Kalteremidou, K. A., & Van Hemelrijck, D. (2018). Exploration of specimen geometry and tab configuration for tensile testing exploiting the potential of 3D printing freeform shape continuous carbon fiber-reinforced nylon matrix composites. *Polymer Testing*, *71*, 318–328. https://doi.org/10.1016/j.polymertesting.2018.09.022
44. Roberson, D. A., Torrado Perez, A. R., Shemelya, C. M., Rivera, A., MacDonald, E., & Wicker, R. B. (2015). Comparison of stress concentrator fabrication for 3D printed polymeric izod impact test specimens. *Additive Manufacturing*, *7*, 1–11. https://doi.org/10.1016/j.addma.2015.05.002
45. Rodríguez-Panes, A., Claver, J., & Camacho, A. M. (2018). The influence of manufacturing parameters on the mechanical behaviour of PLA and ABS pieces manufactured by FDM: A comparative analysis. *Materials*, *11*(8). https://doi.org/10.3390/ma11081333
46. Shi, K., Yan, Y., Mei, H., Chen, C., & Cheng, L. (2021). 3D printing Kevlar fiber layer distributions and fiber orientations into nylon composites to achieve designable mechanical strength. *Additive Manufacturing*, *39*. https://doi.org/10.1016/j.addma.2021.101882
47. Singh, T. J., & Samanta, S. (2015). Characterization of Kevlar Fiber and Its Composites: A Review. *Materials Today: Proceedings*, *2*(4–5), 1381–1387. https://doi.org/10.1016/j.matpr.2015.07.057

48. Sood, A. K., Ohdar, R. K., & Mahapatra, S. S. (2010). Parametric appraisal of mechanical property of Fused deposition modeling processed parts. *Materials and Design*, *31*(1), 287–295. https://doi.org/10.1016/j.matdes.2009.06.016
49. Tekinalp, H. L., Kunc, V., Velez-Garcia, G. M., Duty, C. E., Love, L. J., Naskar, A. K., Blue, C. A., & Ozcan, S. (2014). Highly oriented carbon fiber-polymer composites via additive manufacturing. *Composites Science and Technology*, *105*, 144–150. https://doi.org/10.1016/j.compscitech.2014.10.009
50. Todoroki, A., Oasada, T., Mizutani, Y., Suzuki, Y., Ueda, M., Matsuzaki, R., & Hirano, Y. (2020). Tensile property evaluations of 3D printed continuous carbon fiber reinforced thermoplastic composites. *Advanced Composite Materials*, *29*(2), 147–162. https://doi.org/10.1080/09243046.2019.1650322.6
51. Vălean, C., Marşavina, L., Mărghitaşl, M., Linul, E., Razavi, J., & Berto, F. (2020). Effect of manufacturing parameters on tensile properties of FDM printed specimens. *Procedia Structural Integrity*, *26*, 313–320. https://doi.org/10.1016/j.prostr.2020.06.040
52. Yu, T., Zhang, Z., Song, S., Bai, Y., & Wu, D. (2019). Tensile and flexural behaviors of additively manufactured continuous carbon fiber-reinforced polymer composites. *Composite Structures*, *225*. https://doi.org/10.1016/j.compstruct.2019.111147
53. Ziemian, C., Sharma, M., & Ziemi, S. (2012). Anisotropic Mechanical Properties of ABS Parts Fabricated by Fused deposition modeling. In *Mechanical Engineering*. InTech. https://doi.org/10.5772/3422.63